Ubiquitin-Independent Proteolytic Targeting of Ornithine Decarboxylase

Inaugural-Dissertation

Zur

Erlangung des Doktorgrades

der Mathematisch-Naturwissenschaftlichen Fakultät

der Universität zu Köln

vorgelegt von

Roshini Beenukumar Renukadevi

aus Trivandrum, Kerala, Indien

Köln, 2015

Berichterstatter

Prof. Dr. Jürgen Dohmen

Prof. Dr. Kay Hofmann

Tag der mündlichen Prüfung: 29 June 2015

“Science is the rational way of revealing the existing realities of nature”

My Grandfather

Abstract

Protein degradation mediated by the 26S proteasome is fundamental for cell survival in eukaryotes. There are two known routes for substrate presentation to the 26S proteasome- the ubiquitin-dependent route and the ubiquitin-independent route. Ornithine decarboxylase (ODC) is one of the most well-known ubiquitin-independent substrates of the proteasome. It is a homodimeric protein functioning as a rate-limiting enzyme in polyamine biosynthesis. Polyamines regulate ODC levels by a feedback mechanism mediated by the ODC regulator called antizyme. Higher cellular polyamine levels promote translation of antizyme mRNA and inhibit ubiquitin-dependent proteasomal degradation of the antizyme protein. Antizyme binds ODC monomers and targets them to the proteasome without ubiquitylation. The mechanism of this ubiquitin-independent proteasomal degradation is poorly understood. Therefore, the major aim of this study was to investigate the mechanism of ubiquitin-independent degradation of the ODC by the 26S proteasome. We show that polyamines, besides their role in regulating antizyme synthesis and stability, directly enhance antizyme-mediated ODC degradation by the 26S proteasome. Polyamines specifically enhanced the degradation of ODC by the proteasome both *in vivo* in yeast cells and in a reconstituted *in vitro* system. ODC is shown to be targeted in a manner quite distinct from ubiquitin-dependent substrates as its degradation was enhanced in a mutant lacking multiple ubiquitin receptors. These and other findings indicate, however, that there is a convergence point for the two routes of degradation because ubiquitin-dependent substrates compete with ODC for degradation. Using an *in vitro* assay, it could be shown that the unstructured N-terminal degron, ODS, is essential for binding of ODC to the proteasome. *In vivo* studies using proteasomal ATPase mutants, in which tyrosine residues in so-called pore loops were mutated to alanine (Y-A), further showed that the pore loops of Rpt4 and Rpt5 are of critical importance for ODC degradation and suggested that ODS might be recognized by these ATPase subunits. Additional experiments revealed that antizyme promotes ODC degradation most likely by providing an additional binding site. An ODS-antizyme-Ura3 fusion protein was degraded faster in a ubiquitin-independent but proteasome-dependent manner than ODS-Ura3. Furthermore, a ubiquitin-dependent mode of ODC degradation is also reported. Upon overexpression under the P_{CUP1} promoter, efficient degradation of ODC involved a ubiquitin-dependent mechanism. This degradation of ODC was independent of ODS and antizyme. Together, the findings described in this thesis provide novel insights into the mechanism of proteolytic regulation of ODC. With ODC being a validated target for cancer therapy, a detailed understanding of this mechanism may contribute to the discovery of new therapies targeting the polyamine pathway.

Zusammenfassung

Proteinabbau durch das 26S-Proteasom ist von fundamentaler Bedeutung für das Überleben eukaryotischer Zellen. Substrate können dem Proteasom auf zwei Arten präsentiert warden, entweder Ubiquitin-abhängig oder Ubiquitin-unabhängig. Ornithine decarboxylase (ODC) ist das bekannteste Ubiquitin-unabhängige Substrat des Proteasoms. Es ist ein homodimeres Protein mit einer geschwindigkeitsbestimmenden Funktion in der Biosynthese von Polyaminen. Polyamine regulieren die ODC-Konzentration durch einen *Feedback*-Mechanismus, der durch das ODC-Regulatorprotein Antizym vermittelt wird. Höhere zelluläre Polyamin-Konzentrationen stimulieren die Translation von Antizym-mRNA und hemmen den Ubiquitin-abhängigen Abbau des Antizym-Proteins. Antizym bindet an ODC-Monomere und vermittelt deren Ubiquitin-unabhängigen Abbau durch das Proteasom. Der Mechanismus des Ubiquitin-unabhängigen Proteinabbaus durch das Proteasom ist noch nicht gut verstanden. Das Hauptziel dieser Arbeit war es daher, den Mechanismus des Abbaus der ODC näher zu untersuchen. Es konnte gezeigt warden, dass Polyamine, neben ihrer Rolle in der Regulation der Synthese und Stabilität von Antizyme, einen direkt verstärkenden Effekt auf den Antizym-vermittelten Abbau der ODC durch das 26S-Proteasom sowohl *in vivo* in Hefezellen als auch in einem rekonstituierten *In vitro*-System hat. ODC wird auf eine andere Art und Weise vom Proteasom erkannt als Ubiquitin-abhängige Substratproteine, wie der verstärkte Abbau der ODC in Hefemutanten mit fehlenden Ubiquitin-Rezeptoren zeigte. Diese und andere Ergebnisse deuteten an, dass ODC und Ubiquitin-abhängige Substrate aber auch an einem bestimmten Punkt zusammenkommen, da diese Substrate um den Abbau durch das Proteasom konkurrieren. Durch *In vitro*-Bindungsstudien konnte gezeigt werden, dass das unstrukturierte N-terminale Abbaussignal (ODS) für die Bindung der ODC an das Proteasom essentiell ist. *In vivo*-Experimente mit Hefemutanten, in denen kritische Tyrosinreste in den so genannten *Pore Loops* der ATPase-Untereinheiten zu Alanin mutiert sind, zeigten das diese *Loops* der Untereinheiten Rpt4 und Rpt5 für den Abbau der ODC von kritischer Bedeutung sind, vermutlich indem sie das ODS erkennen. Weitere Experimente erbrachten Hinweise darauf, dass Antizym wahrscheinlich den Abbau der ODC fördert, indem es eine zusätzliche Bindestelle für das Proteasom beisteuert. So wurde beobachtet, dass ein ODS-Antizym-Ura3-Fusionsprotein schneller Ubiquitin-unabhängig abgebaut wurde als ODS-Ura3. Neben dem zuvor genannten Mechanismus wurde auch ein Ubiquitin-vermittelter Abbau der ODC beobachtet, wenn diese in stärkerem Maße in den Zellen synthetisiert wurde. Dieser Abbau erwies sich als unabhängig von ODS und Antizym. Die Ergebnisse dieser Arbeit eröffnene neue Einblicke in die Mechanismen der proteolytischen Kontrolle der ODC. Da ODC bereits als Zielstruktur von Krebstherapien validiert ist, kann ein detaillierteres Verständnis dieser

regulatorischen Mechanismen zur Entwicklung neuer Therapien beitragen, die einer häufig mit der Zellentartung einhergehenden Erhöhung der Polyaminsynthese entgegen wirken.

Table of Contents

1. Introduction

1.1. Proteolysis in eukaryotes

About 70 years ago, it was widely accepted that proteins were stable constituents in living cells (Ciechanover, 2012). After years of pioneering research we now know that protein degradation plays a pivotal role in the maintenance of all cells. Abnormal and unwanted proteins are timely eliminated by the cellular machinery. Proteins are broken down into its constituent amino acids which are then utilized for new protein synthesis. Proteolysis in eukaryotes is carried out via two known systems– lysosome-dependent macroautophagy (autophagy) and ubiquitin-proteasome system (UPS). Lysosomes are organelles that contain an array of enzymes which degrade proteins as well as cellular organelles through the mechanism of autophagy. Alternatively, proteasomal degradation of proteins is achieved by conjugation of target proteins with a post-translational polyubiquitin modification and their subsequent degradation by a barrel shaped complex called the 26S proteasome (Lilienbaum, 2013). Until recently, the two mechanisms were thought to be independent of each other. However, recent studies suggest a cross-talk between them. Impairment of UPS has been shown to induce autophagy (Pandey et al., 2007) and the inhibition of autophagy led to an induction of proteasome activity by up-regulation of proteasomal subunits (Wang et al., 2013). The principles of proteasome-mediated degradation are described in sections below.

1.1.1. The 26S proteasome

During the late 70s, Hershko, Ciechanover and Rose characterized a non-lysosomal energy requiring proteolytic system now known as the ubiquitin-proteasome system (Ciechanover, 2012). A decade later, Hough et al. partially purified the protease responsible for such an ATP-dependent degradation of ubiquitin-conjugated proteins which later came to be known as the 26S proteasome (Hough et al., 1986). Since then, decades of intensive research have increased our understanding of the structure and function of the proteasome. The proteasome is now a validated target for cancer therapies (Almond and Cohen, 2002). In May 2003, Bortezomib, a proteasome inhibitor was approved by the US FDA as a treatment for multiple myeloma.

The 26S proteasome is a ~2.5 MDa multi-subunit degradation machinery which selectively degrades 80-90% of cellular proteins (Lilienbaum, 2013). It consists of two major subcomplexes, the 20S core particle (20S or CP) and the 19S regulatory particle (19S or RP) (Fig. 1A). The crystal structure of the yeast 20S proteasome

revealed that it is composed of four stacked heptametrical rings arranged as an (α1-α7, β1- β7)$_2$ complex. The α-ring consists of seven subunits which are predominantly structural components of the 20S whereas the β-ring houses the catalytic domains of the proteasome. Out of the seven subunits of the β-ring, the β1, β2 and β5 subunits harbor the proteolytic active sites (Tomko and Hochstrasser, 2013).

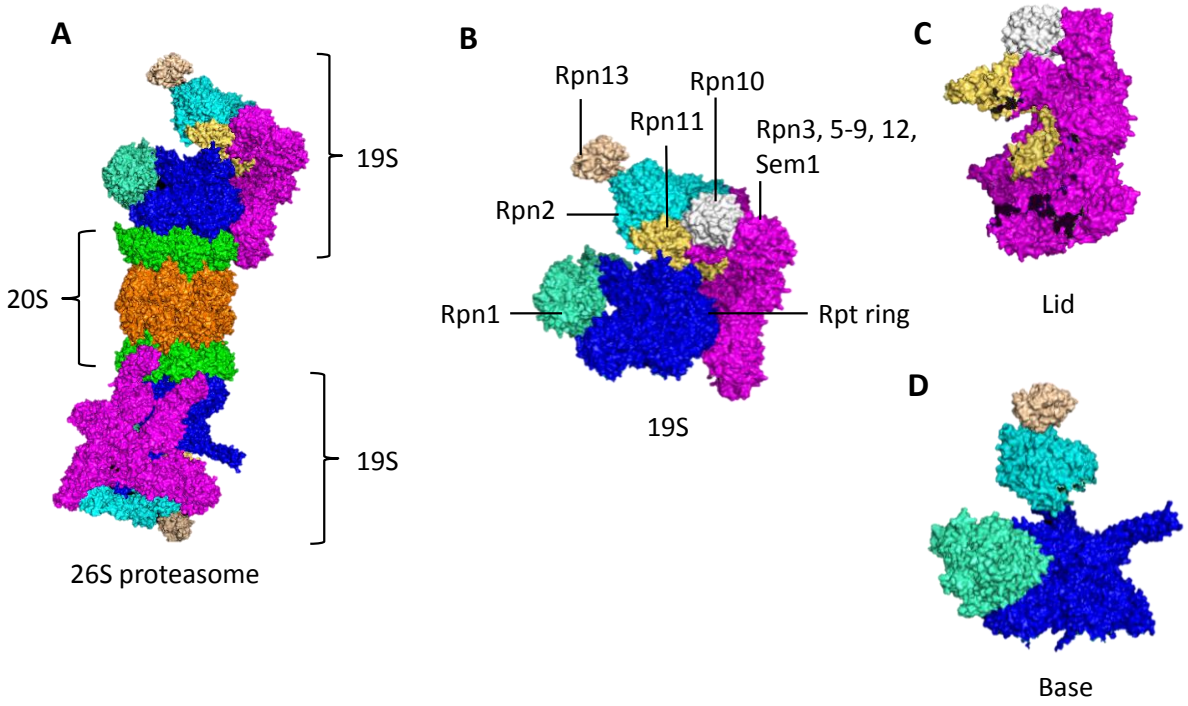

Fig.1: Structure of the 26S proteasome. (A) Surface representation of the 26S proteasome structure with the 20S core particle capped on both sides by the 19S regulatory particles (RP). **(B)** Surface representation of the 19S RP structure showing the relative positions of the subunits of the lid and base subcomplexes. **(C)** Surface representation of the lid subcomplex. **(D)** Surface representation of the base subcomplex. All structural representations were obtained using the PDB structures 4CR and 1RYP and viewed using the 3D molecular visualization software PyMOL™.

The 19S RP (Fig. 1B) caps the CP, thereby regulating substrate entry into the CP. It does so by harbouring receptors for ubiquitin binding, detaching ubiquitin tags, opening the 20S CP gate, as well as by unfolding and translocating the substrate into the CP. Under certain *in vitro* conditions, the RP was shown to dissociate into two subcomplexes, the base and the lid (Michael H. Glickman, 1999). The base consists of a heterohexameric AAA+ ATPase ring (consisting of the subunits, Rpt1-Rpt6) and three non-ATPase subunits, namely Rpn1, Rpn2 and Rpn13 (Fig. 1B and 1D). The major functions of the base are 20S gate opening and substrate unfolding and

translocation into the 20S. The unfolded substrates are then threaded through the narrow 20S pore by using the chemical energy from ATP hydrolysis. The Rpn1 and 2 are the largest subunits of the proteasome. Rpn1 serves as the docking sites of extrinsic ubiquitin receptors such as Rad23, Dsk2 and Ddi1. Rpn1 and 2 are hypothesised to serve as a loading platform for incoming substrates. Apart from these, the Rpn13 functions as a ubiquitin receptor. The RP lid consists of 9 Rpn subunits-Rpn3, 5-9, 11, 12 and Sem1 (Fig. 1B and 1C). The lid is essential for the degradation of ubiquitylated substrates. Rpn11 functions as the deubiquitylating enzyme (DUB). Rpn10 is an intrinsic ubiquitin receptor (Forster et al., 2009; Nickell et al., 2009; Tomko and Hochstrasser, 2013; Walz et al., 1998).

It took more than a decade after the solving of the crystal structure of the 20S CP to resolve the structure of the 19S RP. An atomic structure of the latter by crystallography could not be achieved mainly because of its dynamic nature. In 2012, two laboratories independently published subnanometer CryoEM structures of the yeast 19S RP (Beck et al., 2012; Lander et al., 2012). This was achieved using various techniques combined with CryoEM, including a novel approach for heterologous co-expression in *E.coli*, antibody and GST-fusion labelling and the use of deletion mutants. Interestingly, the lid subcomplex was found to be attached to the side of the 19S RP, which contrasted with previous ideas (Fig. 1B and 1C). The Rpt subunits of the base (marked as Rpt ring in Fig. 1B) were shown to be arranged in a spiral staircase, and the pore of the Rpt ring does not align with the pore of the 20S. The ubiquitin receptors, Rpn10 and Rpn13, are flexibly attached to the periphery of the RP. The Rpn11 deubiquitylase subunit is positioned directly above the entrance of the pore of the Rpt ring. Rpn1 is very closely associated with the ATPase ring, whereas Rpn2 is placed distally along the long axis of the proteasome and a part of it is positioned above the pore of the Rpt ring (Fig. 1B and 1D).

In a recent review, Inobe and Matouschek have described three different modes of substrate recognition by the proteasome: (1) ubiquitin-dependent, (2) adaptor-mediated, and (3) ubiquitin-independent. The first two modes depend on ubiquitin-tagging of the substrate for proteasome recognition whereas the third one is independent of ubiquitin-tagging. In all three modes of proteasome recognition, a common principle is the engagement of an unstructured domain in the substrate by the ATPase ring to initiate degradation (Inobe and Matouschek, 2014). The modes of proteasomal targeting are detailed in the subsections below.

1.1.2. Ubiquitin-dependent proteasomal targeting

There are a growing number of proteins whose cellular function is regulated by their timely elimination by the ubiquitin-proteasome system (UPS). The UPS is known to be involved in many vital cellular processes ranging from DNA repair, cell cycle regulation, and cell migration to immune responses (Melvin et al., 2013). On the clinical side, therapies targeting the UPS are underway for several diseases. Two drugs, Bortezomib and Carfilzomib, both proteasome inhibitors, are already in the clinic as a treatment for multiple myeloma (Melvin et al., 2013). It is therefore critical to further understand the details of the mechanisms of protein degradation by the UPS.

The ubiquitin-dependent substrate targeting and recognition is the more extensively studied route of proteasome targeting. It involves a series of enzymatic reactions wherein ubiquitin, a 8.5 KDa protein modifier, is conjugated to a target protein as detailed in Fig. 2. In *Saccharomyces cerevisiae*, there is only one known E1 enzyme encoded by *UBA1*, 11 known E2s and 42 different E3s. (Lee et al., 2008; McGrath et al., 1991). In most cases, ubiquitin conjugation takes place via a peptide bond formed between the Gly76 of ubiquitin and a lysine residue in the substrate. Polyubiquitin chains are formed by attaching another ubiquitin to a lysine residue (e.g. Lys48) of the preceding ubiquitin (Glickman and Ciechanover, 2002). This process is reversible as cells also contain deubiquitylating enzymes (DUBs) which remove the ubiquitin chains from substrates (Komander et al., 2009).

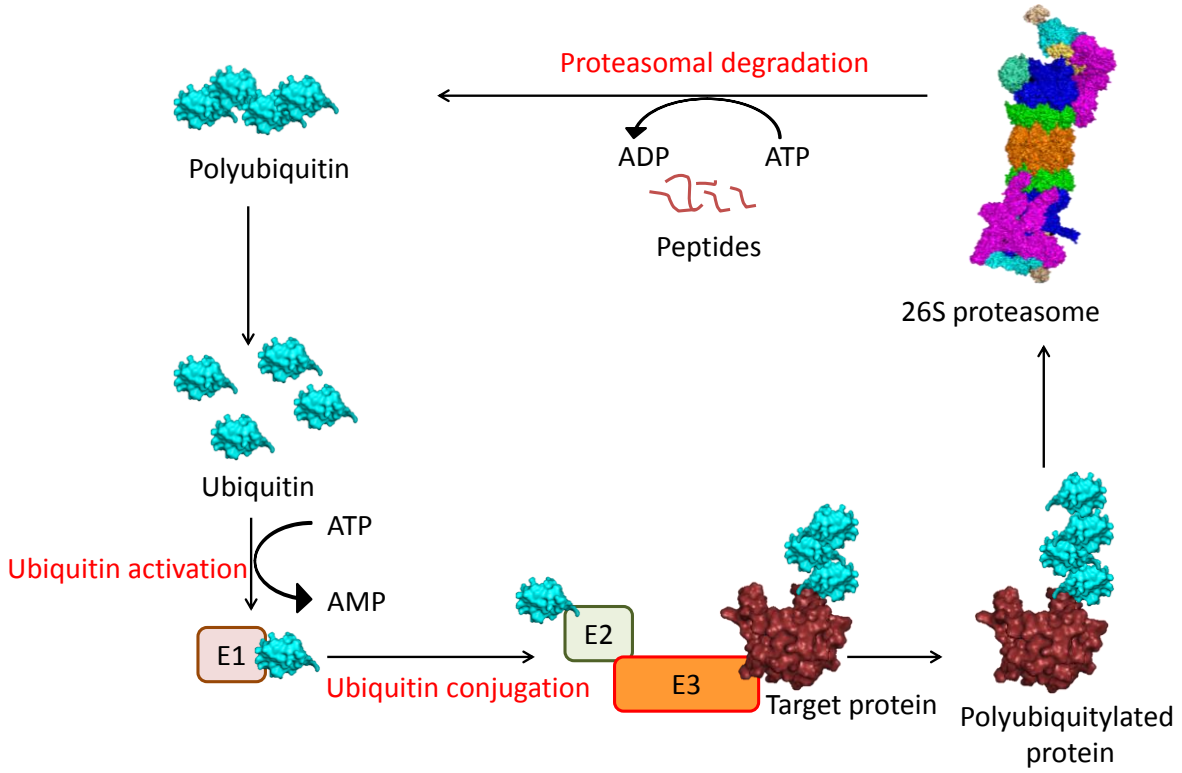

Fig. 2: The ubiquitin-proteasome system. Shown are the steps involved in the ubiquitin-dependent degradation of a target protein. Individual ubiquitin moieties are activated in an ATP dependent manner by the E1 ubiquitin-activating enzyme. The ubiquitin is then transferred to an E2, ubiquitin-conjugating enzyme. Subsequently, the activated ubiquitin-loaded E2 interacts with a specific E3, which are protein ligases directly in contact with a substrate. Ubiquitin is then covalently attached to one or more lysines within the target protein. Polyubiquitylation is achieved by attaching additional ubiquitins to the initial ubiquitin via one of its seven lysines. The polyubiquitylated substrate is then recognised by the shuttle factors or intrinsic ubiquitin receptors in the 19S RP. The ubiquitin chain is cleaved off from the substrate by the deubiquitylase, Rpn11 and recycled. The substrate is unfolded by the Rpt1-6 ATPases and translocated into the CP for degradation.

Recently, a more detailed understanding of the ubiquitin-dependent substrate targeting to the proteasome has emerged. The various steps involved in this process are detailed in Fig. 3. Apart from the ubiquitin tag, an unstructured region in the substrate is required for efficient proteasomal degradation (Prakash et al., 2004). Recent CryoEM structure of an actively translocating 26S proteasome shows that this unstructured initiation region makes contact with the N-ring (the ring formed by the N-terminal domains of the ATPases) once the substrate is tethered to the proteasome via a ubiquitin receptor. Furthermore, the active site of the Rpn11 deubiquitylase is masked to prevent premature deubiquitylation. Upon substrate

engagement by the Rpt ring, the proteasome undergoes structural changes. As a result, a continuous central channel to the 20S core is formed for substrate degradation. The Rpn11 active site is unmasked as it shifts to a position directly above the N-ring thereby scanning and removing ubiquitin chains from the translocating polypeptide.

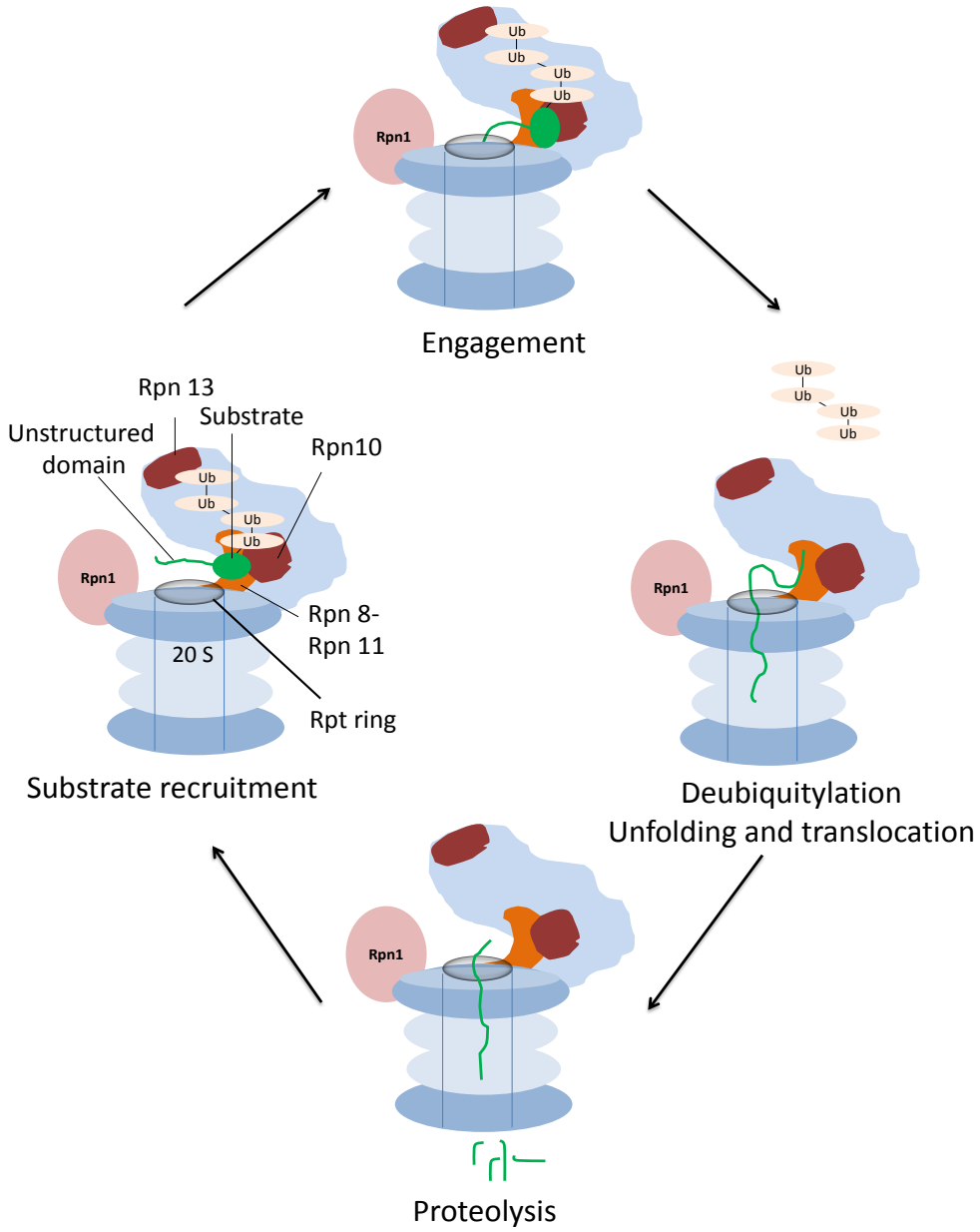

Fig. 3: Proteasomal degradation of a ubiquitylated substrate. Upon substrate recognition through polyubiquitin binding to the receptors Rpn13 and Rpn10, the Rpt ring of the proteasome initiates degradation at an unstructured region in the substrate. Structural rearrangements upon successful engagement lead to unfolding and translocation of the substrate to the 20S CP as well as cleavage of the ubiquitin tag. The substrate is completely unfolded and cleaved into peptides. Adapted from (Bhattacharyya et al., 2014).

1.1.3. Ubiquitin-independent proteasomal targeting

Most of the known proteasomal substrates require ubiquitylation for their degradation. However, there are a significant number of proteins the degradation of which does not require ubiquitin conjugation. This mode of degradation is hypothesised to be a remnant of the ubiquitin-free degradation observed in the archaea and bacteria (Erales and Coffino, 2013; Inobe and Matouschek, 2014). Such substrates are characterized by observing their proteasomal degradation when ubiquitylation is impaired either by inactivating the ubiquitin-activating enzymes or by mutating all receptor lysines on the protein (Jariel-Encontre et al., 2008). The mechanism of such a ubiquitin-independent proteasomal targeting still remains unclear. However, it has been speculated that presence of an unstructured domain in these proteins is sufficient for proteasome association (Inobe and Matouschek, 2014). Based on biochemical analyses of mammalian lysates, Baugh et al. have reported that more than 20% of cellular proteins are regulated by degradation in an ubiquitin-independent manner by both the 20S and 26S proteasomal species (Baugh et al., 2009). Using *in vitro* experiments, it was shown that oxidatively damaged proteins can be degraded by the 20S proteasome, independent of ubiquitin (Davies, 2001). Ornithine decarboxylase (ODC), Rpn4 and thymidylate synthase are examples of ubiquitin-independent substrates, degradation of which is strictly ATP-dependent and therefore requires the 26S proteasome (Erales and Coffino, 2013). Taken together, these observations bring us to two different modes of ubiquitin-independent proteasomal degradation, one that is ATP-dependent mediated solely by the 26S proteasome and another ATP-independent one mediated mainly by the 20S proteasome. This thesis deals with the former mode of ubiquitin-independent proteasomal degradation in particular with the ubiquitin-independent degradation of ornithine decarboxylase (ODC) in yeast.

ODC is the best-studied ubiquitin-independent substrate. It is conserved from yeast to humans (Palanimurugan et al., 2014). In 1989, Bercovich et al. observed that the degradation of ODC occurs in a ubiquitin-independent but ATP-dependent manner in reticulocyte lysates (Bercovich et al., 1989) which was later shown to occur *in vivo* in mammalian cells as well (Rosenberghasson et al., 1989). Since then several laboratories have tried to further understand this mechanism of ubiquitin-independent degradation of ODC. However, this mechanism is still not fully understand and is therefore a major focus of this thesis.

1.2. Feedback regulation of polyamines in eukaryotes

ODC is the rate-limiting enzyme in the biosynthesis of a class of molecules called polyamines. The current understanding of the feedback regulation of polyamines involving ODC and other players is described in subsections below.

1.2.1. Polyamine types and their biosynthesis

Polyamines are ubiquitous polycations essential for cell survival. Polyamines play multiple roles in the cell and are involved in almost all cellular processes. These include DNA replication, apoptosis, transcription, translation and membrane stability (Palanimurugan et al., 2014). Spermidine and spermine derived from the diamine precursor putrescine are the major polyamines in the cell (Fig. 4). Spermidine is formed from putrescine and spermine from spermidine by the addition of an aminopropyl group (Wallace, 2009).

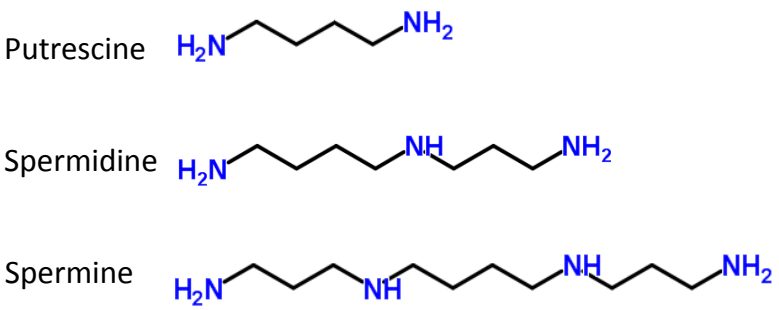

Fig. 4: Polyamine types and their structure.

Biosynthesis of polyamines in *S. cerevisiae* is outlined in Fig. 5. The polyamine biosynthetic pathway and it regulation is highly conserved from yeast to humans. Therefore, *S. cerevisiae* serves as a useful model organism to delve deeper into the regulatory mechanisms of this pathway.

Polyamines are regulated not only at the level of their biosynthesis but also at their catabolism and transport. Acetylated polyamines are either exported from the cell or subjected to oxidation by polyamine oxidase (Fms1 in yeast; shown in Fig. 5). In mammals, oxidation of N-acetylspermine and N-acetylspermidine produces spermidine or putrescine respectively, along with 3-aceto-aminopropanal and hydrogen peroxide (H_2O_2) (Palanimurugan et al., 2014). In mammals, the spermidine/spermine N1-acetyltransferase (SSAT) is a well-characterized enzyme in polyamine catabolism (Casero and Pegg, 1993). Liu et al. have recently

characterized a yeast gene that encodes a polyamine acetyltransferase called Paa1. All polyamine types were shown to be acetylated by Paa1 *in vitro* (Liu et al., 2005).

The polyamine biosynthetic pathway is an established chemopreventive and chemotherapeutic target (Nowotarski et al., 2013). The major reasons as summarized by Wallace are (1) polyamines are essential for cell growth (2) elevated polyamine levels are observed in cancer cells (3) ODC is designated as an oncogene as its levels are also elevated in cancer cells (4) inhibition of polyamine biosynthesis inhibits cell growth (Wallace, 2009).

Numerous tumour types have been associated with altered polyamine levels. These include breast, colon, prostrate and skin cancers. The ODC inhibitor 2-difluoromethylornithine (DFMO)/eflornithine was once a promising candidate for chemotherapy although later the clinical trials did not validate its effectiveness (Nowotarski et al., 2013). However in recent clinical trials, DFMO showed promise as a chemopreventive agent. For example, recent phase II clinical trials for prostate cancer have shown that the ODC inhibitor difluoromethylornithine (DFMO) reduced prostate polyamine levels in patients at risk for invasive prostate cancer (Meyskens et al., 2014). AdoMetDC and polyamine oxidases are also potential targets for therapy. Methylglyoxal bis(guanylhydrazone) (MGBG) and 4-Amidoinoindan-1-one-2'-amidinhydrazone (SAM486A) are inhibitors of AdoMetDC. N,N1-Bis(2,3-butadienyl)-1,4-butanediamine (MDL 72527) is an inhibitor of polyamine oxidases (Nowotarski et al., 2013). An alternative approach for inhibiting the polyamine pathway is by using polyamine analogues (Porter and Bergeron, 1988). Polyamine analogues like BENSpm can be easily taken in by the cell using the polyamine transport pathway thereby inhibiting polyamine biosynthesis and increasing polyamine catabolism. For example BENSpm downregulates ODC and AdoMetDC while inducing SSAT and SMO (spermine oxidase) (Nowotarski et al., 2013).

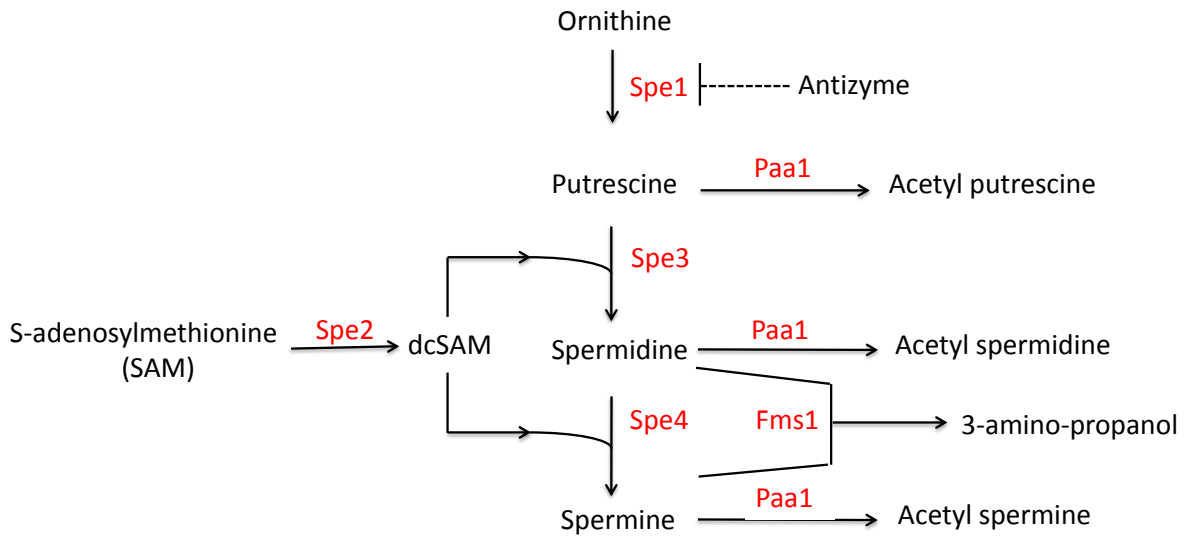

Fig. 5: Biosynthesis of polyamines in yeast. Ornithine, the precursor for polyamine biosynthesis is decarboxylated to the diamine putrescine by Spe1/ODC (Ornithine decarboxylase). Putrescine is then converted to the triamine spermidine by Spe3 (Spermidine synthase) and subsequently to the tetraamine spermine by Spe4 (Spermine synthase). The aminopropyl moieties for spermidine and spermine synthesis come from decarboxylated S-adenosylmethionine (dc-SAM) upon decarboxylation of s-adenosylmethionine (SAM) by Spe2 (SAM decarboxylase). Spermine can be converted back to spermidine by Fms1 (Polyamine oxidase). The polyamines can be converted to several acetylated forms by the enzyme Paa1 (Polyamine acetyltransferase). Adapted from (Rato et al., 2011).

1.2.2. Regulation of ODC by antizyme

Due to their myriad roles in the cell, polyamines are subjected to tight regulation. Polyamines regulate their biosynthetic enzymes through feedback control. This is mainly accomplished by controlling ODC levels in the cell (Igarashi and Kashiwagi, 2010). In mammals, ODC levels are regulated at the level of transcription, translation as well as degradation. *Odc* gene promoter contains elements responsive to hormones and growth factors. ODC is also a target of the oncogene c-*myc*. ODC mRNA has a long 5´-untranslated region (UTR) which contributes to its translational regulation. High levels of the translation initiation factor, eIF-4E, therefore enhances the translation of ODC mRNA, which is suggested to be involved in malignant transformation. The ODC 5´-UTR also contains an upstream open reading frame (uORF) that has been shown to regulate ODC translation *in vitro* (Pegg, 2006; Perez-Leal and Merali, 2012).

ODC is one of the most short-lived enzymes in eukaryotic cells with a half-life estimated between 10 and 60 min in mammals (Persson, 2009). This rapid turnover is mediated by the 26S proteasome in a ubiquitin-independent manner. Fig. 6 depicts

an overview of the post-translational regulation of ODC by polyamines. ODC degradation is regulated through the synthesis of a regulatory protein called ODC antizyme (Kahana, 2009). In mammals four different ODC inhibiting antizyme isoforms are known. Among these, the most predominant is antizyme-1 which has a wide tissue distribution. Though expressed at lower levels, antizyme-2 is similar to antizyme-1 and promotes ODC degradation *in vivo*. Antizyme-3 is a testis specific protein, which is restricted to a late stage in spermatogenesis. It however does not target ODC for degradation. There is also an antizyme-4 but it is not very well characterized (Olsen and Zetter, 2011). In yeast, however, only one isoform is known that is encoded by *OAZ1* (Palanimurugan et al., 2004). Antizyme levels are also strictly regulated by cellular polyamines. It occurs at the level of translation of antizyme mRNA as well as at its degradation, which is inhibited in response to increased cellular polyamine levels (Palanimurugan et al., 2004). The translational control of antizyme takes place via a conserved mechanism of +1 ribosomal frameshifting (Matsufuji et al., 1995; Palanimurugan et al., 2004). Antizyme mRNA is unique as it has a stop codon in its reading frame. For synthesis of full length protein, the ribosome has to skip the inner stop codon and continue till it reaches the stop codon at the end of the mRNA. This process is regulated by cellular polyamine levels, the mechanism for which remained elusive for a long time. Recent studies from our laboratory have shown that polyamine binding to a PRE (polyamine responsive element) on the nascent antizyme polypeptide is the key that regulates antizyme translation. At low cellular polyamine concentrations, ribosomes that undergo +1 ribosomal frameshifting within a polysome on antizyme mRNA, stall close to the end of the coding sequence thereby preventing completion of translation. When polyamine levels rise, the binding of polyamines to the PRE deregulates the inhibition resulting in the release of full length antizyme polypeptide. Although this study was carried out in yeast, there is an indication that this is a conserved phenomenon as they also showed that polyamines bind human antizyme *in vitro* (Kurian et al., 2011). The second level of antizyme regulation is by its ubiquitin-dependent proteasomal degradation. High polyamine levels stabilize antizyme by preventing its degradation, the mechanism of which is not yet fully understood (Palanimurugan et al., 2004).

In mammals, antizyme is also regulated by a ODC-like protein called antizyme inhibitor. Unlike ODC, under physiological conditions antizyme inhibitor is a monomer and therefore binds antizyme with an affinity greater than ODC. This interaction inactivates antizyme thereby resulting in higher cellular polyamine concentrations by

synthesis and uptake. Antizyme inhibitor is rapidly degraded in a ubiquitin-independent manner. To date, two different isoforms of antizyme inhibitor are known -antizyme inhibitor-1 and antizyme inhibitor-2 (Kahana, 2009; Olsen and Zetter, 2011).

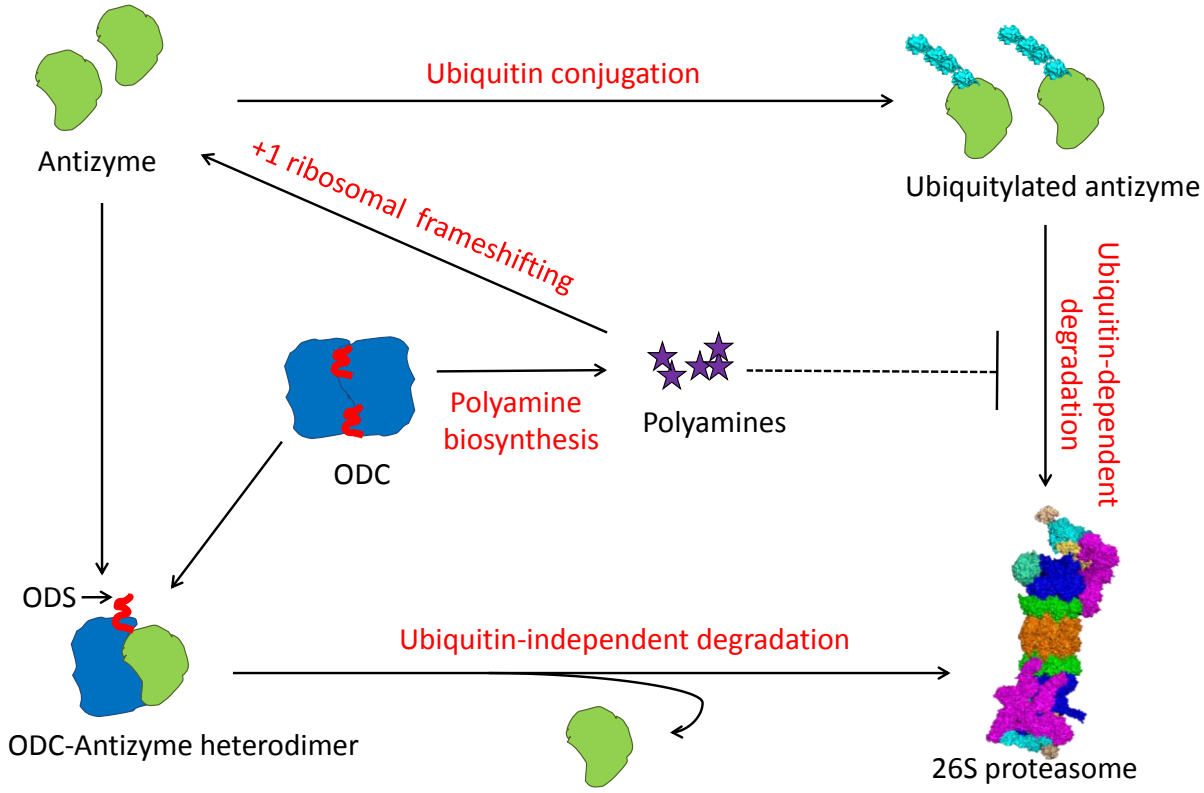

Fig. 6: Feedback regulation of polyamines in yeast. Shown here is an overview of the feedback regulation of cellular polyamines via ODC and antizyme. Following high cellular polyamine levels, antizyme synthesis is augmented via a unique +1 ribosomal frameshifting of antizyme mRNA. Antizyme forms heterodimers with ODC monomers resulting in the exposition of an N-terminal unstructured domain in ODC termed ODS (ODC degradation signal). ODC is subsequently targeted to the 26S proteasome in a ubiquitin-independent manner whereas the antizyme is recycled. Moreover, antizyme levels are controlled posttranslationally by its ubiquitiylation followed by proteasomal degradation. Polyamines inhibit this ubiquitin-dependent degradation of antizyme.

1.2.3. ODC degradation: the story so far

ODC is a 52 KDa protein functional only in its homodimeric form. The ODC monomer exists in equilibrium with the homodimer (Coleman et al., 1994). Antizyme binds to ODC monomers and facilitates their ubiquitin-independent degradation by the 26S proteasome. A 37 amino acid C-terminal region of mouse ODC (termed cODC) was found to be essential for its degradation. cODC was later confirmed as the degron by sequence comparison of mODC with ODC from *Trypanosoma brucei* (TbODC) which

lacks cODC and is therefore a stable protein in mammalian cells. cODC functioned as a transplantable degron as it mediated ubiquitin-independent degradation of TbODC once transplanted. Antizyme is not essential for the turnover of mODC but it greatly enhances it. Antizyme binding is thought to expose the cODC which is otherwise buried in the ODC homodimer. However, it remains unclear whether antizyme plays a further role in mODC degradation (Erales and Coffino, 2013). In *S. cerevisiae*, however, antizyme is essential for the degradation of ODC (Palanimurugan et al., 2004). The yODC (yeast ODC) degron is a ~45 residue N-terminal unstructured domain called ODC Degradation Signal (ODS) which is exposed upon antizyme binding. This degron is both transplantable and replaceable. However, the transplantable nature of the degron depends on the structural context of the receptor protein. An alpha helical domain succeeding the unstructured domain was found to be a contributing factor in degradation (Godderz et al., 2011; Li and Coffino, 1993).

1.3. Other ubiquitin-independent substrates

There are only a handful of well-characterized ubiquitin-independent substrates. Apart from ODC, yeast Rpn4, a transcriptional regulator of proteasome genes, and mammalian thymidylate synthase (TS), an enzyme involved in the synthesis of DNA precursors are the other known substrates. Presence of an unstructured domain containing degron is the common feature among these substrates (Erales and Coffino, 2013). Rpn4 distinguishes itself from the other two as it is degraded via the ubiquitin-dependent as well as ubiquitin-independent modes (Ju and Xie, 2004). Like yeast ODC, the ubiquitin-independent degron of Rpn4 is at its N-terminus consisting of the first 80 residues. Recently, Ha et al. have reported that the N-terminal degron of Rpn4 interacts with the proteasomal subunits Rpn2, Rpn5 and Rpt1 by using a cross-linking label transfer technique (Ha et al., 2012). On the other hand, *in vivo* data from our laboratory showed that the proteasome lid is dispensable for ODC degradation (Godderz et al., 2011). Therefore, the mode of proteasomal reception of ubiquitin-independent substrates still remains to be elucidated. Similar to ODC and Rpn4, the degron of TS consists of an N-terminal unstructured domain spanning residues 1-28. Besides this degron, the presence of an N-terminal proline and the residues 9-15 was also critical for TS degradation. Another common feature with ODC was the α-helix following the degron which contributed to the efficiency of degradation (Pena et al., 2009).

Apart from these, there are substrates that are ubiquitylated but also degraded in a ubiquitin-independent manner. The mode of their degradation is still under debate. These comprise p21/Cip1, the TCRα subunit of the T cell receptor, IκBα, c-Jun and calmodulin (Hoyt and Coffino, 2004). p21 is a loosely folded protein that is ubiquitylated *in vivo*. However, a lysine-less variant of p21 is still unstable showing that its degradation does not completely rely on ubiquitylation (Sheaff et al., 2000). Later, p21 was shown to be polyubiquitylated at the free amino group of its N-terminal methionine which was shown to be sufficient for its degradation (Bloom et al., 2003). Therefore, the exact mode of degradation of p21 in mammalian cells still remains uncertain. It is possible that both pathways might be involved.

2. Aim of current study

Recent structural studies of the 19S regulatory particle have shed light on the mechanistic details of ubiquitin recognition and subsequent engagement of substrates by the proteasome. This model was based on the relative positions of ubiquitin receptors, the deubiquitylase Rpn11 and the ring formed by the 6 Rpts. (Beck et al., 2012; Lander et al., 2012) However, the ubiquitin-independent recognition of substrates is still poorly understood. This study is aimed at elucidating the mechanism of reception and engagement of ubiquitin-independent substrates by the proteasome. ODC is the primary ubiquitin-independent substrate studied in this thesis although other substrates such as p21 and artificial fusion proteins are also employed in comparative approaches. The major questions addressed in this thesis can be summarized as follows.

1. Do polyamines directly influence ODC degradation?
2. Does ODC bind the proteasome through its unstructured domain, ODS?
3. What are the receptors in the proteasome for ODS and other unstructured domains?
4. Does antizyme have a binding site on the proteasome?
5. Is there a ubiquitin-dependent component for ODC degradation?

3. Materials and Methods

3.1. Materials

3.1.1. *Saccharomyces cerevisiae* strains

Strain	Genotype	Lab stock	Source
JD47-13C	*MATa his3Δ200 leu2-3,112 lys2-801 trp1Δ63 ura3-52*	Sc. 188	(Ramos et al., 1998)
BY4741	*MAT*a *his3*Δ1 *leu2*Δ0 *met15*Δ0 *ura3*Δ0	Sc. 1195	Euroscarf
MO24	*MATa his3Δ200 leu2-3,112 lys2-801 trp1Δ63 ura3-52 pre1::PRE1-FLAG-6xHIS*	Sc. 3534	(Kock et al., 2015)
DG10	*MATa his3Δ1 leu2Δ0 met15Δ0 ura3Δ0 oaz1Δ::Kan-MX5*	Sc. 2583	Euroscarf
spe4-Δ	*MATa his3Δ1 leu2Δ0 met15Δ0 ura3Δ0 spe4Δ::Kan-MX5*	Sc. 1202	Euroscarf
paa1-Δ	*MATa his3Δ1 leu2Δ0 met15Δ0 ura3Δ0 paa1Δ::Kan-MX5*	Sc. 3188	Euroscarf
YGA40	*MATa his3Δ200 leu2-3,112 lys2-801 trp1Δ63 ura3-52 P_{GAL1} HSP82::Nat hsc82Δ::Kan-MX6 pdr5Δ::Hph*	Sc. 3112	(Kandasamy, 2014)
YGA95	*MATα his3Δ200 leu2-3,112 lys2-801 trp1Δ63 ura3-52 P_{GAL1}-HSP82::Nat hsc82Δ::Kan-MX6, pdr5Δ::Hph rpn10-UIM::Phe rpn13-KKD::Trp1 rad23Δ::His dsk2 Δ::Kan*	Sc. 3335	(Kandasamy, 2014)
YHI29/1	*MATα pre1-1 his3-11,15 leu2-3 ura3 Can^S*	Sc. 324	Lab collection
JD77-ts26	*MATa uba1Δ::HIS3 pRSts26-1(uba1-ts-26) leu2-3,112 lys2-801 ura3-52*	Sc. 440	Lab collection
JD59	*MATa ump1Δ::HIS3 his3Δ200 leu2-3,112 lys2-801 trp1Δ63 ura3-52*	Sc. 227	(Ramos et al., 1998)
YAH96	*MATα his3-Δ200 leu2-3,112 lys2-801 trp1-1 ura3-52 rpn11::RPN11-3xFLAG-HIS*	Sc. 3936	(Erales et al., 2012)
JE03	*MATα his3-Δ200 leu2-3,112 lys2-801 trp1-1 ura3-52 rpn11::RPN11-3xFLAG-HIS Rpt1::rpt1 (Y283A)*	Sc. 3937	(Erales et al., 2012)
MHY292	*MATα his3-Δ200 leu2-3,112 lys2-801 trp1-1 ura3-52 rpn11::RPN11-3xFLAG-HIS Rpt2::rpt2 (Y256A)*	Sc. 3938	(Erales et al., 2012)
RB18	*MATα his3-Δ200 leu2-3,112 lys2-801 trp1-1 ura3-52 rpn11::RPN11-3xFLAG-HIS Rpt3::rpt3 (Y246A)*	Sc. 3968	This study
MHY294	*MATα his3-Δ200 leu2-3,112 lys2-801 trp1-1 ura3-52 rpn11::RPN11-3xFLAG-HIS Rpt4::rpt4 (Y255A)*	Sc. 3940	(Erales et al., 2012)
MHY295	*MATα his3-Δ200 leu2-3,112 lys2-801 trp1-1 ura3-52 rpn11::RPN11-3xFLAG-HIS Rpt5::rpt5 (Y255A)*	Sc. 3941	(Erales et al., 2012)
RB19	*MATα his3-Δ200 leu2-3,112 lys2-801 trp1-1 ura3-52 rpn11::RPN11-3xFLAG-HIS Rpt6::rpt6 (Y222A)*	Sc. 3969	This study

AM33	*MATa pdr5Δ::KanMX5 his3Δ200 leu2-3,112 lys2-801 trp1Δ63 ura3-52*	Sc. 1954	Lab collection
RB4	*MATα his3Δ200 trp1Δ63 met15::Nat ura3Δ::Kan Leu2::P_{ODC}-ODC-LEU2::Hph Can::P_{OAZ1}-OAZ1-T_{OAZ1}*	Sc.3518	This Study
JN54	*MATa his3-11,15 leu2-3,112 lys2 trp1-Δ1 ura3-52*	Sc. 1032	(Nelson et al., 1992)
YMF15	*MATa ssa1-45 ssa2Δ::LEU2 ssa3Δ::URA3 ssa4::LYS2*	Sc. 1203	(Fröhlich, 2005)

3.1.2. *Escherichia coli* strains

Strain	Genotype	Source
XL1Blue	*F^- φ80 lacZΔM15 Δ(lacZYA-argF)U169 deoR recA1 endA1 hsdR17(rk^-, mk^+) phoAsupE44 thi-1 gyrA96 relA1 $λ^-$*	Lab collection
MC1061	*hsdR2 $hsdM^+$ $hsdS^+$ araD139 Δ(ara-leu)7697Δ(lac)X74 galE15 galK16 rpsL (Strr) mcrA mcrB1*	Lab collection
Rosetta™ 2(DE3) pLysS	*F^- ompT hsdSB(rB^- mB^-) gal dcm (DE3) pLysSRARE2 (Cam^R)*	Lab collection
BL21 codon	*F^- ompT gal dcm lon $hsdS_B$(r_B^- m_B^-) λ(DE3 [lacI lacUV5-T7gene 1 ind1 sam7 nin5])*	Lab collection

3.1.3. Plasmids

Name	Details	Lab stock	Source
YCplac33	CEN/URA3	Ec. 201	(Gietz and Sugino, 1988)
YCplac111	CEN/LEU2	Ec. 202	(Gietz and Sugino, 1988)
YCplac22	CEN/TRP1	Ec. 200	(Gietz and Sugino, 1988)
pPM323	P_{CUP1}-2xMyc-OAZ1-if-T_{CYC1}, CEN/URA3	Ec. 3842	(Kurian et al., 2011)
pDG240	pET11a-6His-OAZ1(codon optimised for *E.coli*)	Ec. 2770	(Kurian et al., 2011)
pDG246	pET11a-6His-$OAZ1_{L245A,L246A,K247A,W251A}$ (codon optimised for *E.coli*)	Ec. 2776	Lab collection
pRB11	pET11a-6His-OAZ1(codon optimised for *E.coli*)-pQE-ODC-2xHa	Ec. 3038	This study
pRB12	pET11a-6His-OAZ1(codon optimised for *E.coli*)-pQE-$ΔN_{47}$-ODC-2xHa	Ec. 3039	This study
pPM97	P_{ODC}-ODC-2xHa-T_{CYC1}, CEN/LEU2	Ec. 3089	(Godderz et al., 2011)
pMAF17	P_{CUP1}-Ub-R-Ha-eK-URA3-T_{CYC1}, CEN/LEU2	Ec. 2380	Lab collection

pMAF18	P_{CUP1}-Ub-V76-Ha-eK-URA3-T_{CYC1}, CEN/LEU2	Ec. 3665	Lab collection
pGEX-4T-2	GST	Ec. 2445	GE Healthcare
pDG241	pGEX4T-2-GST-OAZ1(codon optimized for *E.coli*)	Ec. 2771	Lab collection
pDG273	pET11a-ODC-FLAG	Ec. 2803	Lab collection
pRB24	pET11a-ODC-2xHa-6His	Ec. 3339	This study
pDG269	p_{CUP1}-hp21-2xHa-T_{CYC1}, CEN/URA3	Ec. 2799	Lab collection
pDG258	P_{ODC}-ODC_{1-42}-URA3-2xHa-T_{CYC1}, CEN/LEU2	Ec. 2788	(Godderz et al., 2011)
pDG268	P_{ODC}-URA3-2xHa-T_{CYC1}, CEN/LEU2	Ec. 2798	(Godderz et al., 2011)
pFS1	P_{ODC}-URA3-2xHa-T_{CYC1}, CEN/LEU2	Ec. 3551	(Stadelmayer, 2014)
pFS2	P_{ODC}- OAZ1-if $_{L245A,L246A,K247A,W251A}$ URA3-2xHa-T_{CYC1}, CEN/LEU2	Ec. 3552	(Stadelmayer, 2014)
pRB40	P_{ODC}- ODC_{1-47}OAZ1-if $_{L245A,L246A,K247A,W251A}$-$T_{CYC1}$, CEN/LEU2	Ec. 3553	This study
pRB41	P_{ODC}- ODC_{1-47}OAZ1-if $_{L245A,L246A,K247A,W251A}$-URA3-2xHa-$T_{CYC1}$, CEN/LEU2	Ec. 3577	This study
pRB45	P_{ODC}- ODC_{1-47}OAZ1-if $_{L245A,L246A,K247A,W251A}$-URA3-2xHa-$T_{CYC1}$, CEN/TRP1	Ec. 3649	This study
pJDRZ1	p_{GAL1}-Ub-R-LacZ, 2µ/HIS3	Ec. 3257	Lab collection
pPM96	p_{CUP1}- ODC-2xHa-T_{CYC1}, CEN/LEU2	Ec. 3088	(Rangasamy, 2005)
pPM106	p_{CUP1}-ΔN_{47}-ODC-2xHa-T_{CYC1}, CEN/LEU2	Ec. 3096	(Rangasamy, 2005)
pRB14	p_{CUP1}- ODC-T_{CYC1}, CEN/LEU2	Ec. 3193	This study
pRB15	p_{CUP1}-ΔN_{47}-ODC-T_{CYC1}, CEN/LEU2	Ec. 3194	This study
pMAF59	P_{CUP1}-Ub-R-e^K-DHFR-2xHa-T_{CYC1}, CEN/LEU2	Ec. 3451	Lab collection

3.1.4. Oligonucleotides

Name	Sequence	Description
RB4115	GAGGATCCATTAAAGAGGAGAAATTAACTATGTCTAGTACTCAAGTA	BamH1-SD (PQE)-ODC-FP
RB4116	CTGGATCCTACTAGTTGAGCTCTCTAGACTGCATAGTCAGGTACG	Ha-stop-Sac1-Spe1-BamH1-RP
RB4117	GAGGATCCATTAAAGAGGAGAAATTAACTATGAACCAAGATTTGGAA	BamH1-SD (PQE)-ΔODS-ODC-FP
RB4118	GGTTGGTGGCAAACTGAT	pRB11-sequencing-FP
RB4119	GATATAGTTCCTCCTTTCAGC	pRB11-sequencing-RP
RB4133	ACGAATTCATGTCTAGTACTCAAGTA	EcoR1-ODC-FP
RB4134	ACGAATTCATGAACCAAGATTTGGAA	EcoR1-dODS-ODC-FP

RB4135	TTGGATCCTCAATCGAGTTCAGAGTCTAT	ODC-stop-BamH1-RP
RB4343	GACGAGCTCATCGAGTTCAGAGTCTATGT	ODC-nostop-Sac1-RP
RB4623	CGCCTCGAGGCATTCAAACTCTAAAATAACAAAG	Xho1-nostop-OAZ1-RP
RB4688	GAAGAAAAGCCTGACGTTACTTA	RPT1-int-FP
RB4689	TCAATTATATTGCATATAACGCGA	RPT1-stop-RP
RB4690	GGTTTCGGTCATGAAAATGGATA	RPT2-int-FP
RB4691	TCACAAGTATAAACCTTCTAAATT	RPT2-stop-RP
RB4692	TGACGTCACTTATGCAGATGTTG	RPT3-int-FP
RB4693	TCATTTGTAGAAGTCGAATTTATC	RPT3-stop-RP
RB4694	GTATAATATGACCAGTTTTGAAC	RPT4-int-FP
RB4695	TCATAATTTTTGGTATTCTATAGT	RPT4-stop-RP
RB4696	GAATTTGATTCTCGTGTAAAAGC	RPT5-int-FP
RB4697	TTATGCATAAAAGGATACCGATTT	RPT5-stop-RP
RB4698	GACCCACTAGTTTCGTTGATGAT	RPT6-int-FP
RB4699	TCACTTGAACAGCTTGGCGACAGA	RPT6-stop-RP

3.1.5. Enzymes

Enzyme	**Supplier**
Alkaline Phosphatase	NEB
DnaseI	Roche
DreamTaq DNA Polymerase	Thermo Scientific
Lysozyme	Sigma
Phusion® High-Fidelity DNA Polymerase	NEB
Restriction Endonucleases	Thermo Scientific
T4-DNA Ligase	NEB
β-glucoronidase	Roche

3.1.6. Antibodies

Antibody	**Derived from**	**Supplier**
Anti-βeta2	Rabbit	Lab collection
Anti-Cdc11	Rabbit	Santa Cruz Biotechnology
Anti-GST	Rabbit	Santa Cruz Biotechnology
Anti-HA (16B12 clone)	Mouse	HISS Diagnostic
Anti-HA (3F10 clone)	Rat	Roche
Anti-HSP90	Rabbit	Lab collection
Anti-FLAG (M2 clone)	Mouse	Sigma
ANTI-FLAG® M2 Affinity Gel	Mouse	Sigma
Anti-MYC (9B11 clone)	Mouse	Cell Signaling Technology
Anti-Mouse, HRP	Goat	Sigma

Anti-Mouse, 680	Goat	Invitrogen
Anti-Oaz1	Rabbit	Lab collection
Anti-ODC	Rabbit	Lab collection
Anti-PGK	Mouse	Invitrogen
Anti-Rabbit, HRP	Donkey	GE Healthcare, UK
Anti-Rabbit, 800	Goat	Rockland
Anti-Rat, HRP	Goat	Abcam
Anti-Rpn5	Rabbit	Lab collection
Anti-Rpn11	Rabbit	Santa Cruz Biotechnology
Anti-RPT5	Rabbit	Abcam
Anti-TPI	Rabbit	Lab collection

3.1.7. Chemicals

Chemical	**Supplier**
Acetic Acid	Merck
N1-Acetylspermidine	Wako
N8-Acetylspermidine	Wako
Acrylamide	Roth
Adenine	Applichem
Adenosine triphosphate	Apllichem
Agarose	Sigma
Ammonium persulfate	Sigma
Ampicillin	Sigma
L-Arginine	Roth
Agar	MP Biomedicals
β-Mercaptoethanol	Sigma
Boc-LLR-AMC	Bachem
Bradford-Reagent	Bio-Rad
Bromophenol Blue	Serva
Calcium chloride ($CaCl_2$)	Acros
Chloramphenicol	Sigma
Complete protease inhibitors EDTA free	Roche
Coomassie Biliant Blue R-250	Merck
Copper (II) sulfate	Acros
Deoxyribonucleotides triphosphate (dNTPs)	Sigma
N1, N8-Diacetylspermidine	Wako
di-Sodiumhydrogenphosphate (Na_2HPO_4)	Roth
Dimethylformamid (DMSO)	Roth
Dithiothreitol (DTT)	AppliChem

Ethanol	VWR
Epoxomycin	Enzo life sciences
FLAG peptide	Sigma
5-Fluoroorotic acid (5-FOA)	Sigma
Formaldehyde	Riedel-de Haën
D(+) Galactose	VWR International
Geneticin disulfate (G418)	Sigma
Glas beads (*E. coli*) 0.10- 0.11mm	Satorius Stedium
Glass beads (yeast) 0.4- 0.6mm	Satorius Stedium
D(+) Glucose	Roth
Glutathione sepharose 4B	GE Healthcare
Glycerol	AppliChem
Glycine	Merck
L-Histidine	AppliChem
4-(2-hydroxyethyl)-1-piperazineethanesulfonic acid (HEPES)	Serva
Imidazole	Sigma
L-Isoleucine	Merck
Isopropanol	VWR
Isopropyl-β-D-thiogalactoside (IPTG)	Formedium
L-Leucine	AppliChem
Lithium acetate	Alfa Aesar
L-Lysine	Roth
LumiLight Western Blot Substrate	Roche
Magnesium chloride ($MgCl_2$)	Roth
m-Cresol purple sodium salt	Sigma
Methanol	Roth
L-Methionine	Merck
MG132	Sigma
Milk powder	Roth
Nourseothricin sulfate	Jena bioscience
Ni-sepharose	GE Healthcare
Polyethylene Glycol (PEG) [3350]	Sigma
Peptone	Formedium
L-Phenylalanine	Roth
Pierce ECL Plus Western blotting substrate	Thermo Scientific
Ponceau S solution	Sigma
Potassium acetate	Merck
Potassium chloride	Acros
Potassium dihydrogen phosphate	Roth

Sodium dodecyl sulfate (SDS)	VWR
Sodium azide	Sigma
Sodium carbonate	Sigma
Sodium chloride	AppliChem
Sodium hydroxide	Roth
Di-sodium hidroxyphosphate	Fluka
Sodium phosphate	Merck
Sodium thiosulphate	Sigma-Aldrich
Spermidine	Sigma
Spermine	Sigma
[3H]-Spermidine	PerkinElmer
Suc-LLVY-AMC	Bachem
N, N, N', N'-tetramethylethylenediamine (TEMED)	AppliChem
L-Threonine	Roth
Tris	Roth
Triton X-100	Sigma
L-Tryptophan	AppliChem
Tryptone	Formedium
TWEEN 20	Sigma
Uracil	Sigma
Urea	Usb
Yeast extract powder	Formedium
Yeast Nitrogen Base	Formedium

3.1.8. Instruments

Major Instruments	**Source**
Centrifuge Avanti J-20 XP, Optima TLX Ultracentrifuge 120,000-rpm, Allegra X-22R, Scintillation counter LS5000 TD	Beckman Coulter
Curix 60-System developer machine	Agfa
FLUOstar Galaxy Microplate Reader	BMG Labtech
Incubators	New Brunswick
Mini-gel gel electrophoresis, Blotting chamber	Bio-Rad
Mixer Mill MM400	Retsch
Odyssey Infrared imaging system LI-COR biosciences, USA	LI-COR
Thermocycler	Biometra
Refrigerated centrifuge 5417R, centrifuge 5415D, Thermomixer compact, BioSpectromoter	Eppendorf

3.2. Methods

3.2.1. Molecular biology and genetic techniques

3.2.1.1. Isolation of plasmid DNA from *E. coli*

E. coli cells harbouring the plasmid of interest were grown overnight (or a minimum of 7 hours) at 37°C with constant shaking in LB medium supplemented with the appropriate antibiotics (ampicillin at 70 µg/ml and chloramphenicol at 34 µg/ml). Cells were collected by centrifugation and plasmid DNA was isolated using E.Z.N.A.® Plasmid Mini Kit I (Omega Bio-Tek) according to manufacturer's instructions.

LB media	
Tryptone	1 %
Yeast extract	0.5 %
NaCl	1 %
Agar (for plates)	2 %

3.2.1.2. Estimation of DNA concentration

DNA concentration was measured using the preprogrammed method and Eppendorf µCuvette™ in an Eppendorf BioSpectrometer®.

3.2.1.3. Isolation of genomic DNA from yeast

Yeast cells were grown overnight at 30°C with constant shaking in 5 ml YPD medium. Cells were collected by centrifugation and genomic DNA was isolated using E.Z.N.A.® Yeast DNA Kit (Omega Bio-Tek) according to manufacturer's instructions.

3.2.1.4. PCR amplification

Polymerase chain reaction (PCR) amplification of DNA fragments for cloning was performed using the Phusion® High-Fidelity DNA Polymerase (NEB) according to manufacturer's instructions.

The PCR reaction mix was set up as follows.

Component	100 µL Reaction	Final Concentration
Ultra pure water (Milli-Q®)	to 100 µL	
5X Phusion HF or GC Buffer	20 µL	1X
10 mM dNTPs	2 µL	200 µM
100 µM Forward Primer	0.5 µL	0.5 µM
100 µM Reverse Primer	0.5 µL	0.5 µM
Template DNA		< 500 ng
Phusion DNA Polymerase	1 µL	2.0 units/100 µL Reaction

Thermocycling conditions:

Step		Temperature	Time
Initial denaturation		98°C	30 seconds
Denaturation	30X	98°C	10 seconds
Annealing		Tm-5	30 seconds
Extension		72°C	30 seconds/kb
Final extension		72°C	5-10 minutes
Hold		4°C	

PCR products were purified from the reaction mix using the High Pure PCR Product Purification Kit (Roche) as per manufacturer's instructions

Normal fidelity PCR reactions, were performed using the DreamTaq™ PCR master mix (Thermo Scientific) according to the following protocol. This PCR mix contains DreamTaq™ DNA polymerase, DreamTaq™ buffer, $MgCl_2$ and dNTPs.For colony PCR, the template was prepared by resuspending a small amount of cells (yeast or *E. coli*) in 1 µL of nuclease-free water and boiling it for 1 min.

The PCR reaction mix was set up as follows.

Component	100 µL Reaction	Final Concentration
Ultra pure water (Milli-Q®)	to 100 µL	
DreamTaq PCR Master Mix (2X)	50 µL	1X
100 µM Forward Primer	0.5 µL	0.5 µM
100 µM Reverse Primer	0.5 µL	0.5 µM
Template DNA		< 500 µg

Thermocycling conditions:

Step		Temperature	Time
Initial denaturation		95°C	5-10 min
Denaturation	30X	95°C	30 seconds
Annealing		Tm-5	30 seconds
Extension		72°C	1 minute/kb
Final extension		72°C	5-10 minutes
Hold		4°C	

3.2.1.5. Agarose gel electrophoresis

Agarose gel electrophoresis was performed to resolve and analyze DNA samples. Optimal separation results were obtained using 0.8-1 % (w/v) agarose gels in TAE buffer (40 mM Tris-Cl, 20 mM sodium acetate,1 mM EDTA). The DNA samples were mixed with 6X Gel Loading Dye, Purple without SDS (NEB). For visualization of the DNA fragments, 1.5 - 2 µL of SERVA DNA Stain G was added to 100 ml of agarose gel solution before casting. The bands were visualized under UV light. Appropriate DNA ladders (NEB) were loaded along with the samples for molecular weight estimation.

3.2.1.6. Extraction of DNA from agarose gels

Elution of DNA fragments from agarose gels was performed after cutting out the band of interest from the agarose gel and recovery using the High Pure PCR Product Purification Kit (Roche) as per manufacturer's instructions

3.2.1.7. Restriction digestion of DNA

Plasmid DNA and PCR products after purification were digested with sequence-specific endonucleases. 1 µL of FastDigest™ enzymes (Thermo Scientific) was used to cleave 1 µg of substrate DNA in a universal FastDigest buffer. The reaction was performed between 5-15 min according to the enzyme used as per manufacturer's instructions. If necessary, the digested DNA fragments were separated by agarose gel electrophoresis and purified as described above.

3.2.1.8. Ligation of DNA fragments

Ligation of DNA fragments was performed using T4 DNA Ligase (NEB) according to the following protocol. A vector: insert molar ratio of 1:4 was used.

Ligation mix	
Ultra pure water (Milli-Q®)	to 20 µL
10X T4 DNA Ligase Reaction Buffer	2 µL
T4 DNA Ligase (NEB)	1 µL
vector DNA	~ 40 ng
insert DNA	~ 30 ng

Ligation mix was incubated for either 1 hour at 22°C or overnight at 4°C prior to transformation of competent *E.coli* cells. 10 µL of the ligation mix was used for transformation.

3.2.1.9. Preparation of chemically competent *E.coli* cells

The desired *E. coli* strain was grown overnight at 37°C in 20 ml LB medium. Sub-culturing was done in 100 ml LB medium inoculated at OD600= 0.2 and grown till OD600= 0.6. This culture was then transferred to pre-cooled 50 ml tubes and centrifuged at 900x*g* for 10 min at 4°C. The supernatant was discarded and 25 ml ice-cold, sterile $CaCl_2$ was added to the pellet. The pellet was then gently re-suspended and incubated on ice for 20 min followed by centrifugation at 900x*g* for 10 min at 4°C. The supernatant was discarded and the pellet was re-suspended in 0.1 M $CaCl_2$ containing 15% ice-cold glycerol. This mixture was incubated on ice for 1 hour. The resulting competent *E. coli* cells were stored as 50 µL aliquots at -80°C.

3.2.1.10. Transformation of chemically competent *E. coli* cells

50-100 µL of chemically competent *E. coli* cells were incubated with the desired plasmid DNA for 5 min on ice. This mixture was subjected to heat shock at 42°C for 45 sec and later recovered on ice for 5 min. The recovered cells were resuspended in 900-950 µL of LB media without antibiotics and incubated at 37°C with shaking for at least 45 min to allow the expression of the antibiotic resistance gene. The cells were collected by centrifugation in a table top centrifuge at 18500x*g* for 2 min and plated on LB agar plates supplemented with appropriate antibiotics. The plates were incubated at 37°C till colonies appeared.

3.2.1.11. Cultivation of yeast cells

Yeast cells were streaked out on either YP or minimal media agar plates and grown at 30°C unless otherwise stated. For liquid cultures, cells from single yeast colonies were inoculated in liquid YPD, YPGalactose or in selective synthetic media and incubated with shaking (160 rpm) at appropriate temperatures. Unless stated

otherwise, cultures were grown to exponential phase (OD600=0.8 to 1) by diluting the culture in the same media.

Media compositions are given below.

YP media	
Yeast extract	1 %
Peptone	2 %
Glucose/Galactose	2 %
Agar (for plates)	2 %

SD media	
Yeast nitrogen base (without amino acids)	0.67 % (w/v)
Glucose	2 %
Agar (for plates)	2 %

Amino acids and nucleobases were added to SD media as required.

Amino acids and nucleobases	**Concentration (w/v)**
L-Arginine	0.002%
L-Histidine	0.001%
L-Isoleucine	0.006%
L-Leucine	0.006%
L-Lysine	0.004%
L-Methionine	0.001%
L-Phenylalanine	0.006%
L-Threonine	0.005%
L-Tryptophan	0.004%
Uracil	0.004%
Adenine	0.002%

3.2.1.12. Yeast phenotypic analysis by spot tests

Cells from freshly streaked out yeast colonies were picked using sterile toothpicks and resuspended in 400 µL of sterile water and the OD600 was determined. The different cell suspensions were diluted with sterile water to an OD600 of 0.5 and made up to a total volume of 200 µL. These suspensions or their serial dilutions were then transferred to 96-well plates and spotted onto appropriate agar plates using a frogger and grown for 2-3 days.

3.2.1.13. Yeast mating type testing and crossing of haploids

In order to cross haploid yeast cells, they were mixed in approximate equal amounts on a YPD plate and incubated overnight at 30°C. This was followed by replica-plating on selective media were only the diploids would grow. Single colonies were picked and re-streaked on selective media to obtain the desired diploids. To test the mating type of a haploid yeast strain, the strain was crossed to a different auxotroph background strain to test for correct mating types on SD plates. KMY38 (*MATα trp5*) and KMY39 (*MATa trp5*) were used as tester strains. Haploid cells carrying the *trp1-Δ63* mutation were mated with the mating type tester strains yielding prototrophic diploid cells that grew on SD plates without tryptophan.

3.2.1.14. Sporulation and tetrad dissection

Sporulation and tetrad dissections were carried out to modify yeast strains. After crossing, the diploid strains were grown on YPD plates at 30°C for two days. To induce meiosis and sporulation, the cells were inoculated in 3 ml liquid sporulation medium (1% potassium acetate, 0.005% zinc acetate, 0.04 mg/ml adenine, 0.02 mg/ml uracil, 0.006 mg/ml L-leucine, 0.003 mg/ml L-lysin, 0.004 mg/ml L-tryptophan, 0.002 mg/ml L-histidine) and incubated for 5 days at 25°C, followed by 3 days at 30°C. 100 µL of the culture were taken, centrifuged for 1 minute at 14000x*g* at room temperature and re-suspended in 200 µL of sterile water. To disrupt the ascus wall, 3 µL of β-glucoronidase were added to the suspension and incubated for 5 minutes at 37°C. 20 µL of the suspension were carefully poured onto a YPD plate to form a line across the plate. The tetrad dissection was done under a microscope using a micromanipulator. After incubation for 2-3 days at 30°C, the spore clones were isolated and analysed for genotype and mating type.

3.2.1.15. High efficiency yeast transformation (Gietz and Woods, 2006)

Yeast cells were grown to an OD600 of 0.6 to 1.0 in 5 ml of appropriate medium and harvested by centrifugation at 3000x*g* for 5 min. The pelleted cells were subsequently washed once with 5 ml of sterile water before adding the following transformation mix.

Yeast transformation mix	
50 % (w/v) PEG-3350	240 µL
1 M LiAc	36 µL
E. coli DNA	2 µL
Plasmid DNA	2.5 µL (each)
Sterile distilled water	to 360 µL

The transformation mix was vortexed vigorously for at least a minute until the pellet was completely re-suspended. This mixture was then incubated at 30°C for 15 min followed by another incubation at 42°C (heat shock) for 15 min. Afterwards, the cells were collected by a short-spin and washed with sterile water. In the case of plasmid transformation, cells were immediately plated on the appropriate selective medium whereas for gene disruptions or modifications, cells were plated on selective medium only after incubation in non-selective medium for at least 3 hours. Plates were incubated for 2-5 days at 30°C until yeast colonies appeared.

3.2.2. Biochemical and immunological methods

3.2.2.1. Yeast cell lysis with glass beads (Dohmen et al., 1995)

10-50 ml cells were pelleted and re-suspended in 1:1 volume of cold lysis buffer (150 mM NaCl, 5 mM EDTA, 50 mM HEPES (pH 7.5), 1 % Triton X-100, 1X protease inhibitor mixture, EDTA free) and glass beads (0.4- 0.6 mm) at 4°C. The suspension was shaken on a Vibrax shaker (VXR basic IKA Vibrax) for 5 min at 2000 mot/min 4°C. Cells were then briefly centrifuged for 10 seconds. The supernatant was collected and marked as “total” lysate. The relative protein amounts were determined using Bradford method and the total protein amounts were normalized between various samples. The normalized samples were centrifuged at 30000x*g* for 30 min at 4°C. In certain cases, the samples were subjected to ultracentrifugation at 35000 rpm (Beckman Optima™ TLX ultracentrifuge with rotor TLA-55) for 30 min at 4°C. The resultant “pellet” and “supernatant” fractions were separated and transferred to pre-cooled tubes. The fractions were then boiled with LLB and analysed by SDS-PAGE

3.2.2.2. Yeast cell lysis by boiling

Yeast cells were pelleted, resuspended in 2x LLB with 1% β-mercaptoethanol and boiled at 100°C for 5 min. Samples were cooled down to room temperature and cell debris was pelleted by short centrifugation.

1x Laemmli loading buffer (LLB)	
Tris-Cl (pH 6.8)	62.5 mM
SDS	2 %
Glycerol	10 %
M-Cresol purple	0.0001 g/ml

3.2.2.3. Yeast cell lysis by grinding

Exponentially growing cultures of yeast cells were centrifuged at 5000x*g* and washed once with distilled water before snap-freezing in liquid nitrogen. Proteins were extracted by grinding using a Mixer Mill MM400 (Retsch). The frozen cell pellets were placed in one or two grinding jars containing grinding balls all of which were pre-cooled with liquid nitrogen. Radial oscillations in a horizontal position were done for 1 min at 30 Hz. The resulting cell powder was transferred to a 50 ml falcon tube, frozen in liquid nitrogen and stored at -80°C until further analysis.

3.2.2.4. Estimation of protein concentration

To estimate the protein concentration, 2- 4 µL of samples was made up to a volume of 800 µL using distilled water and mixed with 200 µL of Bradford reagent (BioRad). This mixture was incubated for 5 min at room temperature. Bradford reagent contains coomassie brilliant blue G which changes its absorbance maximum from 465 nm to 595 nm upon binding to protein. The absorbance of samples to be assayed was measured at 595 nm and correlated to a protein standard curve that was obtained with BSA solutions. For purified proteins, the concentrations were measured using the Eppendorf µCuvette™ in an Eppendorf BioSpectrometer®. The programmes were set for each protein/protein complex based on their corresponding extinction coefficients.

3.2.2.5. SDS polyacrylamide gel electrophoresis (SDS-PAGE) (Laemmli, 1970)

Protein extracts were analysed by SDS-PAGE using a standard protocol. The composition of resolving and stacking gels are given below.

Resolving gel	
Acrylamide/bisacrylamide (37:5:1)	10% or 12% (w/v)
Tris-HCl pH 8.8	375 mM
SDS	0.1% (w/v)
APS	0.05% (w/v)
TEMED	0.033% (v/v)
Stacking gel	
Acrylamide/bisacrylamide (37:5:1)	4% (w/v)
Tris-HCl pH 6.8	125 mM
SDS	0.1% (w/v)
APS	0.05% (w/v)
TEMED	0.055% (v/v)

After casting the resolving gel, it was overlayed with isopropanol and allowed to fully polymerize. The gel was then gently washed with water to remove the isopropanol. The stacking gel was casted on top of the resolving and combs with the desired number of wells were inserted. The samples were loaded onto the wells along with a protein ladder for molecular weight determination (PageRuler^{TM} Plus Prestained Protein Ladder). After electrophoresis, gels were subjected to either western blot analysis or directly stained with coomassie brilliant blue R 250.

Coomassie blue R-250 staining solution	
Methanol	40% (v/v)
Acetic acid	10% (v/v)
CBB-R250	0.025% (w/v)
Destaining solution	
Methanol	40% (v/v)
Acetic acid	10% (v/v)

The gels were incubated in staining solution for 10-30 minutes and destained for up to 24 hours till clear protein bands appeared.

3.2.2.6. Western blot analysis

Western blotting was done to analyse proteins after separation by SDS-PAGE or Native-PAGE. The proteins were first transferred from the gel to either a nitrocellulose or a PVDF membrane using the semi-dry protein transfer system (Bio-Rad) using the transfer buffer (25 mM Tris-HCl pH 8.3, 192 mM glycine, 20% (v/v) methanol). A current of 0.8 mA/cm^2 was applied for 75 min for efficient transfer of proteins. After transfer, the membrane was incubated in blocking solution (3% milk in PBS) for 1 hour. The membrane was then incubated overnight at 4°C with specific primary antibodies diluted in blocking solution. The next day, the membrane was washed for 4 times (5 min duration each) with either 1x PBST (for ECL detection) or 1x PBS (for Odyssey detection) before incubation with secondary antibody coupled to HRP (for ECL detection) or fluorophores 800 nm, 680 nm (for Odyssey detection) for 1 hour. Finally, the membrane was washed 4 times (5 min each) with either 1x PBST or PBS. For ECL detection, the membrane was incubated with Lumi-light Plus reagent (Roche) for 1 min before exposing to light sensitive X-ray film. For membranes probed with the fluorophore-coupled secondary antibody, the signal was detected by using the Odyssey Infrared imaging system (LI-COR). The signal was visualized and quantified using the Odyssey v1.2 software.

3.2.2.7. Reprobing of western blot membranes

Western blot membranes were stripped off their original antibodies and reprobed with different primary antibodies to visualize several proteins on the same membrane. The membrane was initially washed with 0.2 N NaOH for 15 min and then with water to remove bound antibodies. It was then incubated for 10 min with blocking solution followed by incubation with primary and secondary antibodies as described above.

3.2.2.8. Analysis of protein stability by cycloheximide chase

Cycloheximide, an inhibitor of protein biosynthesis was used to analyse the stability of proteins in log-phase yeast cultures. Yeast cells were grown to an OD600 of 0.6-0.8 and 100 µg/ml of cycloheximide was added to block protein translation. Cells were harvested at different time points after cycloheximide addition and lysates were prepared by glass-bead or boiling method. The samples were further analysed by SDS-PAGE and western blotting.

3.2.2.9. ODC-Oaz1 interaction analysis

For analysis of ODC-Oaz1 interactions, proteins were extracted from *E. coli* BL21 cod+ cells harbouring either pDG241 (GST-Oaz1), pGEX-2TX (GST), pDG273 (ODC-Flag) or pUC19 (mock) by glass bead lysis in ice-cold lysis buffer (50mM Na-HEPES (pH 7.5), 5mM EDTA, 1% Triton X-100) containing protease-inhibitor cocktail (Roche). Total protein amounts were equilibrated between GST-Oaz1 and GST lysate using the mock lysate. 800 µg of total proteins were incubated with 100 µL of glutathione beads (GE Healthcare) at 4°C for 2h. From this step onwards, 1 mM spermine was added to certain tubes as indicated in Fig.11. The beads were washed two times with lysis buffer, and further incubated after the addition of ODC-Flag lysate at 4°C for 2h. Bound proteins were eluted by incubation with 125 µL elution buffer [25 mM Glutathione (Sigma), 20 mM NaOH in lysis buffer] at 4°C for 90 min. The samples were then analysed by SDS-PAGE and western blotting as described above.

3.2.2.10. Purification of proteasomes from yeast (Ha et al., 2012)

26S proteasomes were purified from yeast strain MO24, in which the *PRE1* gene, encoding the 20S core particle subunit Pre1, has been stably modified to express a C-terminally Flag-6His tagged version. 3 L of yeast culture was grown to an OD600 of 2, divided into 3 equal parts and harvested by spinning at 3500x*g* for 8 min at 4°C. Each pellet was washed once with 40 ml cold water before snap freezing in liquid nitrogen. Lysis was carried out using using a Mixer Mill MM400 (Retsch) as

described above. The yeast cell powder was collected in a 50 ml tube, snap-frozen and stored at -80°C. The pellet was thawed by adding 2 pellet volumes of Buffer A (50mM Tris.Cl, pH 7.5, 150 mM NaCl, 10% Glycerol, 0.2% Triton-X-100) containing 4mM ATP and 1x ARS (buffer AAA). This mixture was incubated in ice till complete suspension of the pellet (approx. 45 min) followed by centrifugation in an pre-cooled Beckman 25.50 rotar for 20 min at 17000 rpm at 4°C. The supernatant was filtered using a Acrodisc PF Syringe Filters with Supor Membrane (0.2 µ 0.8/0.2 µm, 32 mm) into a pre-cooled 15 ml tube. Anti-Flag agarose beads (1ml/15,000 OD) were equilibrated by washing twice with 5 volumes of buffer AAA with alternating incubations at 4°C for 5 min. The beads were collected by spinning at 200x*g* for 3 min. The filtered supernatant was then added to the pre-equilibrated anti-FLAG agarose beads and incubated at 4°C for 3h in a rotating wheel. The beads were collected by spinning at 200x*g* for 3 min. The beads were washed twice with 5 volumes of buffer AAA (with 5 min mild rotation at 4°C) and rinsed (re-suspended and pelleted without incubation) twice with 5 volumes of buffer B (25 mM HEPES, pH 7.8, 5 mM MgCL2, 25 mM KCl, 10% glycerol) supplemented with 2 mM ATP (buffer BA). The bound proteasomes were eluted with 300 µL of buffer BA containing 150 µg/ml of Flag peptide, transferred to a 2 ml tube and incubated at 4°C for 1h in a rotating wheel. If necessary, elution was repeated with another 300 µL of elution buffer.

3.2.2.11. Purification of Oaz1, ODC and ODC/Oaz1 heterodimer

6His-Oaz1 was affinity-purified from *E. coli* strain Rosetta (Merck) transformed with pDG240 (6His-Oaz1) as described earlier (Kurian et al., 2011). Cells were grown in LB medium supplemented with ampicillin and chloramphenicol to OD600=0.6 and expression was induced by adding 1mM IPTG for 4h. Cell were harvested and re-suspended in 10 ml binding buffer (50 mM Tris, pH 7.8 at 4 °C). This mixture was frozen in liquid nitrogen and stored at −80 °C. For lysis, the cells were thawed in water and 10 mg of lysozyme (Sigma), 1 mg of DNase I (Roche) and 1X protease inhibitor mix (Roche) were added. Lysis was initiated by vortexing six times for 10 sec at 25 °C followed by incubation on ice for 45 min. The lysate was then clarified by centrifugation at 25000x*g* for 30 min at 4 °C. Amylose resin (200 µL; NEB) was equilibrated with binding buffer before adding the supernatant. This suspension was incubated for 2h at 4 °C for with mild rotation. Unbound material was removed by centrifugation at 200x*g* for 3 min at 4 °C. The beads were washed five times with 10 ml of binding buffer supplemented with 20 mM imidazole. Bound protein was eluted in 350 µl binding buffer containing 250 mM imidazole for 1h at 4 °C for with

mild rotation. 6His-Oaz1/ODC-2xha or 6His-Oaz1-ΔODS-ODC-2xha were co-expressed in *E. coli* strain Rosetta and Ni-affinity-purified as described above with a few variations. The lysis buffer used was buffer B (25 mM Na-HEPES, pH 7.8, 5 mM $MgCL_2$, 25 mM KCl, 10% glycerol). After elution of the protein, imidazole was removed using NAP^{TM}-5 (GE Healthcare) columns. The purity of the eluted proteins was evaluated by SDS-PAGE followed by coomassie staining. The purified proteins (in buffer with 10% glycerol) were stored as 20-50 µL aliquots at -80 °C.

3.2.2.12. Analysis of proteasomes by Native-PAGE (Elsasser et al., 2005)

The purity and of the proteasomes were analysed by Native-PAGE followed by either coomassie staining or in-gel chymotrypsin-like activity degradation assay.

The composition of the gel is given below.

Native gel	
Acrylamide/bisacrylamide (37:5:1)	3.5%(w/v)
Tris	90 mM
Boric acid	90 mM
$MgCl_2$	5 mM
EDTA	0.5 mM
ATP- $MgCl_2$	1 mM
APS	0.1% (w/v)
TEMED	0.1% (v/v)

10-15 ml of the above gel mixture was used to prepare 1 mini native gel. The gel was cast at room temperature and was later allowed to cool down at 4°C. The samples were prepared in 5x sample buffer (250mM Tris-HCl, pH 7.4 50% glycerol, 60 ng/ml xylene cyanol). After sample loading the gels were run at 4°C at 100 V for 3 h. After separation, proteasomes was detected by an in-gel proteasome assay using Suc-LLVY-AMC (N- succinyl- leucine- leucine- valine- tyrosine- 7- amino- 4- methyl coumarin), or by coomassie staining.

The in-gel proteasome activity assay was performed by incubating the gel in the following solution for 10 min at 30°C.

Tris-HCl pH 7.4	25 mM
$MgCl_2$	10 mM
ATP	1 mM
DTT	1 mM
Glycerol	10% (v/v)
Suc-LLVY-AMC	0.1 mM

Proteasome bands were visualized upon exposure to a UV lamp and imaged using a Gel Doc™ (Bio-Rad). 20S bands can be visualised better with addition of 0.002% SDS to the assay mixture.

3.2.2.13. Proteasomal peptidase activity assay (Dohmen et al., 2005)

The chymotrypsin-like proteasomal activity assay was done by measuring the release of the fluorescent 7 amino-4-methylcoumarin (AMC), after cleavage from Suc-LLVY-AMC, at 440 nm by using an excitation wavelength of 380 nm. 0.06 µg of purified 26S proteasome and varying amounts of spermine (as shown in Fig. 10B) were diluted in buffer B supplemented with 1 mM ATP and 1 mM DTT to a volume of 90 µL followed by addition of 10 µL of 1:10 dilution of substrate stock solution (10 mg/ml). The reactions were set up in a 96 well plate and measured using a fluorimeter (FLUOstar Galaxy Microplate Reader). The measurement was done in 40 cycles and the enzymatic activity in each fraction was calculated based on the increase of fluorescence per time.

3.2.2.14. *In vitro* proteasomal degradation assay (Ha et al., 2012)

A degradation assay was set up in a 15 µL reaction containing purified proteasomes and ODC/Oaz1 heterodimer as substrate in buffer B (25 mM HEPES, pH 7.8, 5 mM MgCL2, 25 mM KCl, 10% glycerol) supplemented with 1 mM ATP and 1 mM DTT. The amounts of 26S proteasome and substrate used are as indicated in Figs. 8 and 9. To inhibit proteasomal activity; proteasomes were pre-treated with 100 µM epoxomycin (Enzo life sciences) at 30°C for 45 min before adding to the degradation assays. Wherever indicated (Fig. 9), the reactions were supplemented with either spermidine or spermine. The degradation reactions were carried out at 30°C for various time periods as indicated in Figs. 8 and 9 followed by SDS-PAGE and western blotting.

3.2.2.15. Polyamine binding assay (Palanimurugan and Dohmen, 2012)

Polyamine binding mixtures were composed of 10 µM of purified 6His-Oaz1 mixed with 10 µM of [^{3}H]-spermidine and one of the three acetyl polyamines N1-acetylspermidin, N8-acetylspermidine and N1, N8-diacetylspermidine (concentrations as indicated in Fig.13A) and made up to 100 µL with 50 mM Tris, pH 7.8 at 4 °C. This was then gently mixed and incubated on ice for 60 min. This mix was then transferred to a centrifugal filter (modified polyethersulfone (PES) 10K, VWR) mounted on top of a 1.5 ml collection tube. The unbound polyamines were filtered by spinning at 2500xg for 5 min at 4°C. Microcentrifuge tubes with 1 ml scintillation liquid

(two tubes with scintillation liquid for every filter device used) were prepared and kept at room temperature. 10 µL of the retentate from inside the cut-off filter device was removed and added to a microcentrifuge tube with scintillation liquid (retentate). Next, 10 µL of filtrate from the collection tube of the filtration device was added to a second microcentrifuge tube with scintillation liquid (filtrate). The tubes were vortexed for 10s before proceeding with scintillation counting. From the resulting CPM (counts per minute) values, the percentage of protein-bound polyamines was calculated using the following formula.

$$\text{Percentage polyamine Binding} = \{(CPM_{retentate} - CPM_{filtrate}) / CPM_{retentate}\} \times 100$$

3.2.2.16. Native-PAGE analysis of proteasomal binding

The binding mixture was prepared similar to the degradation assay mixture. 4 µg of 26S proteasome and 50 ng of substrate were mixed in 10 µL buffer B supplemented with 1 mM ATP and 1 mM DTT and 50 µM MG132. The latter inhibitor was added to prevent any degradation of the substrates by the proteasomes. This mixture was incubated in ice for 3h. 2.5 µL of 4x Native PAGE sample buffer (Life technologies) was added and mixed with the sample. This mixture was then centrifuged at 30000x*g* for 10 min to remove all insoluble material that might interfere with the Native PAGE. The samples were analysed using the NativePAGE™ Novex® Bis-Tris Gel System (Life technologies) followed by western blotting as per manufacturer's instructions.

4. Results

4.1. Characterization of the direct role of polyamines in ODC targeting

Polyamines regulate cellular ODC levels by two known mechanisms involving ODC antizyme. They induce ribosomal frameshifting during the translation of antizyme and also inhibit the ubiquitin-dependent degradation of antizyme (Kurian et al., 2011; Palanimurugan et al., 2004). However, there is a third possible mechanism of regulation of ODC by polyamines. Using a stable mutant of antizyme (Oaz1-4res), Gödderz showed that polyamines directly enhanced the degradation of ODC *in vivo* (Gödderz, 2010). The Oaz1-4res mutant [in frame version (Palanimurugan et al., 2004)] was used because its levels were not altered by polyamine addition. Upon addition of spermidine, the steady state levels of ODC was lowered albeit similar antizyme levels indicating a direct enhancement of ODC degradation by polyamines. This observation was further clarified using wild-type Oaz1 (in frame version). The presence of spermidine caused a remarkable decrease in ODC levels in spite of similar Oaz1 levels established using a copper-inducible, P_{CUP1} promoter-driven *OAZ1* gene. These data showed that polyamines directly promote ODC degradation *in vivo* in yeast cells (Beenukumar et al., in press).

4.1.1. *In vitro* recapitulation of proteasomal degradation of ODC

To study the direct effect of polyamines on ODC degradation, it was a goal of the present work to reconstitute ODC degradation *in vitro*. Hoyt et al. have previously reproduced key features of ubiquitin-independent ODC degradation using mouse ODC and purified 26S proteasome (Hoyt et al., 2003). Moreover, another *in vitro* study using yeast ODC and Oaz1 had shown that antizyme promotes ODC degradation in a ubiquitin-independent and ATP-dependent manner (Porat et al., 2008). Subsequently, Gödderz et al. showed using *in vivo* experiments in yeast that binding of ODC monomers to antizyme is required to expose an N-terminal degron of yeast ODC called ODS (ODC Degradation Signal) (Godderz et al., 2011). Here, I reconstituted ODS-dependent degradation of ODC *in vitro*. 26S proteasomes were affinity-purified using anti-Flag beads from a yeast strain with a Flag-His_6-tagged β4/Pre1 subunit. Native-PAGE analysis showed that these preparations mainly yielded active forms of the proteasome in its singly (SC) or doubly capped (DC) form, i.e. CP with one or two RPs (Fig. 7A) (Elsasser et al., 2005). ODC/Oaz1 or ΔODS-ODC/Oaz1 heterodimers were affinity-purified using Ni-NTA beads from *E. coli* cells overexpressing 6His-Oaz1 and ODC-2xHa or ΔODS-ODC-2xHa and characterized by SDS-PAGE. ODC-2xHa purified as a double band, the faster migrating form of which apparently, due to premature termination or to proteolytic processing, lacks

one of the Ha epitopes as it is not detected with the same sensitivity as the slower migrating form (compare Figs. 7B and 8A). The different ODC/Oaz1 heterodimers were mixed with 26S proteasomes in a buffer supplemented with ATP, and incubated at 30^0C for specific time periods followed by SDS-PAGE analysis. As expected, ODC was degraded over time, whereas antizyme remained stable (Fig. 8A; lanes 4-6). In the control without 26S proteasomes, in contrast, ODC was not degraded (Fig. 8A; lanes 1-3). Around 75% inhibition of degradation was observed upon addition of epoxomicin (Meng et al., 1999), a selective proteasome inhibitor (Fig. 8A; lanes 7-9). In a similar experiment using the ΔODS variant of ODC, only around 30% degradation was observed compared to the 80% degradation observed for the full-length ODC (Fig. 8B). These results show that ODS is critical for efficient degradation of ODC in line with the *in vivo* data reported earlier (Godderz et al., 2011).

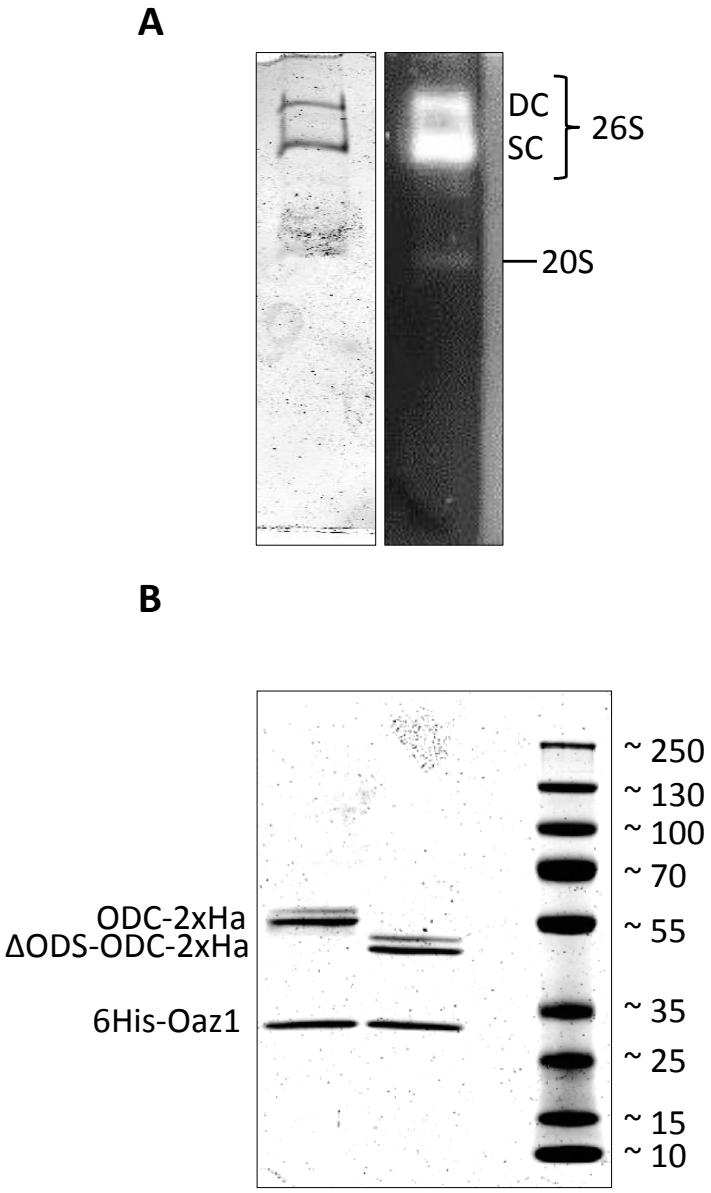

Fig. 7: Purification of 26S proteasome and ODC/Antizyme heterodimer. (A) Flag-tagged proteasome affinity-purified from yeast cells was analyzed by native-PAGE and coomassie staining (left) or activity staining by overlay with the fluorogenic peptide Suc-LLVY-AMC (right). Proteasomes in this preparation were either doubly-capped (DC) with two RPs on both sides of the core particle (CP), or singly-capped (SC) with only one RP attached to the CP. 20S CPs without any RPs attached to them were also present in the preparation. **(B)** SDS-PAGE analysis and coomassie staining of 6His-Oaz1 co-purified from *E.coli* cells as heterodimers either with full length ODC (ODC-2xHa) or with N-terminally truncated ODC lacking the first 47 residues (ΔODS-ODC-2xHa).

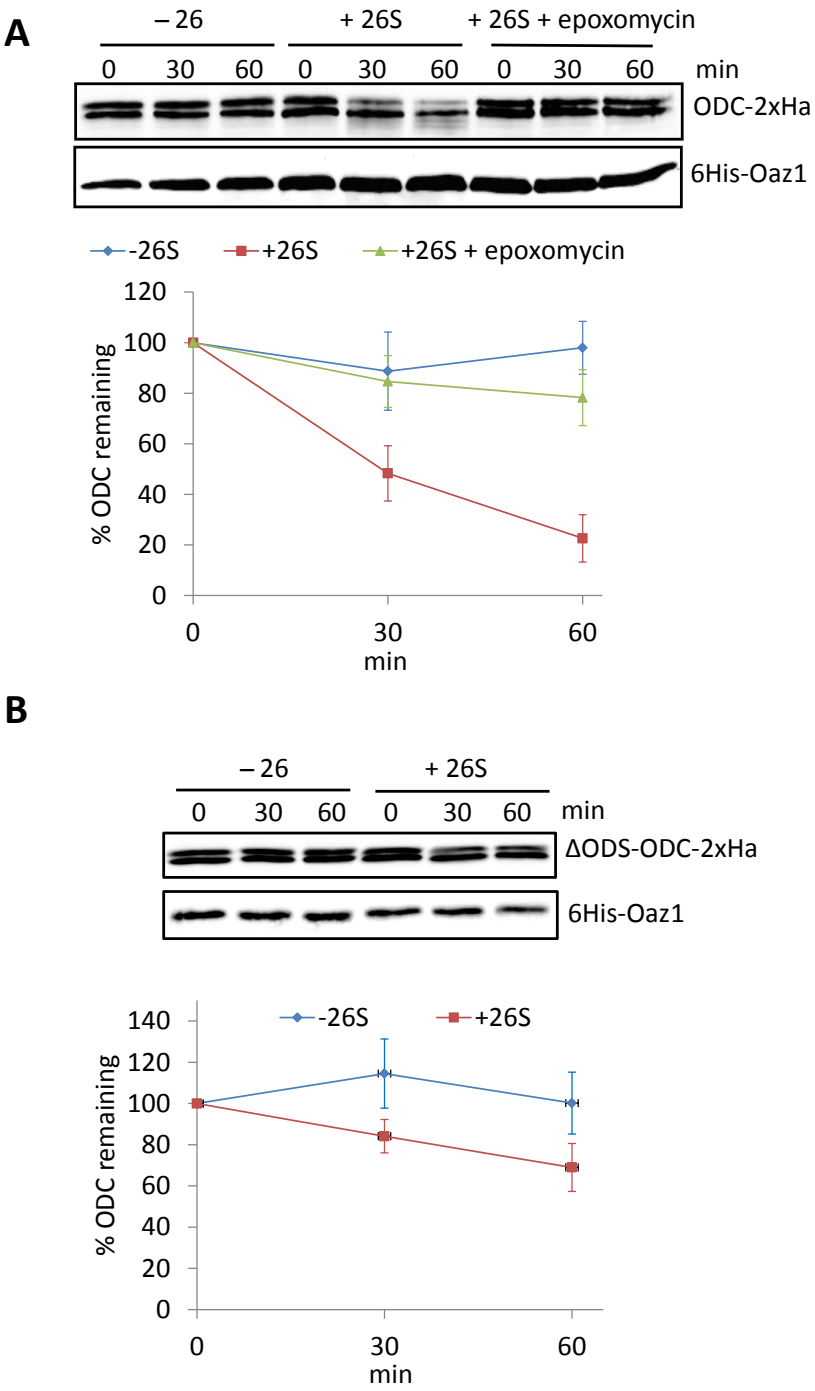

Fig. 8: *In vitro* characterization of proteasomal degradation of ODC. (A) *In vitro* degradation assays with purified 26S proteasomes and purified ODC/Oaz1 heterodimer as a substrate showing the degradation of ODC over time. 50 ng of ODC/Oaz1 heterodimer (40 nM) and 3 µg of 26S proteasome (80 nM) in a volume of 15 µL were used. As controls, otherwise identical samples were assayed without 26S proteasome (-26S), or with the proteasome inhibitor epoxomycin (100 µM). In the graph, values for the 0 time points were set to 100%. Error bars, s.d.; *n* = 3. **(B)** Experiments were performed as described for Fig. 8A, except that ΔODS-ODC-2xHa was used instead of the full length ODC.

4.1.2. Polyamines directly promote proteasomal degradation of ODC *in vitro*

I used the *in vitro* ODC degradation system described above to study the direct effects of polyamines on ODC degradation. Consistent with the *in vivo* results, increased degradation of ODC was observed with increasing concentrations of either spermidine or spermine (Fig. 9). Spermine showed a greater effect on ODC degradation than spermidine. This finding is compatible with the higher binding affinity of Oaz1 observed for spermine compared to spermidine (Kurian et al., 2011).

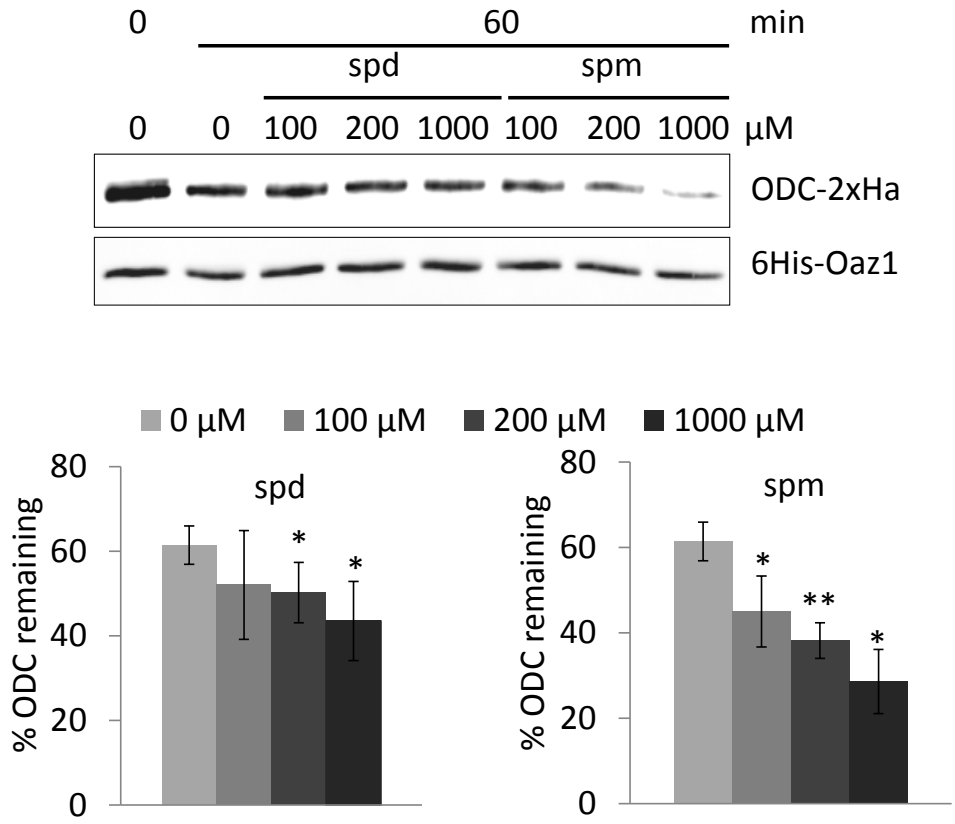

Fig. 9: Degradation of ODC by the proteasome is directly enhanced upon polyamine addition. *In vitro* degradation of ODC with 0.06 µg of 26S proteasome (1.6 nM) and 100 ng of ODC/Oaz1 (80 nM) as substrate in a volume of 15 µL as described in Fig. 8A except that varying concentrations of either spd or spermine (spm) were added as shown. The graph shows the quantification of ODC-2xHa signals. Error bars, s.d.; *n* = 3. Paired T test values are represented as asterisks above the bars; P ≤ 0.05 (*) and P ≤ 0.01 (**).

4.1.3. Polyamines do not enhance ubiquitin-dependent proteasomal degradation

To investigate the specificity of the observed effect of polyamines on ODC degradation, I asked if polyamines have any general effect on proteolytic degradation. To address this possibility *in vivo*, two well characterized ubiquitin-dependent substrates, an N-end rule substrate (Ub-R-e^{K}-Ha-Ura3) and a Ubiquitin Fusion Degradation (UFD) pathway substrate (Ub-V76-e^{K}-Ha-Ura3) were used (Ghislain et al., 1996; Varshavsky, 1996). No significant effect on degradation of these two substrates was observed upon polyamine addition to polyamine-depleted cells (Fig. 10A). Additionally, the chymotrypsin-like activity of purified 26S proteasome was measured in the presence of increasing spermine concentration. A small reduction in proteasome activity was observed with polyamine addition (Fig. 10B). Taken together, the results presented above demonstrate that polyamines directly and specifically enhance ODC degradation by the proteasome.

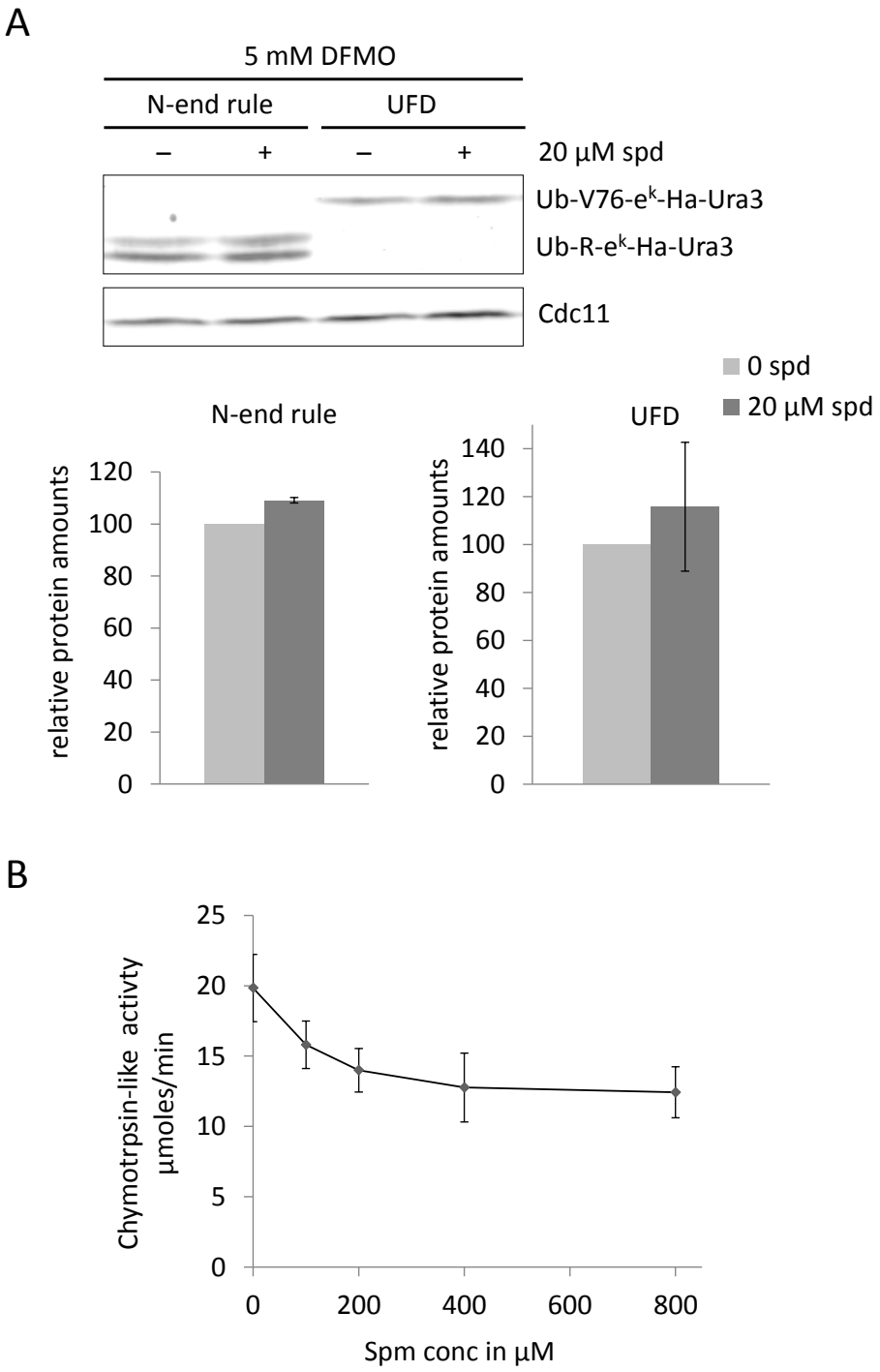

Fig. 10: Polyamines do not enhance the degradation of ubiquitin-dependent substrates by the proteasome. (A) Western blot analysis of steady state levels of Ub-R-e^k-Ha-Ura3 and Ub-V76- e^k-Ha-Ura3 from wild-type cells grown in the presence of 5 mM DFMO. 20 µM spermidine (spd) was added as indicated. Ha signals were quantified normalized to the Cdc11 loading controls and given relative to the level of protein without spermidine, which was set to 100%. Error bars, s.d.; *n* = 2. **(B)** Assay of chymotrypsin-like activity with purified proteasome in the presence of increasing spermine (spm) concentrations. Error bars, s.d.; *n* = 4.

4.1.4. Polyamines do not alter the affinity of ODC/antizyme interaction

To understand the mechanism behind the effect of polyamines on ODC degradation, I tested whether polyamines changed the affinity of ODC/Oaz1 heterodimer interaction. To address this question, I performed co-pull down assays using epitope-tagged variants of ODC and Oaz1 expressed in *E. coli*. GST-Oaz1 bound beads were exposed to *E. coli* cell extracts overexpressing ODC-Flag in the presence or absence of spermine. Western blot analysis after GST pull down showed no significant difference in ODC-Flag binding between the samples with and without spermine (Fig. 11). These data suggested that polyamines promote ODC degradation without altering ODC/Oaz1 heterodimer interactions.

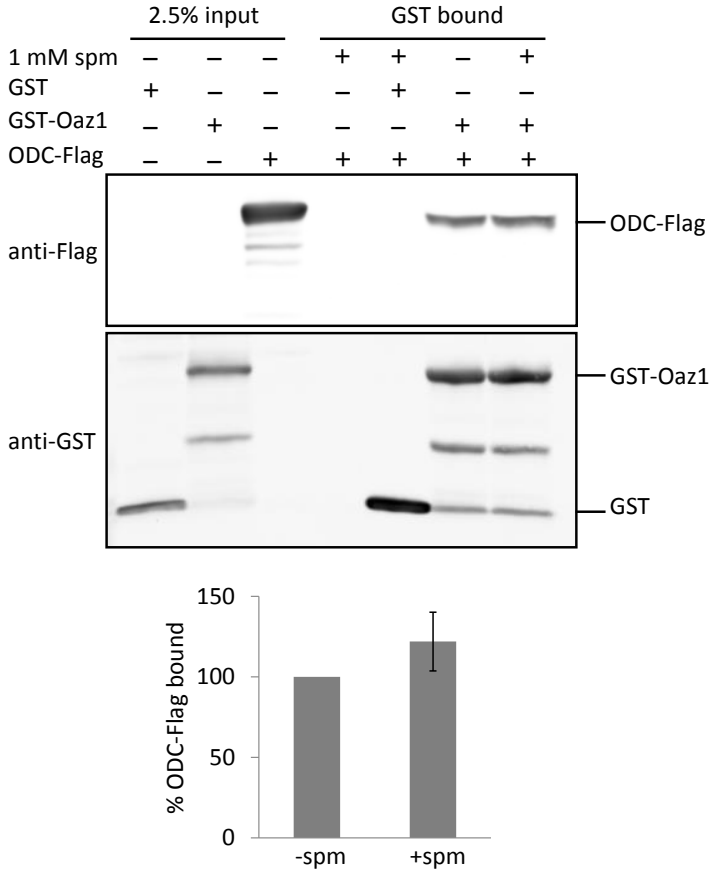

Fig. 11: Spermine does not affect the affinity of ODC/antizyme heterodimer. Co-pull down of Oaz1 and ODC in the presence or absence of 1 mM spermine (spm). Extracts from *E. coli* cells expressing the indicated tagged proteins were subjected to GST-pull down and subsequent quantitative anti-Flag western blotting for ODC-Flag detection and anti-GST for GST-Oaz1 detection. ODC-Flag signals after elution were normalized to GST-Oaz1 signals providing ODC-Flag values obtained in the absence of spermine, the mean of which was set to 100%. Values obtained in the presence of spermine are given in % of those obtained in its absence. Error bars, s.d.; n = 3.

4.1.5. Both spermidine and spermine promote antizyme and ODC degradation *in vivo*

As spermine binds antizyme better than spermidine (Kurian et al., 2011) and also shows a greater effect on the enhancement of ODC degradation *in vitro*, I questioned whether spermine is the major mediator of ODC regulation in yeast cells. Therefore, I compared the effect of spermidine and spermine on antizyme stabilization and ODC degradation in wild-type and *spe4-Δ* strains. *SPE4* encodes spermine synthase, an enzyme that mediates the conversion of spermidine to spermine. Hence, *spe4-Δ* cells are devoid of spermine (Hamasaki-Katagiri et al., 1998). Antizyme degradation was similarly inhibited in both WT and *spe4-Δ* cells upon addition of spermidine or spermine (Fig. 12, top panel). When compared to spermine, addition of spermidine had a stronger effect on the inhibition of antizyme degradation in both strains. Similarly, spermidine had a stronger (stimulatory) effect on ODC degradation than spermine (Fig. 12, middle panel). These results suggest that both spermidine and spermine are capable of mediating ODC regulation in yeast cells. The relatively weak effect of spermine on ODC targeting *in vivo* contrasts with its relatively stronger effect *in vitro* and is likely due to a lower uptake efficiency of spermine by yeast cells (Erez and Kahana, 2001).

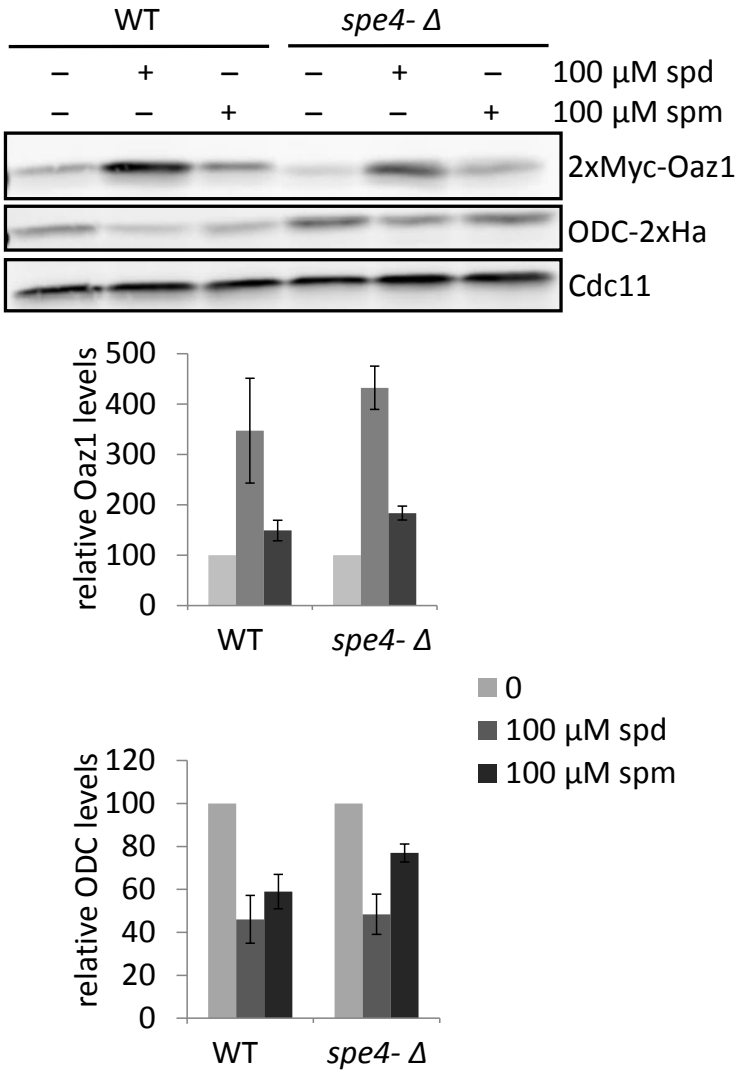

Fig. 12: Role of polyamine subtypes and their modification in the targeting of ODC. Western blot analysis comparing steady state levels of Oaz1 and ODC in either the wild-type or a strain lacking spermine synthase (*spe4-Δ*), grown with or without polyamine supplementation as indicated. The graph shows the results of a quantification of Myc (upper part) and Ha signals (lower part) normalized to the Cdc11 loading control. Levels are given relative to the respective levels of the same proteins in cells grown without polyamine addition, which was set to 100%. Error bars, s.d.; *n* = 3.

4.1.6. Acetylation of polyamines inhibit their binding to antizyme

In mammals, when cellular polyamine levels are high, they are acetylated leading to their breakdown or export from the cells (Casero and Pegg, 1993). High cellular polyamine levels, in addition, lead to antizyme synthesis and hence the down-regulation of ODC. I therefore asked whether acetylated polyamines might be responsible for down-regulating ODC by binding to antizyme. Hence a competition assay with [^{3}H]-spermidine and various acetylated spermidine for Oaz1 binding was performed. In this assay, mono-acetylated spermidine variants showed a clearly reduced binding to antizyme when compared to unmodified spermidine, and di-acetylspermidine showed no competition at all (Fig. 13A). I then asked if acetylated polyamines affected either antizyme or ODC degradation using the *paa1-Δ* mutant. *PAA1* encodes polyamine acetyltransferase, an enzyme that has been shown to acetylate polyamines (Liu et al., 2005). No notable differences were observed between WT and *paa1-Δ* yeast cells in antizyme stabilization and ODC degradation (Fig. 13B). Taken together, these findings suggest that once acetylated, polyamines do no longer participate in the feedback regulation of ODC.

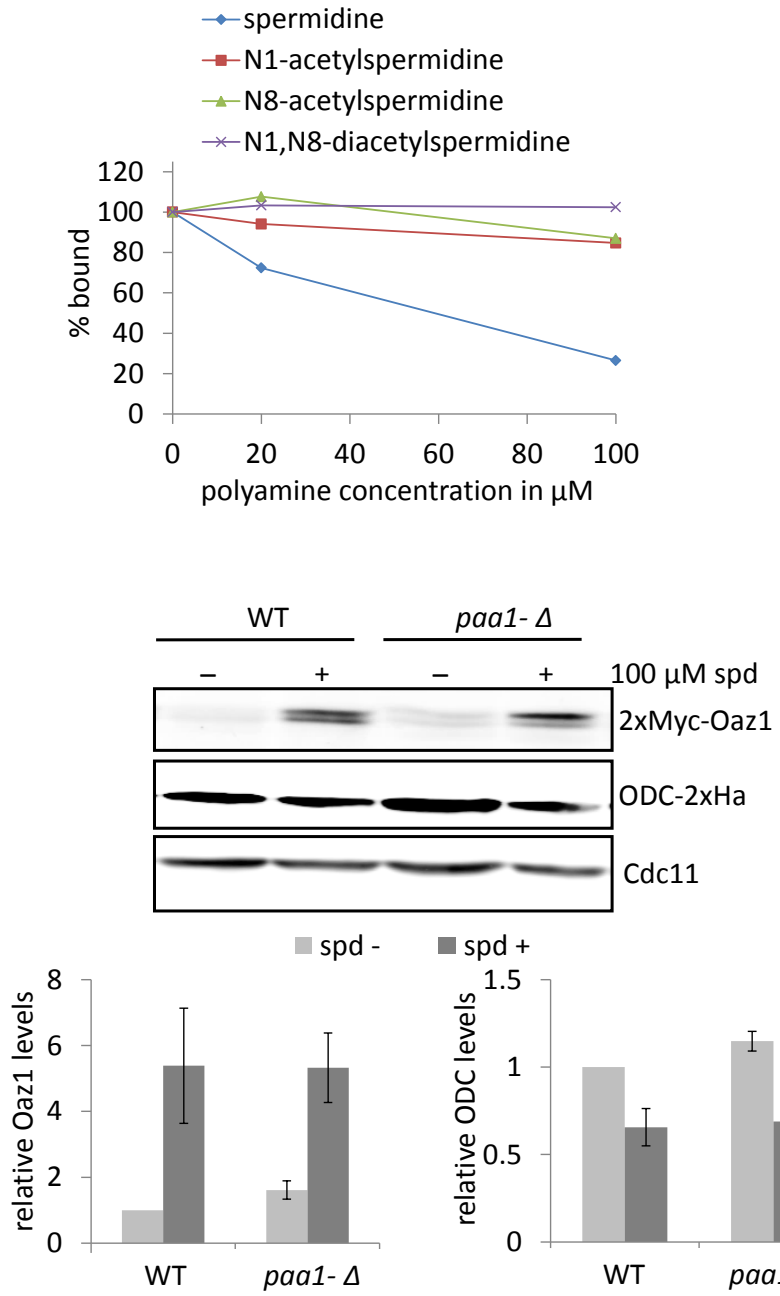

Fig. 13: Role of acetylated polyamines in the feedback regulation of ODC. (A) Acetylation of spermidine inhibits its binding to antizyme. *In vitro* binding assay showing the competition between [^{3}H]-spermidine and different species of acetylated spermidine for binding to 6xHis-tagged antizyme purified from *E. coli.* **(B)** Western blot analysis after SDS-PAGE comparing steady state levels of Oaz1 and ODC in either the wild-type or a strain lacking polyamine acetyltransferase (*paa1-Δ*), grown with or without 100 µM spermidine as indicated. The graph shows the results of a quantification of Myc (left) and Ha signals (right) normalized to the Cdc11 loading control. Levels are given relative to the respective levels of the same proteins in cells grown without polyamine addition, which was set to 100%. Error bars, s.d.; *n* = 3.

4.2. Characterization of ubiquitin-independent substrate recognition by the proteasome

Ubiquitin-dependent substrates have well-characterized proteasomal receptors that recognize polyubiquitin chains (Finley et al., 2012). However, how ubiquitin-independent substrates get recognized by the 26S remains elusive. Several hypotheses have been put forth by various laboratories to explain ubiquitin-independent proteasomal recognition. Zhang et al. suggested that ubiquitylated substrates and ODC-antizyme compete for the same binding sites on the proteasome (Zhang et al., 2003). Inobe and Matouschek suggested in a recent review that ubiquitin-independent substrates have unstructured domains which themselves have sufficient binding affinity to the ATPase ring loops thereby eliminating the requirement for ubiquitin (Inobe and Matouschek, 2014). In this chapter, I explored some of these hypotheses using ODC and other ubiquitin-independent substrates.

4.2.1. ODS is essential for proteasomal binding of ODC

Gödderz et al. showed that ODS is a transplantable and replaceable degron and that it's exposure is essential for ODC degradation (Godderz et al., 2011). For ubiquitin-dependent proteasomal substrates, binding to the proteasome is mediated by polyubiquitin chains and the unstructured region engages the ATPases for substrate translocation and unfolding (Lander et al., 2012; Prakash et al., 2004). For ODC degradation, it remains unclear whether the unstructured region simply engages the ATPases or also takes over the role of ubiquitin and mediates proteasomal binding. To answer this question, a blue native PAGE-based *in vitro* binding assay of purified ODC/Oaz1 heterodimer to purified 26S proteasome was developed as shown in Fig.14. Using this assay, I recapitulated the binding of ODC/Oaz1 heterodimer to the 26S proteasome as shown by the superimposition of the Ha signal (ODC-2xHa) with the signals from various proteasome specific antibodies (Fig. 15; lane 5). As expected, the co-migration of the substrate with the 26S proteasome band was lost in the case of the ΔODS variant as well as of the ODC homodimer (Fig.15; lanes 6 and 7) showing that ODS is essential for proteasome association of ODC/Oaz1 heterodimer. However, this assay does not exclude the presence of another binding element in the heterodimer such as the antizyme.

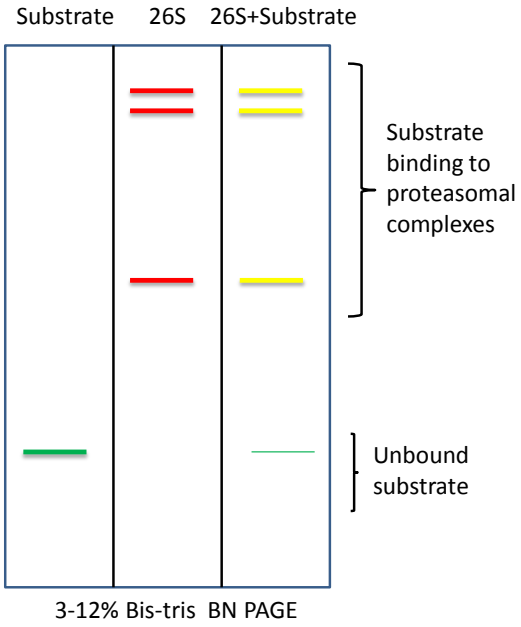

Fig. 14: Schematic representation of the blue native PAGE analysis of binding. A low molecular weight test substrate tagged with an epitope is mixed with 26S proteasomes and then separated on a 3-12% bis-tris BN PAGE gel. Western blot analysis after BN PAGE with the anti-epitope antibody would reveal the migration of the test substrate along with the proteasome, if binding occurs.

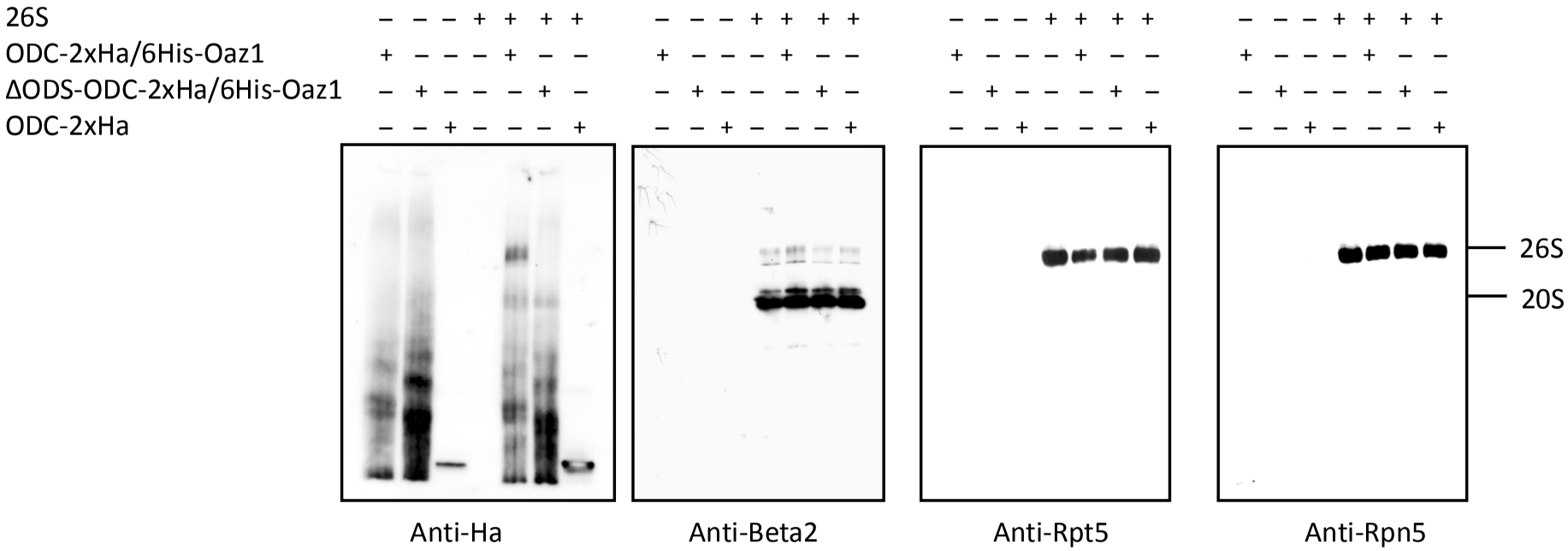

Fig 15: ODS-dependent binding of ODC-Oaz1 to the 26S proteasome. Western blot analysis after a blue native PAGE-based *in vitro* binding assay with purified 26S proteasome and purified ODC-Oaz1 heterodimer showing the binding of ODC-2xHa to 26S proteasome. 50 ng of ODC-Oaz1 and 4 µg of 26S were used. A detailed description of this assay is described in the methods section. After detection of Ha signals (using Anti-Ha 3F10), three different antibodies (Anti-Beta2, Anti-Rpt5 and Anti-Rpn5) were used one after the other by stripping and re-probing to show the co-migration of ODC-Oaz1 with 26S. As negative control, ODC-Oaz1 heterodimer lacking ODS (ΔODS-ODC-Oaz1) and ODC homodimer was used.

4.2.2. Proteasomal lid is dispensable for *in vitro* degradation of ODC by the proteasome

Gödderz et al. showed that the lid subcomplex is not required for ubiquitin-independent degradation of ODC in yeast cells (Godderz et al., 2011). They studied the steady state levels of ODC in the *rpn5-ΔCT* strain in which lid formation was impaired without affecting the base subcomplex (Isono et al., 2007). Steady state ODC levels were not altered whereas the levels of R-DHFR-2xHa, a ubiquitin-dependent substrate were increased. These data suggested that the lid subcomplex might be dispensable for ODC degradation. However, it is possible that the residual amounts of lid in the *rpn5-ΔCT* mutant were enough to carry out ODC degradation. To address this question, 26S particles lacking the lid subcomplex were isolated from yeast cells, and ODC degradation using ODC/Oaz1 heterodimer as a substrate was carried out as described in subsection 4.1.1. The absence of the lid and the presence of other subcomplexes in the proteasome preparation were confirmed using various proteasome-specific antibodies as shown in Fig. 16. As anticipated, ODC was degraded both by the normal 26S particles as well as by proteasomes lacking the lid (26S-lid), whereas the antizyme remained stable. This observation further reinforces the *in vivo* data from Gödderz et al. that the lid is dispensable for ODC degradation.

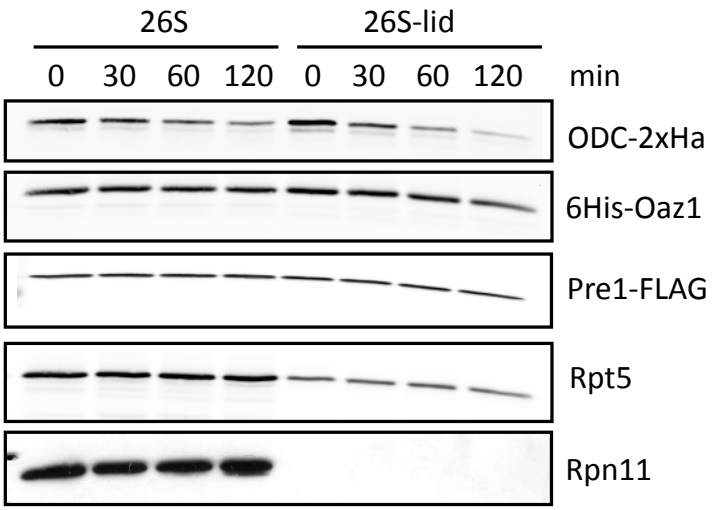

Fig. 16: *In vitro* degradation of ODC by 26S proteasomes lacking the lid subcomplex. Western blot analysis after SDS-PAGE showing *in vitro* degradation of ODC with purified 26S particles and 26S particles lacking the lid (26S-lid). ODC-2xHa and 6His-Oaz1 was detected with anti-Ha and anti-Oaz1 antibodies, respectively. The blot was reprobed with antibodies against the different proteasome subunits as indicated.

4.2.3. ODC is not recognized by the canonical ubiquitin receptors

Zhang et al. showed that both substrate-linked and free polyubiquitin chains compete with mouse ODC for degradation and therefore suggested that ODC might also be recognized by ubiquitin receptors at the proteasome (Zhang et al., 2003). Conversely, Gödderz showed that steady-state levels of ODC are reduced in mutants lacking one or a combination of ubiquitin receptors suggesting that ubiquitin receptors might not recognize ODC (Gödderz, 2010). It is however possible that multiple ubiquitin receptors might be involved in ODC reception at the proteasome. Therefore, steady state levels of ODC were checked in a strain lacking multiple ubiquitin receptors and shuttle factors. This strain lacks the shuttle factors Rad23 and Dsk2 and the ubiquitin interaction motifs of the intrinsic ubiquitin receptors, Rpn10 and Rpn13. The steady state levels of ODC were drastically reduced in the mutant strain compared to wild-type. Upon induction of ODC degradation with 100 µM spermidine, the ODC levels in the mutant were further reduced. Taken together, the data suggest that ODC recognition at the proteasome is not mediated by the canonical ubiquitin receptors and that the faster degradation of ODC in these mutants might be due to reduced competition with ubiquitylated substrates at a step downstream of proteasomal reception.

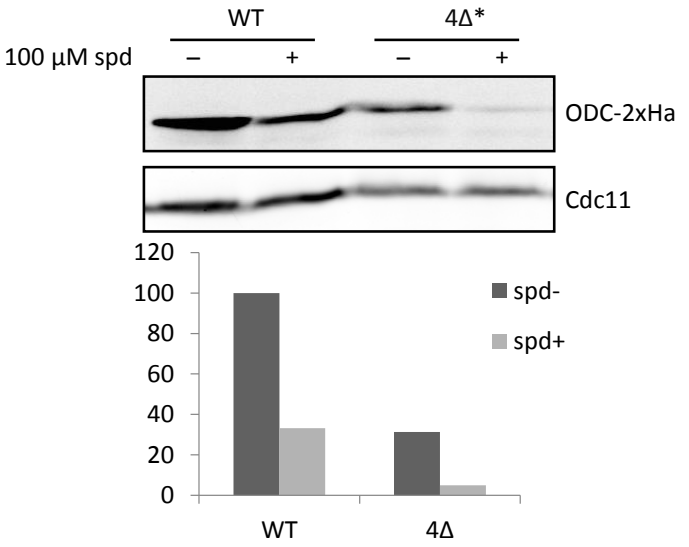

* 4Δ*: rad23-Δ dsk2-Δ rpn10-ΔUIM rpn13-ΔKKD*

Fig. 17: ODC is degraded faster in a mutant lacking multiple ubiquitin receptors. Western blot analysis after SDS-PAGE comparing steady state levels of ODC in wild-type versus the mutant *rad23-*Δ *dsk2-*Δ *rpn10-*Δ*UIM rpn13-*Δ*KKD* grown with or without 100 µM spermidine as indicated. The graph shows the results of a quantification of Ha signals normalized to the Cdc11 loading control. Levels are given relative to the respective levels of ODC-2xHa in cells grown without polyamine addition, which was set to 100%.

4.2.4. Human p21 is degraded by the yeast proteasome and competes with ODC for degradation

p21, the cyclin-dependent kinase inhibitor, is a critical cell cycle regulator in mammals (Sherr and Roberts, 1999). p21 is tightly regulated at the level of its transcription as well as by proteolytic degradation. Ubiquitin dependence of p21 degradation is an unresolved issue. A lysine-less variant of p21 was unstable showing that its degradation does not completely rely on ubiquitylation (Sheaff et al., 2000). However, another group later showed that p21 was polyubiquitylated at its N-terminal methionine which might be sufficient for its degradation (Bloom et al., 2003). In short, it is still not clearly established how p21 is targeted to the proteasome.

p21 is a globally loosely folded protein lacking a proper secondary or tertiary structure which makes it a suitable candidate for ubiquitin-independent degradation pathway (Richard W. Kriwacki 1997). There is no known homologue of p21 in yeast. However, it is interesting to study if the loosely folded structure of p21 would enable its ubiquitin-independent degradation in yeast. Also, it would be a useful substrate for

comparative studies with ODC to elucidate common mechanisms underlying ubiquitin-independent proteolytic pathway.

Therefore, I studied the degradation of human p21 (hp21) in yeast. hp21 tagged at its C terminus with 2xHa was expressed under the $CuSO_4$ inducible cup promoter. The steady state levels of hp21 in a WT strain was compared with the proteasome mutant *pre1-1* and the ubiquitin-activating enzyme (E1) mutant *uba1-ts26* at 30^{o}C after induction with $CuSO_4$. The total protein isolated was fractionated into pellet and supernatant fractions. p21 was non-detectable in all fractions of the WT strain (Fig. 18A; lanes 1-3) whereas in the *pre1-1* mutant, p21 was detected both in the pellet and the supernatant (Fig. 18A; lanes 4-6). Interestingly, in the *uba1-ts26* mutant p21 accumulated mainly in the pellet fraction (Fig. 18A; lanes 7-9). This indicates that the degradation of hp21 occurs via the ubiquitin-dependent as well as -independent modes in yeast. The soluble p21 is degraded via the ubiquitin-independent route whereas the insoluble fractions are most likely taken care of by the quality control pathway which is ubiquitin-dependent.

The results described above establish that p21 is rapidly degraded in yeast. Therefore, it is interesting to ask whether p21 competes with ODC for degradation. To answer this question, the steady state levels of ODC were studied upon hp21 overexpression. The $CuSO_4$ inducible hp21-2xHa was co-expressed with ODC-2xHa expressed under the ODC promoter. ODC-2xHa co-expressed with the vector plasmid served as the control. In a WT strain, no stabilization of ODC was seen when hp21 was overexpressed (Fig18B, right panel). Consequently, the experiment was repeated in the *ump1-Δ* mutant which lacks the proteasome maturation factor Ump1 and therefore has reduced amounts of functional proteasomes (Ramos et al., 1998). Steady state levels of ODC were higher when p21 was overexpressed (Fig18B, left panel). It is however interesting to note that steady state levels of ODC were unaffected in the *ump1-Δ* mutant compared to wild-type (Gödderz, 2010). Therefore, when the proteasome activity is compromised, a competition of ODC with hp21 for degradation in yeast can be demonstrated.

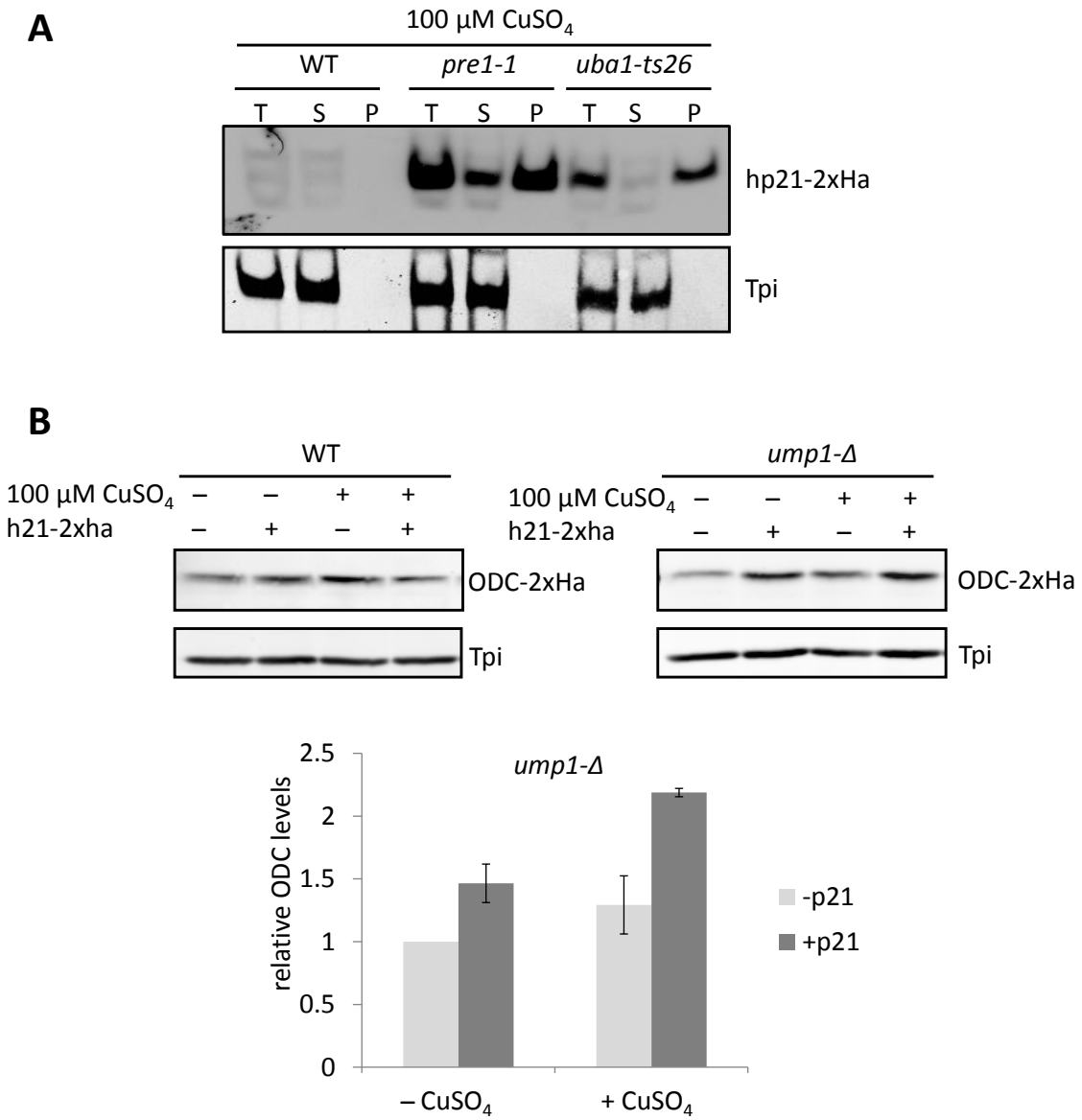

Fig. 18: Ubiquitin-independent proteasomal degrdation of human p21 in yeast and its competition with ODC for degradation. (A) Western blot analysis after SDS-PAGE showing steady state levels of human p21 in *pre1-1* and *uba1-ts26* mutant strains compared to wild-type. The expression of hp21 was induced with 100 µM $CuSO_4$. After glass-bead lysis of the pelleted yeast cells, the total lysate (T) was centrifuged at 30000x*g* for 30 min to separate the supernatant (S) and pellet (P) fractions. **(B)** Western blot analysis after SDS-PAGE comparing steady state levels of ODC with or without co-expression of h21 and grown in the presence or absence of 100 µM $CuSO_4$ as indicated. This comparison was done in WT and *ump1-Δ* strains. The graph shows the results of a quantification of ODC-2xHa signals normalized to the Tpi loading control. Levels are given relative to the respective levels of ODC-2xHa in cells grown without 100 µM $CuSO_4$ and co-expression of hp21, which was set to 1. Error bars, s.d.; *n* = 2.

4.2.5. Specificity of Rpt4 and Rpt5 Ar-Φ loop in substrate engagement and targeting of ODC

The experiments detailed above have demonstrated that ODS mediates proteasomal binding of ODC/Oaz1 heterodimer to the 26S proteasome and that it binds most likely to the base subcomplex as the lid was dispensable for ODC degradation. The base subcomplex consists of the hexameric Rpt1-6 ATPase ring as well as the Rpn1 and Rpn2 subunits. Axially positioned aromatic-aliphatic (Ar-Φ) loops of the six ATPases are thought to make contact to unstructured domains in substrates engaging them for proteasomal targeting (Zhang et al., 2009). Erales et al. showed that the six different ATPases have asymmetric functions. They individually mutated conserved tyrosine residues to alanine (Y-A) in the Ar-Φ loop of each of the six Rpt subunits and showed by analysing the resulting strains that the Ar-Φ loops of the Rpt subunits are functionally different. Interestingly, they also showed that mouse ODC is specifically stabilized when expressed in yeast *rpt4* and *rpt5* Y-A loop mutants (Erales et al., 2012). Therefore, I asked whether the same is true for yeast ODC. Analysis of the steady-state levels of ODC revealed that yeast ODC is also specifically stabilized in *rpt4* and *rpt5* mutants (Fig. 19A). This observation prompted me to ask whether Rpt4 and Rpt5 loops are the most important for the degradation of all proteasomal substrates. Therefore, steady state levels of few other ubiquitin-independent and ubiquitin-dependent substrates were checked in these mutants. The artificial ubiquitin-independent fusion substrate ODS-Ura3 (Godderz et al., 2011) was not stabilized in any of the *rpt* mutants (Fig. 19B). Similar was the case with hp21. However, hp21 is a rapidly degraded protein and therefore its levels are hard to detect in wild-type cells as shown in Fig 18A. No p21 could be detected by western blot in any of the *rpt* mutants indicating that their degradation is not impaired in these mutants (data not shown). I then analysed the steady state levels of three different ubiquitin-dependent substrates, namely, yeast antizyme (Palanimurugan et al., 2004), an N-end rule substrate (Ub-R-e^{K}-Ha-Ura3) and a Ubiquitin Fusion Degradation (UFD) pathway substrate (Ub-V76-e^{K}-Ha-Ura3)(Ghislain et al., 1996; Varshavsky, 1996). Unlike ODC, no specific preferences for any of the Rpt subunits were observed (Fig. 20A-C).

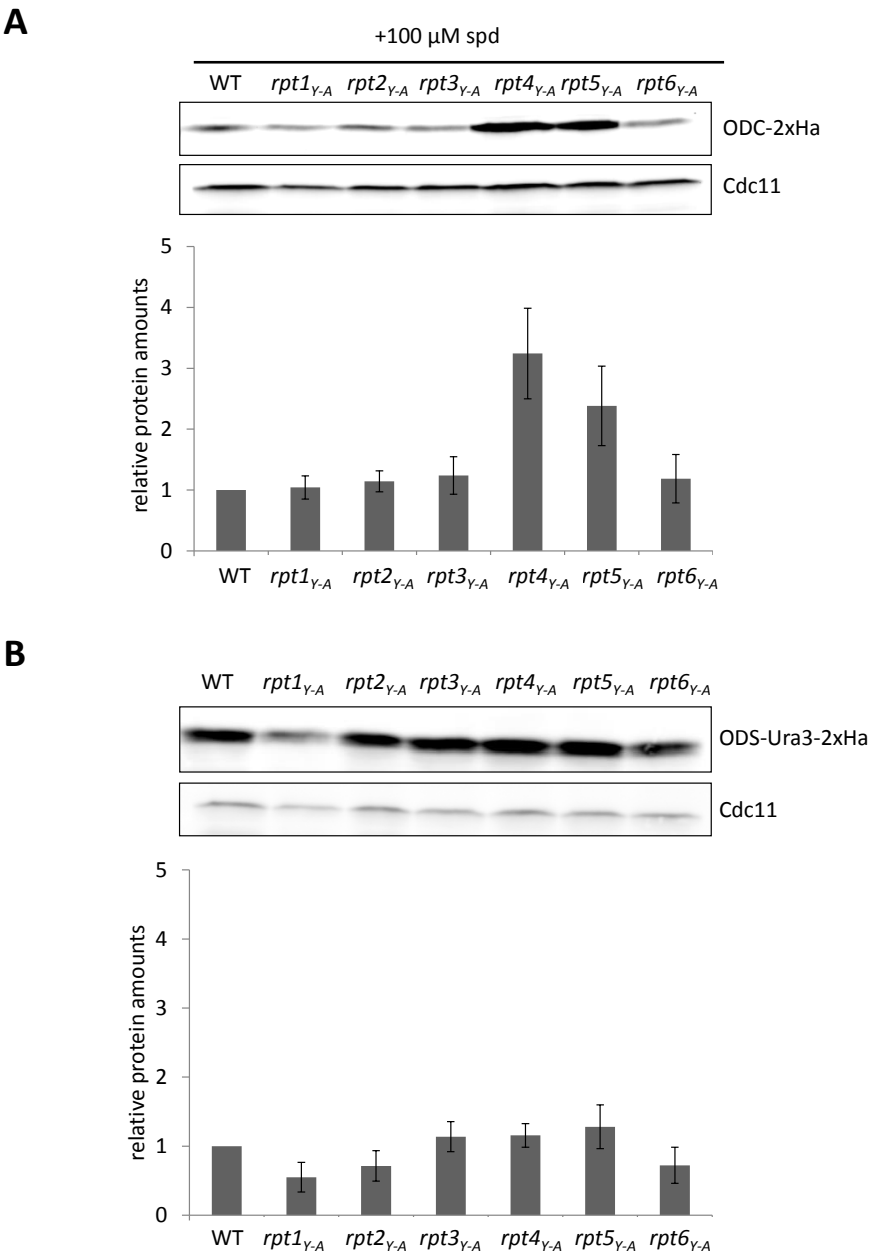

Fig. 19: ODC is stabilized in *rpt4* and *rpt5* loop mutants. (A) Western blot analysis after SDS-PAGE showing steady state levels of ODC-2xHa in $rpt_{Y\text{-}A}$ loop mutants compared to wild-type. The growth media were supplemented with 100 µM spermidine to induce ODC degradation. **(B)** Western blot analysis after SDS-PAGE showing steady state levels of ODS-Ura3 in $rpt_{Y\text{-}A}$ loop mutants compared to wild-type. The graphs show the results of a quantification of the corresponding Ha signals normalized to the Cdc11 loading control. Levels are given relative to WT, which was set to 1. Error bars, s.d.; for A, n =4 and for B, n =3.

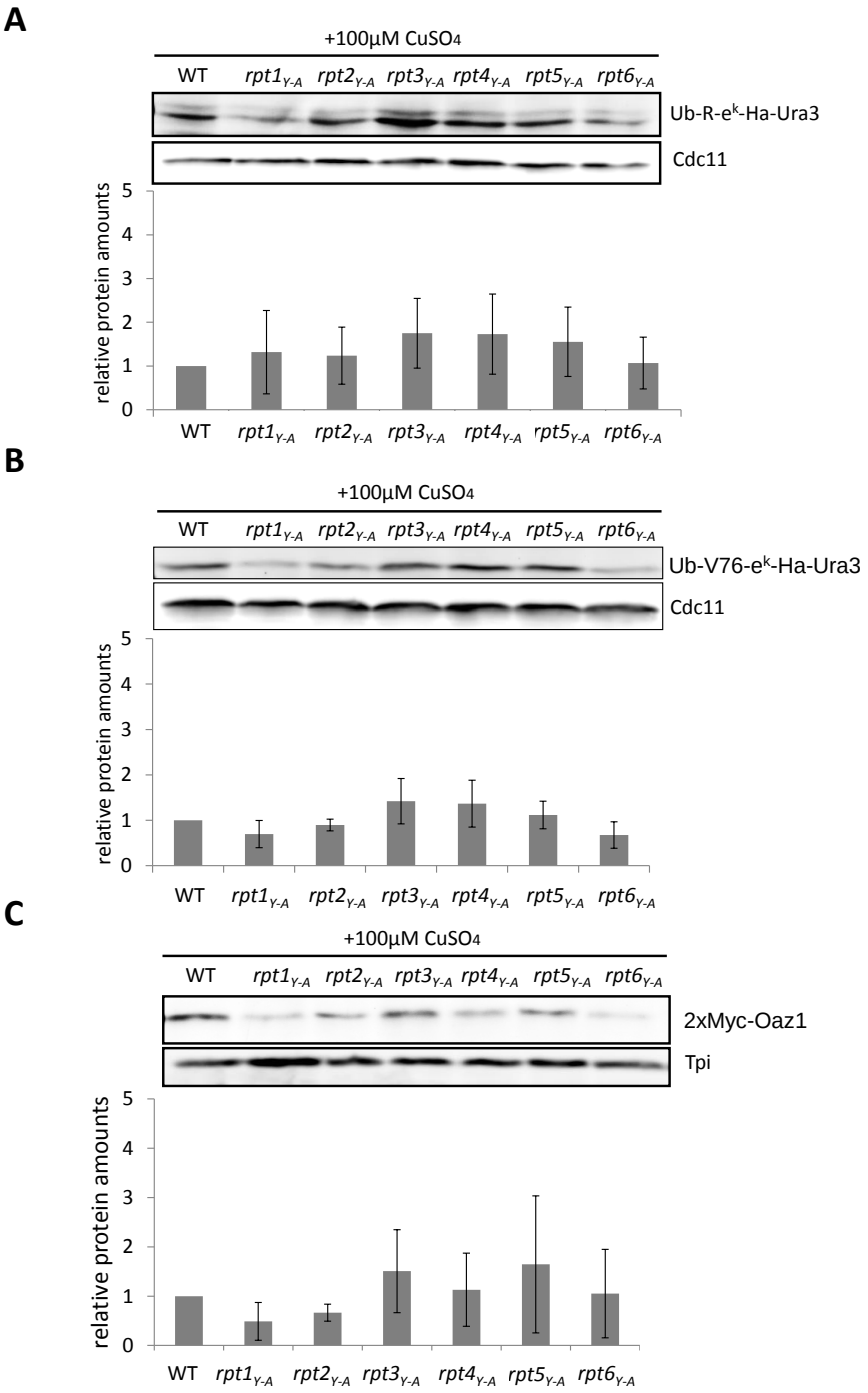

Fig. 20: Ubiquitin-dependent substrates are not strongly stabilized in *rpt4* and *rpt5* loop mutants. (A) Western blot analysis after SDS-PAGE showing steady state levels of Ub-R-eK-Ha-Ura3 in $rpt_{Y\text{-}A}$ loop mutants compared to wild-type. Protein expression was induced with 100 µM $CuSO_4$. Western blot was done with anti-Ha antibody. **(B)** Same as in (A) but with Ub-V76-eK-Ha-Ura3 as a substrate. **(C)** Same as in (A) and (B) with 2xMyc-Oaz1 as a substrate. Anti-Myc antibody was used for western blot analysis. The graphs show the results of a quantification of the corresponding Ha or Myc signals normalized to the Cdc11 or Tpi loading controls. Levels are given relative to WT, which was set to 1. Error bars, s.d.; for A, n =3, for B, n =3 and for C, n=2.

4.3. Characterization of the role of antizyme in ODC targeting

The established role of antizyme in ODC degradation is the formation of a heterodimer with ODC and inducing a conformational change thereby exposing the ODC degradation signal (Godderz et al., 2011; Li and Coffino, 1993). However, it has been hypothesised that antizyme may play a further role in ODC degradation. Li and Coffino showed that an N-terminal half of antizyme is necessary for ODC degradation although it is the C-terminal half of antizyme that mediates the exposition of the degradation signal (Li and Coffino, 1994). Using spacer sequence insertions between ODS and the rest of ODC, Gödderz et al. showed that exposure of ODS alone can trigger Oaz1-independent degradation of ODC in yeast. Interestingly the presence of antizyme further destabilized these ODC variants (Godderz et al., 2011). These observations point to the possibility that antizyme does something more than exposition of ODS. In this section, I explored this hypothesis using an array of antizyme fusion constructs.

4.3.1. ODS fused to stable antizyme is degraded in a ubiquitin-independent manner

In addition to the unstructured domain, antizyme might provide a binding site to the proteasome to mediate ubiquitin-independent ODC degradation. Therefore, a stable version of antizyme (Oaz1-4res) (Fig. 21B) was used to make antizyme fusion constructs to check whether antizyme could target otherwise stable proteins like Ura3 to the proteasome. Four different constructs were made as shown in Fig. 20A. Cycloheximide chase analysis of these constructs revealed that the antizyme fusion to Ura3 does not change the stability of the protein [Fig. 21C; (Stadelmayer, 2014)]. Interestingly however, the ODS-Oaz1-4res fusion protein was unstable (Fig. 21D) as was the ODS-Oaz1-4res-Ura3 fusion (Fig. 21E). It was therefore imperative to ask if this observed degradation is ubiquitin-independent or not and whether it is mediated by the proteasome. This was indeed the case. As observed earlier for ODC, both ODS-Oaz1-4res and ODS-Oaz1-4res-Ura3 were degraded faster in a *uba1-ts26* mutant (Fig. 22A and C). This indicates that these substrates compete with ubiquitin-independent substrates at the proteasome. Addition of the proteasome inhibitor MG132 partially stabilized both fusion proteins showing that they are indeed degraded in a ubiquitin-independent manner by the proteasome (Fig. 22B and D).

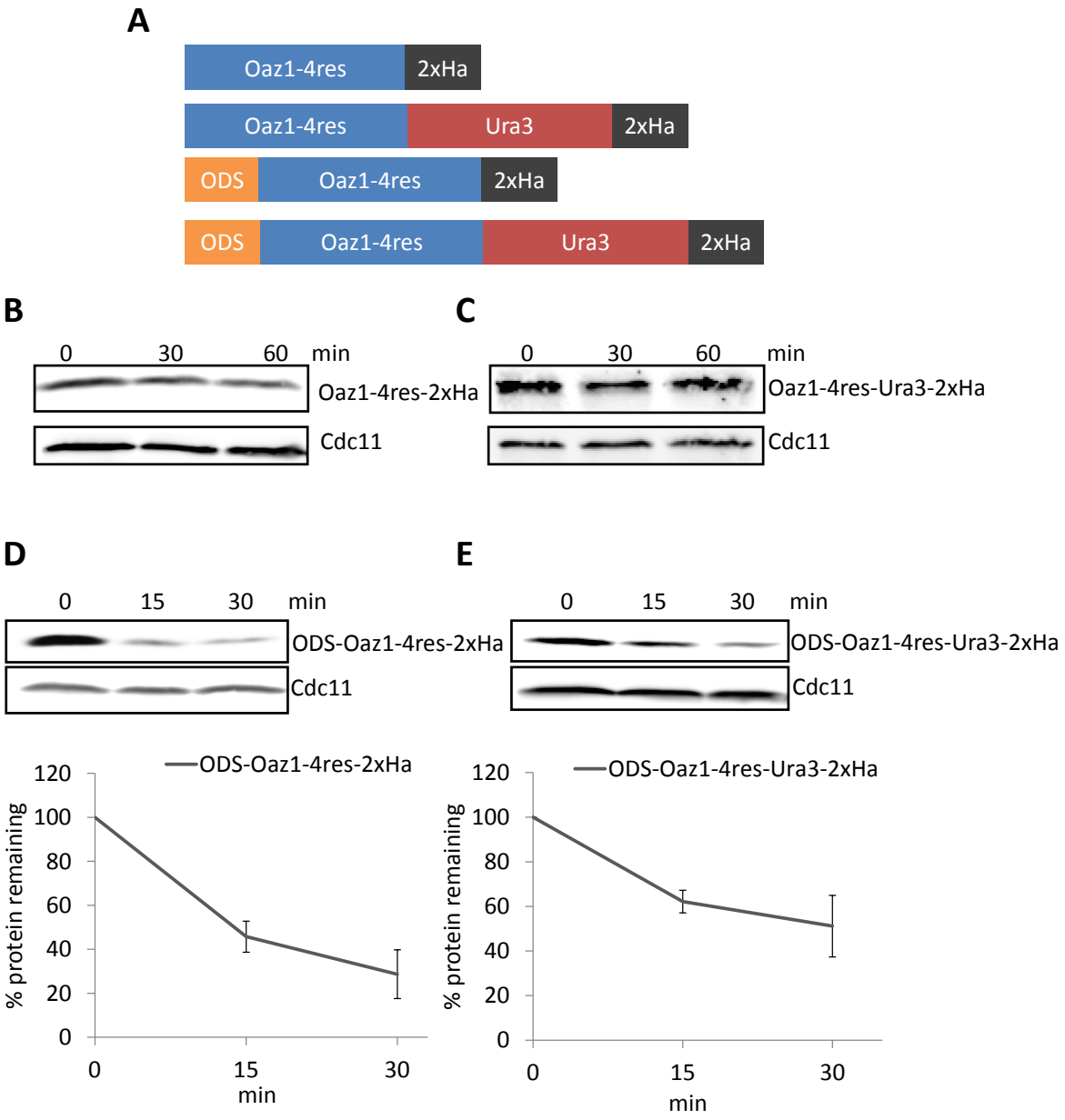

Fig. 21: Stability of various antizyme fusion constructs. (A) Schematic representation of the various antizyme-4res fusion constructs. **(B)** Cycloheximide chase experiments showing that Oaz1-4res-2xHa is a stable protein in yeast. **(C)** Same as in (B) but with the construct Oaz1-4res-Ura3-2xHa. **(D)** Cycloheximide chase experiments showing that ODS-Oaz1-4res-2xHa is rapidly degraded in yeast. **(E)** Same as in (D) but with the construct ODS-Oaz1-4res-Ura3-2xHa. All western blot analyses were done with anti-Ha antibody. Cdc11 served as loading control. The graphs show the results of a quantification of the corresponding Ha signals normalized to Cdc11. Levels are given relative to the protein levels at 0 time point which was set to 100%. Error bars, s.d.; for D, n =3, and for E, n =2

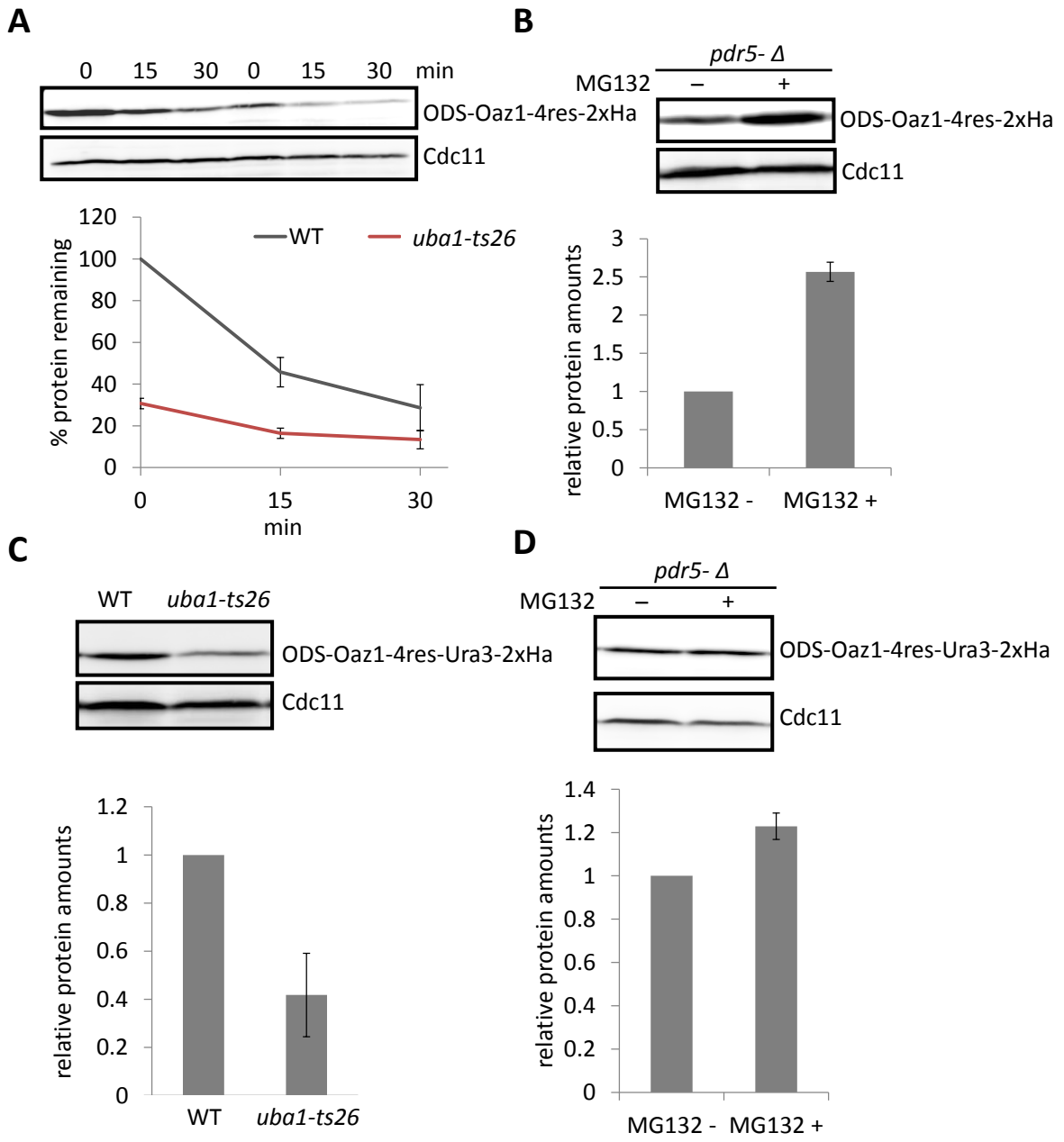

Fig. 22: Ubiquitin-independent proteasomal degradation of antizyme fusion constructs. (A) Cycloheximide chase experiment showing that ODS-Oaz1-4res-2xHa is degraded faster in a *uba1-ts26* mutant compared to wild-type. The graph shows the results of a quantification of the corresponding Ha signals normalized to Cdc11. **(B)** Steady state levels of ODS-Oaz1-4res-2xHa in *a pdr5-Δ* strain with and without proteasome inhibition with 20 µM MG132 for 1 hour. **(C)** Steady state levels of ODS-Oaz1-4res-Ura3-2xHa in *a uba1-ts26* strain compared to wild-type. **(D)** Same as in (B) but with the construct ODS-Oaz1-4res-Ura3-2xHa. All western blot analyses were done with anti-Ha antibody. Cdc11 served as loading control. The graphs show the results of a quantification of the corresponding Ha signals normalized to Cdc11. Levels are given relative to either the protein levels in a wild-type strain or in the control yeast cells without proteasome inhibition which were set to 1. Error bars, s.d.; for A, B, D n =3, and for C, n =4.

4.3.2. Antizyme might have a binding site on the proteasome

Gödderz et al. showed that the fusion of ODS to certain stable proteins like Ura3 can convert them to ubiquitin-independent proteasomal substrates. However, the ODS-Ura3 fusion protein is not degraded as efficiently as ODC in yeast cells. There might be several reasons for its higher stability. One hypothesis is that ODS alone is not sufficient to effectively target proteins to the proteasome. Therefore, I asked if fusing ODS-Ura3 to stable antizyme renders it more unstable. A growth assay was performed and the growth of wild-type yeast harbouring one of these constructs was scored on minimal media lacking uracil. The observed phenotypes indicate that ODS-Oaz1-4res-Ura3 is less stable than ODS-Ura3 or Ura3 (Fig. 23A). This suggests that the presence of both ODS and antizyme enhances the degradation of the Ura3 fusion protein indicated that antizyme helps substrate binding to the proteasome. As in the case of ODC, ODS-Oaz1-4res-Ura3 is stabilized in $rpt4_{Y\text{-}A}$ and $rpt5_{Y\text{-}A}$ loop mutants (Fig. 23B). This is a strong indication that both ODC and this fusion substrate have similar mechanisms of proteasomal targeting.

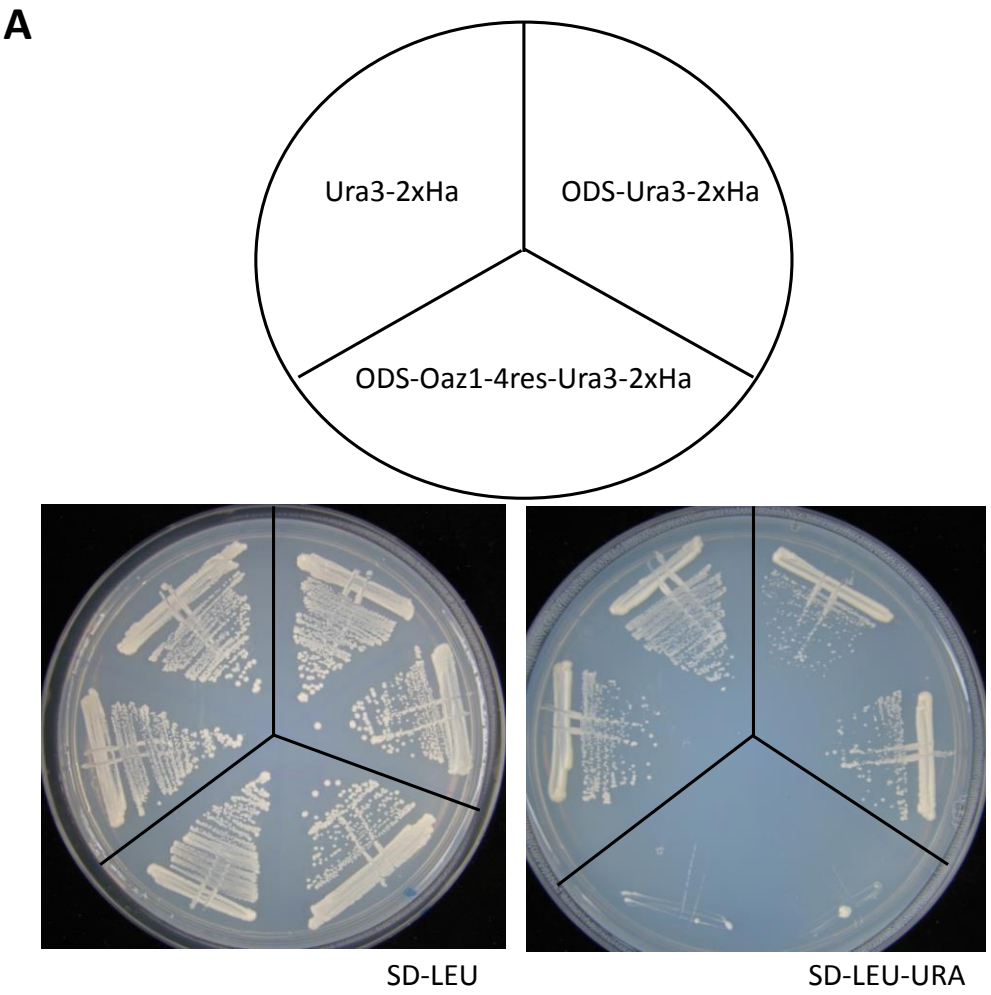

Fig. 23: Antizyme fusion reduces the stability of ODS-Ura3. (A) Growth assay showing the phenotype of a wild-type strain transformed with plasmids encoding Ura3-2xHa, ODS-Ura3-2xHa, and ODS-Oaz1-4res-Ura3-2xHa in minimal medium lacking LEU (left) or LEU-URA (right). **(B)** Growth assay showing the phenotypes of the various $rpt_{Y\text{-}A}$ loop mutants compared to wild-type transformed with the plasmid ODS-Oaz1-4res-Ura3-2xHa in minimal medium lacking LEU (top) or LEU-URA (bottom).

4.3.3. A genetic screen for the isolation of ODC stabilizing mutants

Gödderz had previously performed a genetic screen for the isolation of mutants impaired in ODC degradation (Gödderz, 2010). A similar screen was setup aimed mainly at the identification of factors involved in ODC targeting in particular the binding sites of ODS and antizyme in the proteasome. As shown in Fig. 24, the parent strain harboured a genomic fusion of ODC encoding sequence to the auxotrophic marker *LEU2* inserted into the *LEU2* locus, a plasmid with the ubiquitin-independent proteasomal substrate ODS-Oaz1-4res-Ura3-2xHa described in sections above, and a plasmid expressing the ubiquitin-dependent substrate R-β-gal from the P_{GAL1} promoter. The mutants were selected on minimal media plates lacking histidine and tryptophan (for the section of the plasmids) and either leucine or uracil or both (for selection of mutants that stabilized the reporter proteins). Mutants which are both Leu+ and Ura+ and not stabilizing the R-β-gal protein are the most desired ones as they would most likely be specifically affected in ODC targeting.

The mutants isolated were subjected to various phenotypic analyses as shown in table 1. The dominant or recessive nature of the mutants was analysed by scoring the Leu and Ura phenotype upon crossing to a wild-type strain of the opposite mating type. Out of the several mutants picked from various plates, very few were both Leu+ and Ura+. Most of the mutants were recessive. Mutants 29, 31 and 61 were the most interesting as they were both Leu+ and Ura+ and did not affect the degradation of the R-β-gal protein. Further analysis includes grouping of these mutants into phenotypic classes and mapping their genomic positions. Mapping can be done either using the classical genetic complementation analyses or by whole genome sequencing.

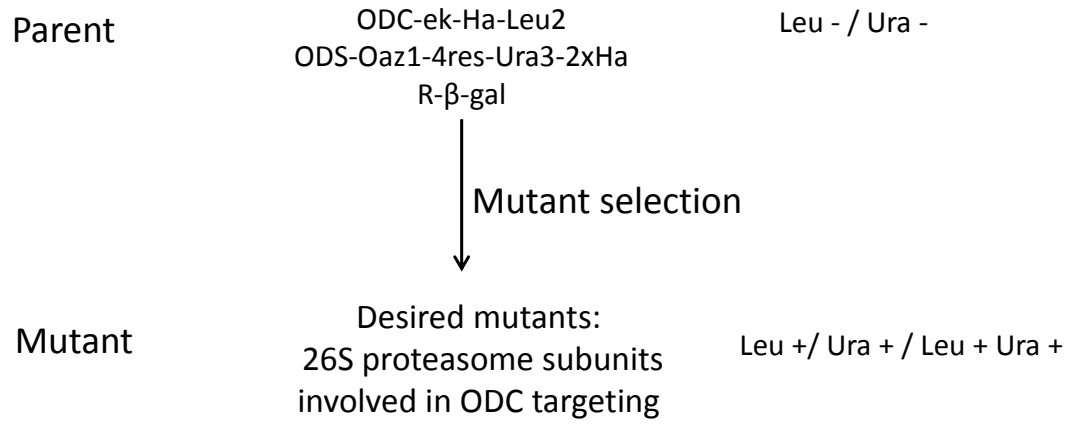

Fig. 24: The setup of the spontaneous mutant screen for the isolation of ODC stabilizing mutants

Table1: Phenotypic analysis of isolated mutants

Mutant No.	Selection plate	Leu	Ura	YPD 37^0C	SD 37^0C	β-Gal	Dominant/ Recessive
1	Ura	–	+++	+++	+++	–	Dom
6	Ura	–	+	+	+	++	Res
9	Leu	+++	–	+++	+++	–	Res
16	Ura	–	+	+	+	white	Res
27	Leu	++	+	+++	+	+++	Res
29	Leu	+++	+	+++	+++	–	Res
31	Leu	+++	+	+++	+++	–	Res
36	Leu	++	–	+++	+++	–	Res
37	Ura	–	(+)	+	+	+	Res
38	Ura	–	++	+++	+++	–	Res
39	Ura	–	+++	+++	+++	–	Res
42	Ura	–	(+)	+	+	–	Res
44	Ura	–	+	++	+	(+)	Res
45	Ura	(+)	(+)	+	+	+	Res
49	Ura	–	++	+	+	–	Res
61	Leu	+++	+	+++	+++	–	Res
64	Leu	++	++	+++	+++	+	Res

– indicated same as WT and + indicates positive deviation from WT

4.4. Ubiquitin-dependent degradation of ODC

ODC is one of the few ubiquitin-independent substrates of the proteasome that is thought to be degraded solely in a ubiquitin-independent manner. Recent data from our lab, however, suggested that this may not be the case. ODC, when expressed under the $CuSO_4$-inducible P_{CUP1} promoter was degraded in an ubiquitin-dependent manner by the proteasome (Gödderz, D, unpublished data). Gödderz observed increased ODC levels in the proteasome mutant *pre1-1* as well as in the E1 mutant *uba1-ts26* compared to wild-type, suggesting that ODC under these conditions is degraded in a ubiquitin-dependent manner by the proteasome. In this chapter, I reproduced this observation and further explored the factors involved in ubiquitin-dependent ODC degradation.

4.4.1. ODC is degraded by the proteasome in a ubiquitin-dependent manner upon overexpression

Previous data from our lab showed that ODC-GFP when overexpressed along with antizyme, formed cellular aggregates upon proteasomal inhibition (Gödderz, 2010). Also when human p21 was expressed from the P_{CUP1} promoter, the ubiquitin-dependent fraction was mainly seen in the pellet showing that aggregated p21 is ubiquitylated and degraded by the proteasome (Fig. 18A). It could therefore be possible that ubiquitin-dependent ODC degrdation is simply a result of its aggregation. To rule out this possibility, I checked whether ODC formed aggregates upon its overexpression along with antizyme. Both ODC and Oaz1 were expressed from the P_{CUP1} promoter and their steady state levels were analysed with and without $CuSO_4$ addition. The cell lysates were subjected to ultracentrifugation (100000x*g*) for 30 minutes and the fractions were separated by SDS-PAGE before western blot analysis (Fig. 25). As observed previously by Gödderz, a clear stablization of ODC was seen both with (Fig. 25A) and without (Fig. 25B) $CuSO_4$ induction in *pre1-1* and *uba1-ts26* mutants. In both cases, ODC accumulated mainly in the soluble fraction. Interestingly however, Oaz1 upon its overexpression was distributed between supernanat (S) and pellet (P) fractions. This is a good indication that Oaz1 is more aggregation-prone than ODC.

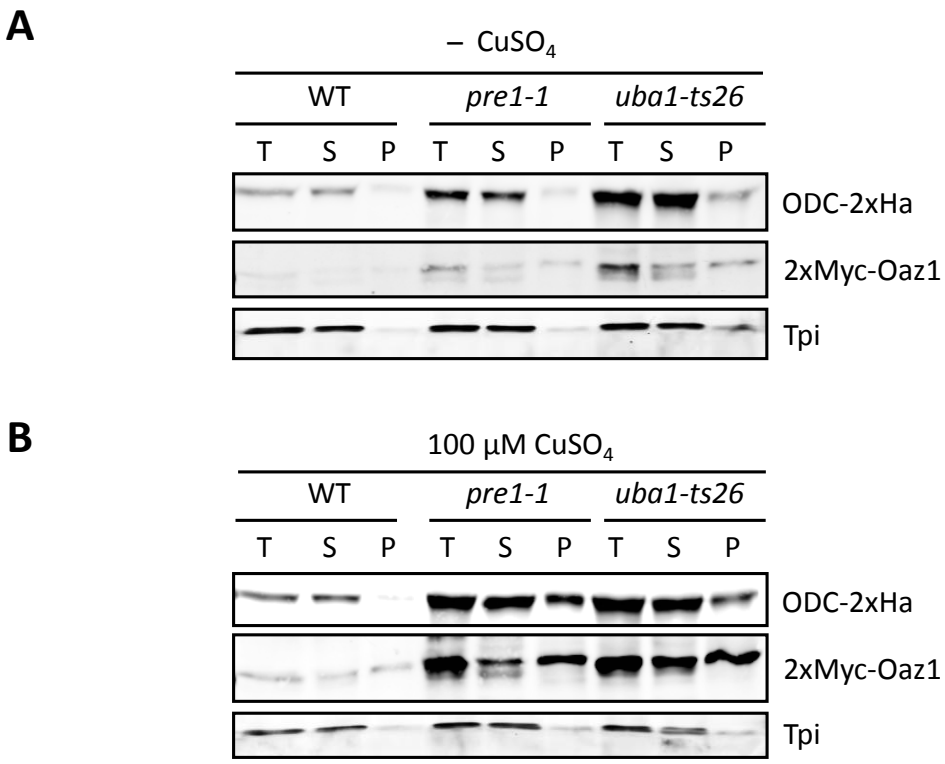

Fig. 25: Ubiquitin-dependent ODC degradation. (A) Western blot analysis after SDS-PAGE showing steady state levels of ODC and Oaz1 in *pre1-1* and *uba1-ts26* mutant strains compared to wild-type. After glass-bead lysis of the pelleted yeast cells, the total lysate (T) was centrifuged at high speed to separate the supernatant (S) and pellet (P) fractions. Tpi served as loading control. **(B)** Same as (A), except that the expression of both ODC and Oaz1 was induced with 100 µM $CuSO_4$.

4.4.2. Ubiquitin-dependent ODC degradation is independent of its unstructured domain

The requirement of the N-terminal unstructured domain (ODS) for ubiquitin-independent ODC degradation was discussed in detail in section 4.2.1. Therefore, an obvious question to ask was whether ODS is relevant for ubiquitin-dependent ODC degradation. Additionally, to rule out any influence of the 2xHa tag on ubiquitin-dependent ODC degradation, ODC and its variant without ODS (ΔODS-ODC) were constructed without any epitope. A rabbit polyclonal antibody against yeast ODC was used for western blot analysis. ODC and ΔODS-ODC were expressed from the P_{CUP1} promoter and their steady state levels were analysed in wild-type, *pre1-1* and *uba1-ts26* strains upon induction with $CuSO_4$. ODC was stabilized in *pre1-1* and *uba1-ts26* mutants compared to wild-type as previously observed, showing that the tag did not have any influence on this phenotype (Fig. 26A; lanes 1-3). Surprisingly, ΔODS-ODC was also stabilized in *pre1-1* and *uba1-ts26* mutants showing that ODS is not required for ubiquitin-dependent degradation of ODC (Fig. 26A; lanes 4-6).

I then asked whether the ubiquitin-dependent degradation of ODC requires polyamines. Steady state levels of ΔODS-ODC-2Xha were compared in a wild-type strain with and without spermidine. The ΔODS variant of ODC was used to rule out the influence of the ubiquitin-independent degradation pathway. No differences in steady state levels were seen showing that this mechanism does not depend on polyamines (Fig. 26B). Figure 26C shows the steady state levels of DHFR-2xHa, a stable protein. This experiment was done as a control to rule out any general influence of the P_{CUP1} promoter in *pre1-1* and *uba1-ts26* mutants. The levels do not change significantly in *pre1-1* and *uba1-ts26* upon induction with $CuSO_4$ showing that the observed effect is specific for ODC.

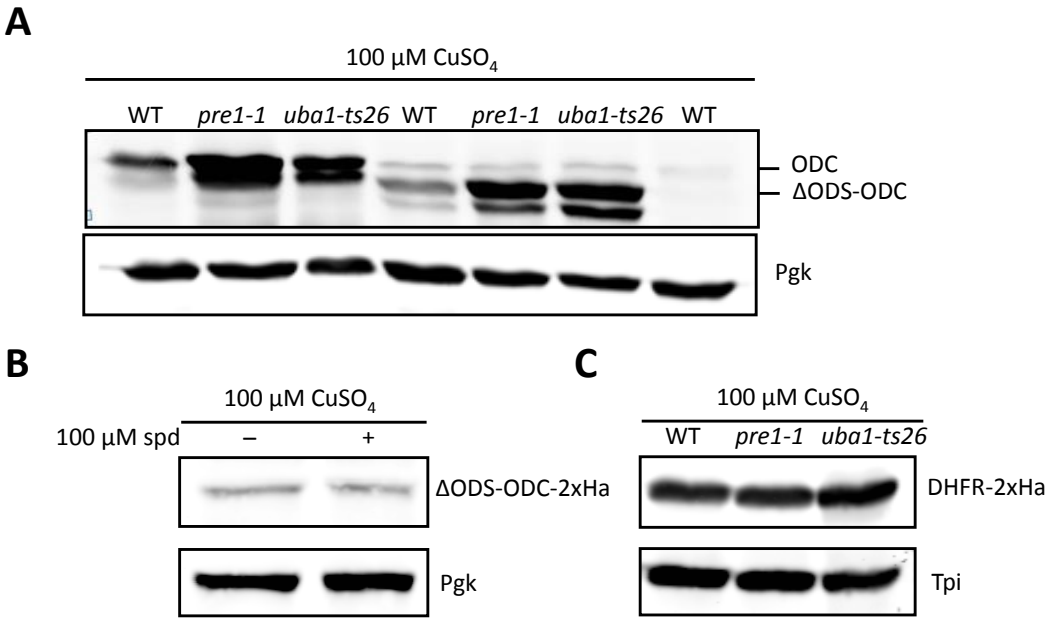

Fig. 26: Ubiquitin-dependent ODC degradation is ODS-independent. (A) Western blot analysis after SDS-PAGE showing steady state levels of ODC and ΔODS-ODC expressed from P_{CUP1} promoter in *pre1-1* and *uba1-ts26* mutant strains compared to wild-type. Expression was induced with 100 µM $CuSO_4$. Western blot was done with anti-ODC polyclonal antibody. The specificity of the antibody is demonstrated by the lack of the specific band in a control with the vector plasmid (last lane). The faint band corresponds to wild-type ODC expressed from the genomic locus. **(B)** Western blot analysis after SDS-PAGE showing steady state levels of ΔODS-ODC-2xHa in a wild-type strain with a without 100 µM spermidine. Expression was induced with 100 µM $CuSO_4$. **(C)** Same as (A), with DHFR-2xHa as substrate. For both (B) and (C), western blots were done with anti-Ha antibody. Pgk and Tpi served as loading controls.

4.4.3. Ubiquitin-dependent ODC degradation is independent of antizyme

The ΔODS-ODC construct is particularly useful for studying the ubiquitin-dependent degradation of ODC as it is degraded solely by this mechanism. In this construct, any influence from the canonical ubiquitin-independent degradation pathway can be eliminated. Therefore it was used to check if ubiquitin-dependent ODC degradation is antizyme-dependent or not. ΔODS-ODC expressed from the P_{CUP1} promoter was introduced into wild-type, *oaz1-Δ* and OAZ^{OE} (overexpression of the in frame version of antizyme) strains and its steady state levels were analysed. Both $CuSO_4$-induced and non-induced states were analysed. In the non-induced state, ΔODS-ODC could not be detected very well in this particular blot. As expected, wild-type ODC encoded by the genomic locus was stabilized in the *oaz1-Δ* mutant whereas it disappeared in the OAZ^{OE} strain (Fig. 27A). Surprisingly, upon $CuSO_4$ induction, there was no difference in the levels of ΔODS-ODC between the tested conditions. This shows that ubiquitin-dependent degradation of ODC is antizyme-independent.

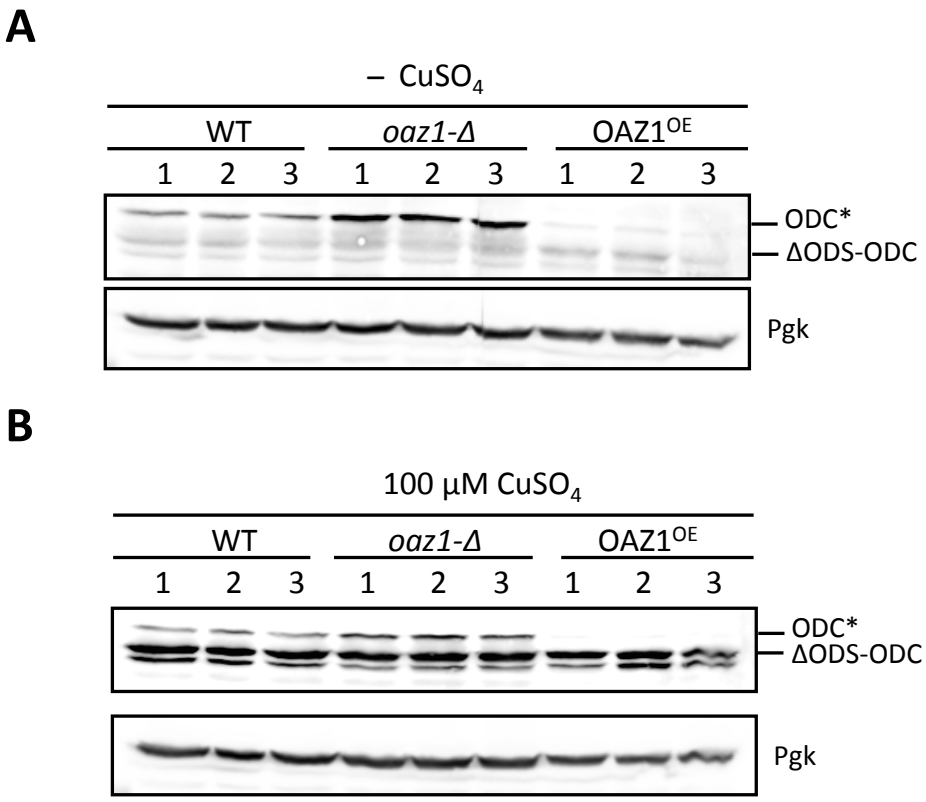

* Wild type ODC is expressed from its genomic locus and is detected by anti-ODC antibody

Fig. 27: Antizyme-independent degradation of ODC (A) Western blot analysis after SDS-PAGE showing steady state levels of ΔODS-ODC expressed from P_{CUP1} promoter in wild-type strain compared to *oaz1-Δ* and $OAZ1^{OE}$. Western blot was done with anti-ODC polyclonal antibody. The numbers 1, 2 and 3 corresponds to the three different yeast transformants used for the experiment. Pgk served as loading control. **(B)** Same as (A) except that protein expression was induced with 100 µM $CuSO_4$.

4.4.4. Protein quality control pathway might not influence ubiquitin-dependent ODC degradation

The Protein Quality Control pathway (PQC) takes care of detrimental misfolded proteins by refolding, degradation or sequestering them in specific cellular compartments (Chen et al., 2011). Molecular chaperones like Hsp70 play a vital role in these processes. Molecular chaperones have been shown to be involved not only in the folding and refolding of polypeptides but also in their proteasomal degradation. (Arndt et al., 2007) The chaperone Hsp70 has been shown to stimulate polyubiquitylation of dentaured substrates via the ubiquitin ligases Ubr1 and Ubr2. (Nillegoda et al., 2010) Therefore, a mutant deficient in the Ssa class of Hsp70 proteins (*ssa1-45*) was used to see if the ubiquitin-dependent degradation of ODC occurs via the PQC pathway (Becker et al., 1996).

Full length ODC-2xHa expressed from the P_{CUP1} promoter was introduced into WT and *ssa1-45* mutant strains. Whole cell lysates were analysed by SDS-PAGE followed by western blotting. Upon induction with $CuSO_4$, ODC-2xHa levels were significantly reduced (Fig. 28B). At this point, the reason for this reduction is not clear. Therefore, the blot was reprobed with antibodies against the proteasome (anti-Rpt5) and the chaperone Hsp90. There were no visible differences between the levels of Rpt5 . However, a slight increase in Hsp90 levels were observed in *ssa1-45* mutants. When the experiment was repeated with ΔODS-ODC-2xHa, upon induction with $CuSO_4$, the protein levels remained the same in both strains (Fig. 28B). This shows that ubiquitin-dependent degradation of ODC is independnet of Hsp70 and therefore might not involve the PQC pathway.

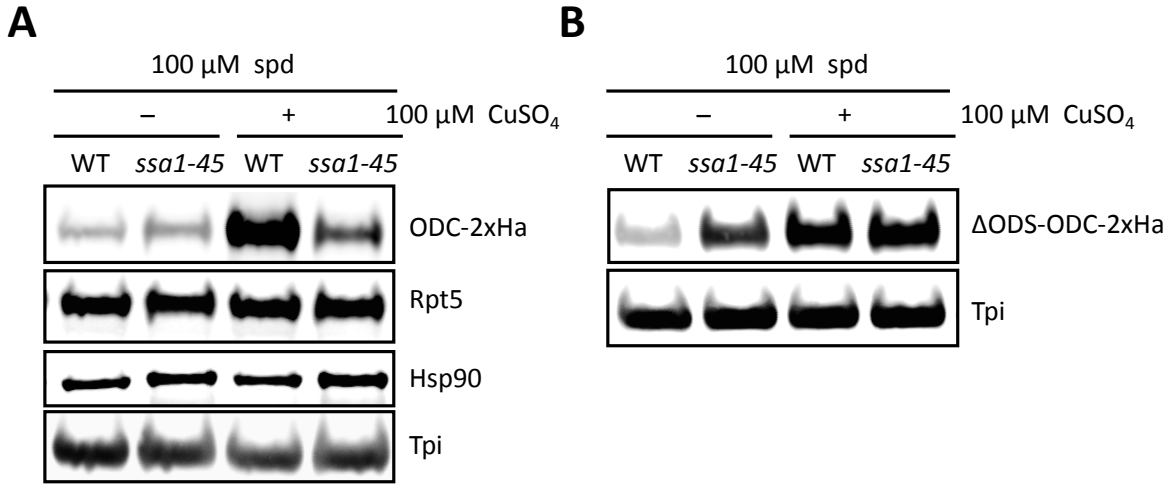

Fig. 28: Ubiquitin-dependent ODC degradation is not influenced by Hsp70. (A) Western blot analysis after SDS-PAGE showing steady state levels of ODC-2xHa expressed from P_{CUP1} promoter in wild-type strain compared to *ssa1-45* mutant with and without induction with $CuSO_4$. Western blot was done with anti-Ha antibody. The blot was later reprobed with antibodies against Rpt5 and Hsp90. Tpi served as loading control. **(B)** Same as (A), except that ΔODS-ODC-2xHa was used.

5. Discussion

5.1. Role of polyamines in feedback regulation of ODC

Polyamines are multivalent cellular polycations whose levels are controlled by a feedback mechanism which involves the regulation of its biosynthetic enzyme ODC. This feedback regulation involving ODC and its regulatory protein antizyme is conserved from yeast to humans (Palanimurugan et al., 2014). As described in the introduction, various enzymes involved in this pathway including ODC are therapeutic targets for cancer and other diseases. In this thesis, yeast was used as a model organism to decipher some of the details of this complex mechanism. Discussed below are some observations and findings that add to this regulatory network.

5.1.1. An additional role of polyamines in ODC degradation

The canonical regulation of ODC by polyamines occurs via up-regulation of the ODC regulatory protein antizyme. The levels of antizyme are strictly regulated by polyamines via two independent mechanisms (Palanimurugan et al., 2014). Firstly, polyamines promote antizyme translation by a mechanism that involves ribosomal frameshifting to bypass an internal stop codon (Matsufuji et al., 1995). Our laboratory has recently elucidated the mechanism of how polyamines regulate translational decoding of antizyme mRNA in yeast cells. Co-translational binding of polyamines to the nascent antizyme polypeptide promotes completion of antizyme synthesis. At low concentrations of polyamines, the nascent antizyme polypeptide causes a stalling of ribosomes, a process that initially requires a low ribosome density that is caused by a pause at the frameshifting site (Kurian et al., 2011). Secondly, polyamines inhibit the ubiquitin-dependent degradation of Oaz1, the mechanism of which remains to be elucidated (Palanimurugan et al., 2004). Complementing earlier *in vivo* data (Gödderz, 2010), a third mechanism of regulation of ODC by polyamines was characterized in the present work. The three modes of regulation of ODC by polyamine are depicted in Figure 29.

Gödderz observed that ODC degradation was enhanced *in vivo* by spermidine in spite of comparable Oaz1 levels (Gödderz, 2010). Using an *in vitro* ODC degradation assay, I complemented her observation by showing that both spermidine and spermine directly enhanced ODC degradation (Fig. 9). Spermine showed a greater stimulatory effect than spermidine on *in vitro* degradation of ODC (Fig. 9). The reason for this *in vitro* effect is not yet clear. Spermine showed a higher binding affinity to antizyme in comparison to spermidine (Kurian et al., 2011). However, it is

not clear whether the binding of polyamines to antizyme mediates this enhanced degradation.

In order to understand the specificity of this effect on ODC degradation, we tested whether polyamines augment general proteasome activity or the degradation of ubiquitin-dependent substrates. Polyamines slightly inhibited chymotrypsin-like activity of the proteasome *in vitro*, and had no effect on the degradation of ubiquitin-dependent substrates *in vivo* (Fig.10). Since polyamines bind antizyme, polyamines might enhance ODC/Oaz1 heterodimer formation thereby enhancing ODC degradation. In co-pull down experiments, however, polyamines did not show any detectable effect on the binding of ODC to Oaz1 (Fig. 11). Nonetheless, it is still possible that this binding assay is not sensitive enough to capture physiologically relevant but small differences in binding affinity. Alternatively, binding of polyamines to the complex might either cause a conformational change in ODC resulting in a better exposure of the unstructured domain thereby enhancing degradation (Godderz et al., 2011) or that polyamine binding to Oaz1 increases its affinity to an additional binding site in the proteasome (Godderz et al., 2011; Li et al., 1996). Additional studies are required to resolve this issue. Structural analyses of the ODC/Oaz1 complex bound to the 26S in the presence and absence of polyamines will be extremely valuable not only in determining the mechanism of this enhanced degradation but also in determining any additional binding interactions between ODC/Oaz1 and the proteasome.

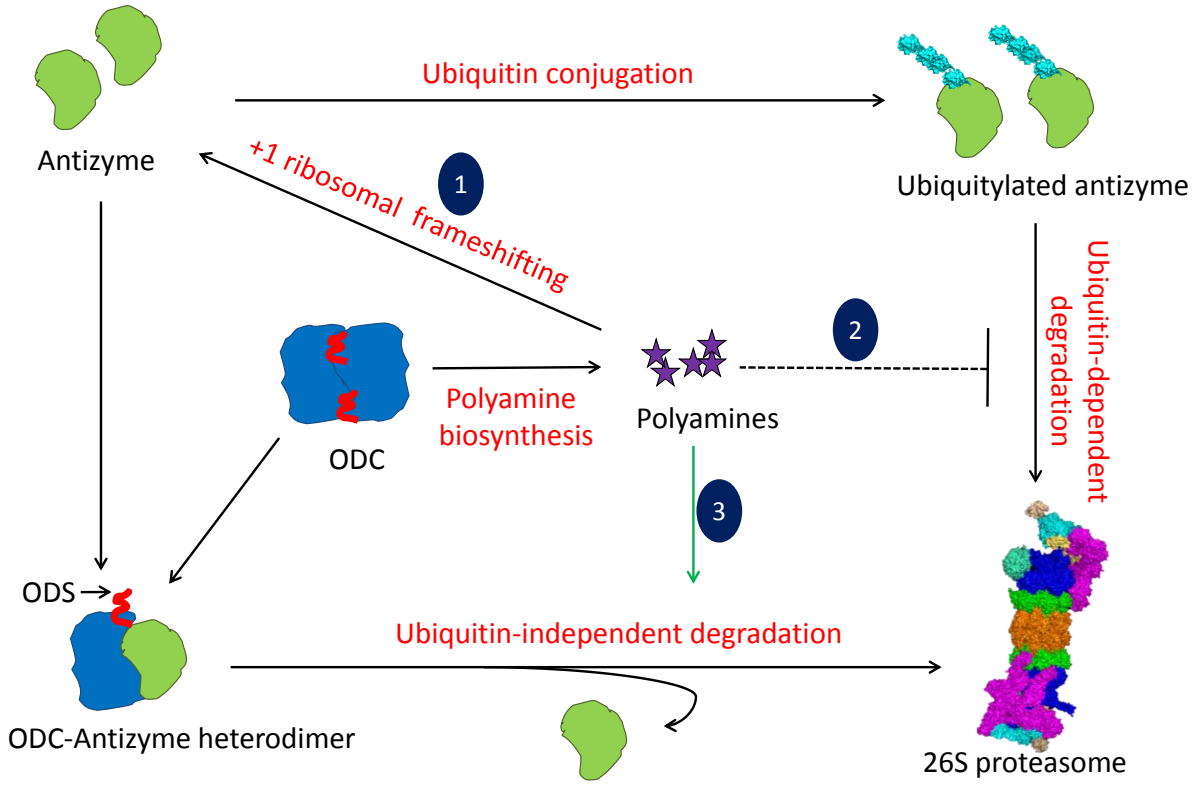

Fig. 29: Modes of regulation of ODC by polyamines. Polyamines regulate ODC levels by **(1)** inducing antizyme translation by mediating +1 ribosomal frameshifting of its mRNA **(2)** inhibiting ubiquitin-dependent degradation of antizyme **(3)** enhancing ubiquitin-independent degradation of ODC

5.1.2. Spermidine and spermine play similar roles in ODC regulation in yeast

Gödderz observed that spermidine addition to the growth media had a much stronger effect on Oaz1 stabilization in wild-type yeast cells than addition of spermine (Gödderz, 2010). However, one cannot conclude that spermidine is the major *in vivo* player that mediates polyamine induced regulation of ODC via antizyme. This is because spermine is taken up less efficiently by yeast cells compared to spermidine (Erez and Kahana, 2001). Therefore the observed differences could merely stem from differences in the uptake of various polyamines. Also, in wild-type yeast cells, both spermine and spermidine can be interconverted to each other. To eliminate the interconversion of spermine to spermidine, I used the strain (*spe4*-Δ) lacking the enzyme spermine synthase. Since there were no significant differences in ODC or Oaz1 levels detectable between wild-type and *spe4*-Δ cells (Fig. 12), we could conclude that formation of spermine from spermidine is not critical for ODC targeting *in vivo,* which does not exclude the possibility that spermine contributes to this regulation.

5.1.3. Role of acetylated polyamines in ODC degradation

Polyamine acetylation is necessary for the catabolism and export of polyamines (Casero and Pegg, 1993). Therefore, acetylation is another way of regulating polyamine levels in the cell. In mammals acetylation is carried out by the highly regulated spermidine/spermine-N(1)-acetyltransferase (SSAT), whereas in yeast the enzyme polyamine acetyl transferase (Paa1) had been suggested as a key enzyme in polyamine acetylation (Liu et al., 2005; Pegg, 2008). In order to understand if there is any cross-talk between the two modes of polyamine regulation, the effects of acetyl-polyamines on ODC degradation and Oaz1 stabilization were analyzed. No significant effect could be seen under the tested conditions in the *paa1*-Δ mutant compared to wild-type (Fig. 13B). Besides, acetylation of spermidine clearly inhibited its binding to antizyme (Fig. 13A). This is most likely due to the neutralization of the positive charges on polyamines by the acetyl groups. These findings indicate that acetylation of polyamines does not play a role in promoting ODC degradation.

5.2. Ubiquitin-independent substrate targeting to the proteasome

Most of the known proteasomal substrates depend on ubiquitin conjugation for recognition at the proteasome. In this thesis, I investigated the mechanism of degradation of certain substrates that does not require ubiquitin for their degradation. I asked whether such ubiquitin-independent substrates have some common features that make them susceptible to degradation. Some of these findings are discussed below.

5.2.1. Factors involved in ODC/Oaz1 targeting to the proteasome

Gödderz et al. showed that an N-terminal unstructured domain in ODC termed ODS (ODC Degradation Signal) is essential for the degradation of yeast ODC. They also showed that ODS is replaceable and need to be a minimum of 25-30 residues in length. By extension of ODS with spacer elements they further demonstrated that ODC can be degraded in yeast without antizyme binding. However, binding of antizyme improved the degradation of ODC indicating that antizyme has an additional function in ODC degradation (Godderz et al., 2011). These findings pointed to the fact that binding of ODC/Oaz1 complex to the proteasome is mediated by ODC but were consistent with the possibility that Oaz1 may contribute an additional binding site. In Fig 15, I showed by means of an *in vitro* binding assay that ODS mediates proteasomal binding of ODC/Oaz1 complex and that its presence is essential for ODC binding. Prakash et al. showed that an unstructured region in the substrate is required for efficient proteasomal degradation of ubiquitin-tagged substrates. In these substrates, however, the unstructured regions are necessary for the proteasome to initiate unfolding rather than mediating proteasome binding as the binding is done by the ubiquitin tag (Prakash et al., 2004). Therefore, the unstructured domains in ubiquitin-dependent substrates might be functionally different from ODS. It was also shown that as few as 20 amino acids can serve as initiation sites for efficient degradation of ubiquitin-dependent substrates (Prakash et al., 2004). In the case of ODC, a 20 amino acid degradation signal is not enough for efficient degradation. This comparison reveals that, these observed differences in function could arise from differences in the length of the unstructured domains present in these substrates. Therefore, a longer unstructured domain like ODS might mediate proteasomal binding as well as engage the ATPases for unfolding and translocation.

Having established that ODS mediates proteasomal binding, the next step was to investigate the receptor(s) for ODC on the proteasome. Gödderz et al. showed that

the lid subcomplex of the proteasome is dispensable for the degradation of ODC *in vivo*. Using isolated 26S proteasomes lacking the lid subcomplex, I complemented the *in vivo* data showing that *in vitro* degradation of ODC is not affected in this mutant proteasome (Fig.16). Zhang et al. had proposed that ODC might also be recognized by ubiquitin receptors at the proteasome (Zhang et al., 2003). However, Gödderz showed that ODC was degraded faster in mutants lacking one or a combination of ubiquitin receptors and shuttle factors. Extending these findings, I could show that ODC is degraded faster in a mutant lacking multiple ubiquitin receptors (Fig. 17). Together, these findings strongly suggest that ubiquitin-dependent and ODC follow different modes of proteasomal association.

5.2.2. Human p21 is degraded by the yeast proteasome in a ubiquitin-independent manner

p21 is a key cell cycle regulator in mammals. There are conflicting evidences showing that p21 act both as a tumour suppressor and an oncogene (Starostina and Kipreos, 2012). p21 is regulated at multiple levels including the post-translational level. It is not firmly established whether p21 is degraded in a ubiquitin-dependent or -independent manner. Multiple pathways seem to regulate p21 at the post-translational level (Jariel-Encontre et al., 2008). It is therefore interesting to ask whether p21 is degraded in yeast and if so, whether the degradation is ubiquitin-dependent or not. Interestingly, p21 was degraded by the yeast proteasome in a ubiquitin-dependent as well as -independent manner resembling the earlier observation made in mammalian cells (Fig. 18A). p21 is a loosely folded protein and therefore a fraction of it was prone to aggregation. This aggregated from of p21 was degraded in a ubiquitin-dependent manner most likely involving the protein quality control pathway. On the other hand, the soluble fraction of p21 was degraded in a ubiquitin-independent manner. These findings are based on the observation that p21 mainly accumulated in the pellet fraction in a *uba-ts26* mutant. Besides, upon co-expression with ODC, p21 competed with ODC for degradation (Fig. 18B). This is an indication that p21 and ODC compete at the proteasome for degradation possibly at the level of proteasomal recognition.

5.2.3. Rpt4 and Rpt5 Ar-Φ pore loops are involved in ODC recognition at the proteasome

Lander et al. showed that in a substrate-free stage, the Rpt subunits within the ATPase ring are arranged in a spiral staircase (Lander et al., 2013). However, upon substrate binding, the ATPase ring rearranges itself to form a ring with uniform

interfaces, a widened central channel coaxially aligned with the 20S CP, and a spiral orientation of pore loops (Matyskiela et al., 2013). Furthermore, Beckwith et al. showed that the three Rpt subunits (Rpt6, Rpt3 and Rpt4), which are located at the top of the pre-engaged spiral staircase are more important than the other three Rpt subunits (Rpt5, Rpt1 and Rpt2) for substrate engagement (Beckwith et al., 2013). In contrast, using mutants of Rpt Ar-Φ pore loops, Erales et al. showed that Rpt4 and Rpt5 are more important than the other Rpts for the degradation of mouse ODC in yeast (Erales et al., 2012). Also, the pore loops are known to make contacts with the unstructured regions of the substrate (Zhang et al., 2009). Therefore, I asked whether there is any specificity for the Rpt subunits in yeast ODC degradation. As in the case of mouse ODC, yODC was specifically stabilized in *rpt4 and rpt5* Ar-Φ pore loop mutants (Fig. 19A). On the other hand, ubiquitin-dependent substrates and the ubiquitin-independent substrate, ODS-Ura3 did not show any clear specificity for the Rpt4 and Rpt5 pore loops (Figs. 19-20). The effect seems to be specific for ODC and therefore is a strong indication that Rpt4 and Rpt5 might be the receptors for ODS at the proteasome (Fig. 30).

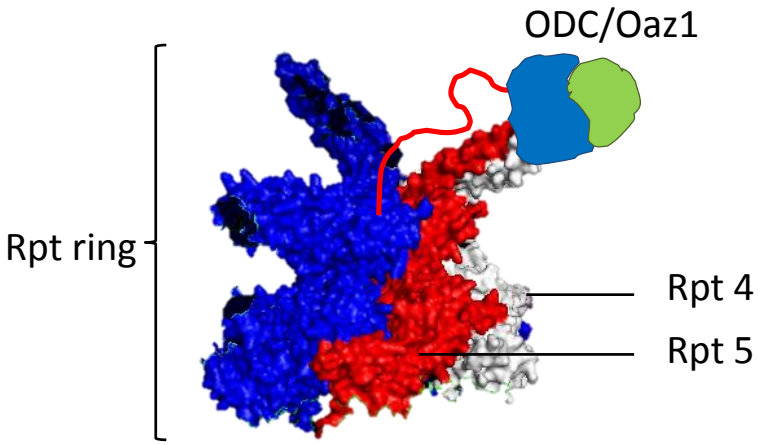

Fig. 30: Model for recognition of ODC at the proteasome. This model depicts the recognition of the unstructured domain of ODC (ODS) by the proteasomal ATPase ring. The Rpt4 (grey) and Rpt5 (red) are more prominent in the recognition of ODS. The rest of the Rpt subunits are coloured in blue.

5.3. Antizyme might provide an additional binding site to the proteasome

The proteasome is a busy cellular machinery with several substrates competing with each other at the same time for degradation. Since ODC is a rapidly degraded protein, it might have more than one way to prolong its staying time at the proteasome. Therefore, elements other than ODS might be involved in proteasomal targeting of ODC. Both polyamines and antizyme influence the degradation of ODC and could therefore promote proteasomal binding as well. Antizyme has been hypothesised to provide a binding site to the proteasome. Zhang et al. compared the K_{cat} and K_m values in an *in vitro* degradation assay of mouse ODC by rat proteasomes in the presence or absence of rat AZ1. The K_{cat} value was little affected by AZ1 (0.22 and 0.20 min^{-1}, respectively, without or with AZ1) whereas the K_m value reduced from 13 to 1.6 mM, consistent with the observed 8-fold stimulation of ODC degradation by AZ1 (Zhang et al., 2003). Based on these values, they suggested that AZ1 improves the association of ODC with the proteasome, not the rate of its processing. The same group had previously shown that N-terminal part of antizyme is necessary to induce degradation of ODC but not for the interaction with ODC (Li and Coffino, 1994). They further showed that this N-terminal fragment of antizyme can target heterologous proteins to the proteasome (Li et al., 1996). Previous experiments from our lab complemented these observations. The extension of ODS by spacer elements made ODC susceptible to proteasomal degradation independent of antizyme. But presence of antizyme improved the degradation of these ODC variants showing that it has an additional function (apart from its role in exposing the unstructured domain) (Godderz et al., 2011). I further dissected the additional role of antizyme using an array of antizyme fusion constructs. Using a phenotypic assay, I showed that fusion of the stable variant of antizyme (Oaz1-4res), decreased the stability of ODS-Ura3 (Fig. 23). ODS-Ura3 was previously shown to be degraded in a ubiquitin-independent manner by the 26S (Godderz et al., 2011). Antizyme fusion further destabilized this fusion protein. Together, the previous findings along with the results presented in this thesis, the mode of targeting of ODC to the 26S has become clearer. I hypothesise that there are two binding elements in the ODC-Oaz1 heterodimer; ODS and antizyme. ODS most likely binds to the pore loops of Rpt4 and Rpt5. Antizyme might provide an additional binding site. It is also clear that antizyme alone cannot mediate binding of the heterodimer to the proteasome because the ΔODS-ODC/Oaz1 heterodimer did not bind the 26S in the *in vitro* proteasome binding assay (Fig. 15). Therefore, ODS is most likely the primary binding element and antizyme might function as an additional factor enhancing

proteasomal association. Further studies are required to prove this hypothesis. A screen for spontaneous mutants stabilizing both ODC and the artificial ubiquitin-independent substrate, ODS-Oaz1-4res-Ura3 has been initiated as part of this work and is ongoing (Fig. 24). This screen is aimed at isolating mutants that are incapable of binding ODS or Oaz1. An initial phenotypic analysis of selected mutants has been completed (Table. 1). The next step is to classify and map the mutations to a particular gene. Mapping can be done using genetic methods like complementation analysis with a yeast gene library or by whole genome sequencing of selected mutants. Additionally, structural analyses of the ODC/Oaz1 complex bound to the 26S proteasome would be helpful in determining the exact interactions between these complexes.

5.4. Ubiquitin-dependent ODC degradation

Many of the known ubiquitin-independent substrates have two modes of degradation. Rpn4 is a classic example. ODC, on the other hand, has so far been known to be degraded solely in a ubiquitin-independent manner. Surprisingly, Gödderz observed that, when ODC is expressed from the P_{CUP1} promoter, it is in part degraded in a ubiquitin-dependent manner (personal communication). This observation was reproduced in Fig. 25. Upon copper induction, the levels of ODC are much higher compared to the levels obtained when the gene is expressed from its own promoter. Unlike in the case of ubiquitin-dependent p21 degradation in yeast, the ubiquitin-dependent ODC degradation was not a consequence of an aggregation of the ODC/Oaz1 heterodimer. Additionally, in a mutant strain impaired in the function of cytosolic heat shock factor Hsp70, ODC was not stabilized under these experimental conditions (Fig. 28). Together, these observations indicate that the ubiquitin-dependent ODC degradation is mainly occurring independent of the protein quality control pathway. Interestingly, ubiquitin-dependent ODC degradation was unaffected by the presence of ODS, antizyme, or polyamines (Figs. 26-27). This indicates that this regulatory mechanism is independent of the canonical negative feedback regulation of ODC by polyamines. Together, the ubiquitin-independent ODC degradation is a result of increased levels of ODC in the cell. The following scenario could be envisioned. Once the ubiquitin-independent pathway of ODC regulation is overwhelmed by high ODC levels (as in the case of copper induction), the ubiquitin-dependent pathway takes over (Fig. 31). The physiological relevance of such a pathway is yet to be discovered. Since ODC levels are abnormally elevated in cancer cells, we could imagine that such an additional regulation might be relevant. This is to the best of our knowledge, the first indication that under certain experimental conditions, ODC can be degraded in a ubiquitin-dependent manner. E2 and E3 enzymes responsible for ubiquitylation are yet to be discovered. Systematic analyses of ODC levels in a collection of known E2 and E3 could reveal the players involved.

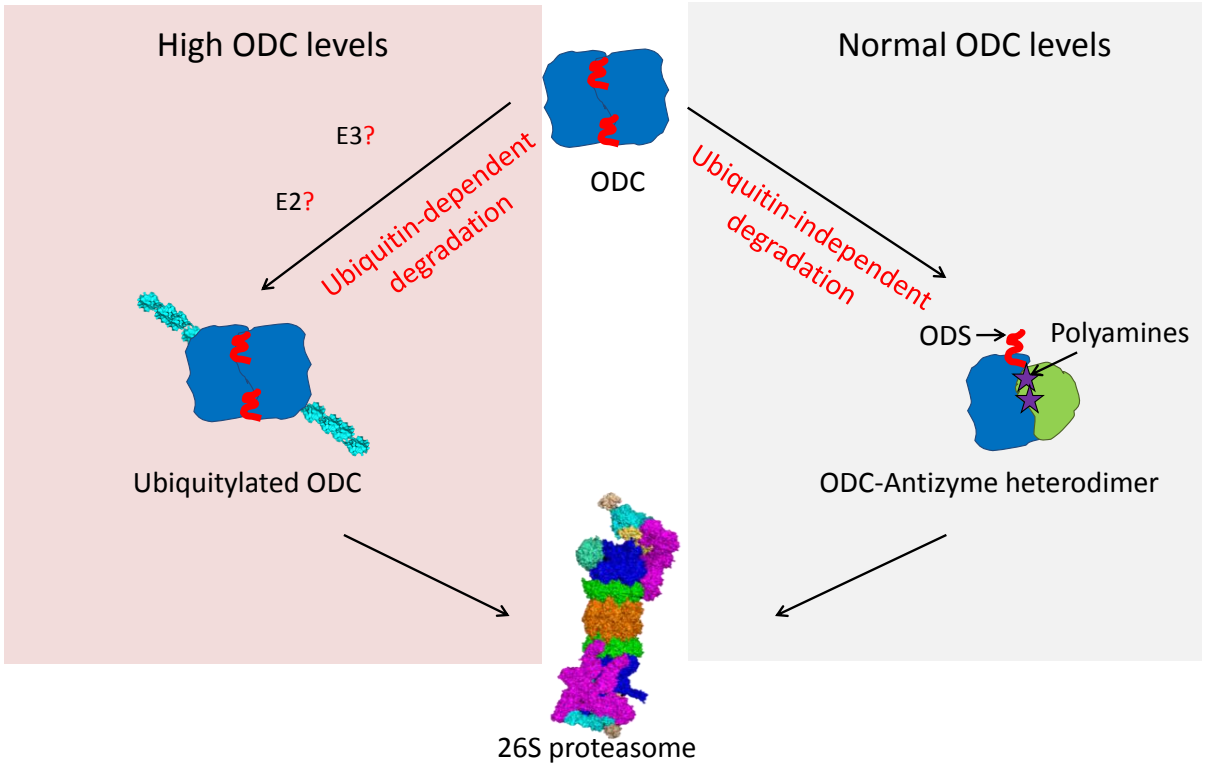

Fig. 31: The two modes of ODC degradation. Depicted above are the two modes of ODC degradation by the 26S proteasome. The part on the right side is the canonical ubiquitin-independent mode of ODC degradation. The left part shows the ubiquitin-dependent ODC degradation mode discussed in the section above.

5.5. Conclusions and outlook

Together, the results presented in this thesis provide some new insights into the mechanism of ubiquitin-independent degradation of ODC. A previously unknown mode of regulation of ODC by polyamines was established. The role of the unstructured domain of ODC in the binding of the ODC/Oaz1 heterodimer to the proteasome was demonstrated using an *in vitro* proteasome binding assay developed in this study. This binding assay can now be used in future studies to check the binding of putative substrates and interactors to the proteasome. I also showed that antizyme might play an additional role in ODC targeting most likely by improving the binding of ODC to the proteasome. Identification of the relevant binding sites on antizyme and the proteasome are challenging topics for future studies. Finally, a new mode of degradation of ODC by ubiquitin conjugation has been described. These findings and observations form a basis for future studies on the regulation of ODC which could lead to new therapies targeting the polyamine regulatory pathway.

6. References

Almond, J.B., and Cohen, G.M. (2002). The proteasome: a novel target for cancer chemotherapy. Leukemia *16*, 433-443.

Arndt, V., Rogon, C., and Hohfeld, J. (2007). To be, or not to be-molecular chaperones in protein degradation. Cellular and molecular life sciences *64*, 2525-2541.

Baugh, J.M., Viktorova, E.G., and Pilipenko, E.V. (2009). Proteasomes can degrade a significant proportion of cellular proteins independent of ubiquitination. Journal of molecular biology *386*, 814-827.

Beck, F., Unverdorben, P., Bohn, S., Schweitzer, A., Pfeifer, G., Sakata, E., Nickell, S., Plitzko, J.M., Villa, E., Baumeister, W.*, et al.* (2012). Near-atomic resolution structural model of the yeast 26S proteasome. Proceedings of the National Academy of Sciences of the United States of America *109*, 14870-14875.

Becker, J., Walter, W., Yan, W., and Craig, E.A. (1996). Functional interaction of cytosolic hsp70 and a DnaJ-related protein, Ydj1p, in protein translocation *in vivo*. Molecular and cellular biology *16*, 4378-4386.

Beckwith, R., Estrin, E., Worden, E.J., and Martin, A. (2013). Reconstitution of the 26S proteasome reveals functional asymmetries in its AAA plus unfoldase. Nature structural & molecular biology *20*, 1164.

Beenukumar, R.R., Gödderz, D., Palanimurugan, R., and Dohmen, R.J. (in press). Polyamines directly promote antizyme-mediated degradation of ornithine decarboxylase by the proteasome. Microbial cell

Bercovich, Z., Rosenberg-Hasson, Y., Ciechanover, A., and Kahana, C. (1989). Degradation of ornithine decarboxylase in reticulocyte lysate is ATP-dependent but ubiquitin-independent. The Journal of biological chemistry *264*, 15949-15952.

Bhattacharyya, S., Yu, H., Mim, C., and Matouschek, A. (2014). Regulated protein turnover: snapshots of the proteasome in action. Nature reviews Molecular cell biology *15*, 122-133.

Bloom, J., Amador, V., Bartolini, F., DeMartino, G., and Pagano, M. (2003). Proteasome-mediated degradation of p21 via N-terminal ubiquitinylation. Cell *115*, 71-82.

Casero, R.A., and Pegg, A.E. (1993). Spermidine Spermine N1-Acetyltransferase - the Turning-Point in Polyamine Metabolism. Faseb Journal *7*, 653-661.

Chen, B., Retzlaff, M., Roos, T., and Frydman, J. (2011). Cellular strategies of protein quality control. Cold Spring Harbor perspectives in biology

Ciechanover, A. (2012). Intracellular protein degradation: from a vague idea through the lysosome and the ubiquitin-proteasome system and onto human diseases and drug targeting. Neuro-degenerative diseases *10*, 7-22.

Coleman, C.S., Stanley, B.A., Viswanath, R., and Pegg, A.E. (1994). Rapid exchange of subunits of mammalian ornithine decarboxylase. The Journal of biological chemistry *269*, 3155-3158.

Davies, K.J. (2001). Degradation of oxidized proteins by the 20S proteasome. Biochimie *83*, 301-310.

Dohmen, R.J., London, M., Glanemann, C., and Ramos, P. (2005). Assays for Proteasome Assembly and Maturation. In Ubiquitin-Proteasome Protocols, C. Patterson, and D. Cyr, eds. (Humana Press), pp. 243-254.

Dohmen, R.J., Stappen, R., McGrath, J.P., Forrova, H., Kolarov, J., Goffeau, A., and Varshavsky, A. (1995). An essential yeast gene encoding a homolog of ubiquitin-activating enzyme. The Journal of biological chemistry *270*, 18099-18109.

Elsasser, S., Schmidt, M., and Finley, D. (2005). Characterization of the Proteasome Using Native Gel Electrophoresis. In Methods in enzymology, J.D. Raymond, ed. (Academic Press), 353-363.

Erales, J., and Coffino, P. (2014). Ubiquitin-independent proteasomal degradation. Biochimica et biophysica acta. *1843,* 216–221

Erales, J., Hoyt, M.A., Troll, F., and Coffino, P. (2012). Functional asymmetries of proteasome translocase pore. The Journal of biological chemistry *287*, 18535-18543.

Erez, O., and Kahana, C. (2001). Screening for modulators of spermine tolerance identifies Sky1, the SR protein kinase of Saccharomyces cerevisiae, as a regulator of polyamine transport and ion homeostasis. Molecular and cellular biology *21*, 175-184.

Finley, D., Ulrich, H.D., Sommer, T., and Kaiser, P. (2012). The ubiquitin-proteasome system of *Saccharomyces cerevisiae*. Genetics *192*, 319-360.

Forster, F., Lasker, K., Beck, F., Nickell, S., Sali, A., and Baumeister, W. (2009). An atomic model AAA-ATPase/20S core particle sub-complex of the 26S proteasome. Biochemical and biophysical research communications *388*, 228-233.

Fröhlich, M.S. (2005). Funktionen molekularer Chaperone in der Qualitätskontrolle zytosolischer Proteine In Mathematics and Natural Sciences. (Cologne, Germany: University of Cologne).

Ghislain, M., Dohmen, R.J., Levy, F., and Varshavsky, A. (1996). Cdc48p interacts with Ufd3p, a WD repeat protein required for ubiquitin-mediated proteolysis in *Saccharomyces cerevisiae*. Embo J *15*, 4884-4899.

Gietz, R.D., and Sugino, A. (1988). New yeast-*Escherichia coli* shuttle vectors constructed with *in vitro* mutagenized yeast genes lacking six-base pair restriction sites. Gene *74*, 527-534.

Gietz, R.D., and Woods, R.A. (2006). Yeast transformation by the LiAc/SS Carrier DNA/PEG method. Methods Mol Biol *313*, 107-120.

Glickman, M.H., and Ciechanover, A. (2002). The ubiquitin-proteasome proteolytic pathway: destruction for the sake of construction. Physiol Rev *82*, 373-428.

Gödderz, D. (2010). Antizyme-mediated targeting of Ornithine Decarboxylase to the proteasome. In Mathematics and Natural Sciences (Cologne, Germany: University of Cologne).

Godderz, D., Schafer, E., Palanimurugan, R., and Dohmen, R.J. (2011). The N-terminal unstructured domain of yeast ODC functions as a transplantable and replaceable ubiquitin-independent degron. Journal of molecular biology *407*, 354-367.

Ha, S.W., Ju, D., and Xie, Y. (2012). The N-terminal domain of Rpn4 serves as a portable ubiquitin-independent degron and is recognized by specific 19S RP subunits. Biochemical and biophysical research communications *419*, 226-231.

Hamasaki-Katagiri, N., Katagiri, Y., Tabor, C.W., and Tabor, H. (1998). Spermine is not essential for growth of *Saccharomyces cerevisiae:* identification of the SPE4 gene (spermine synthase) and characterization of a *spe4* deletion mutant. Gene *210*, 195-201.

Hough, R., Pratt, G., and Rechsteiner, M. (1986). Ubiquitin-Lysozyme Conjugates - Identification and Characterization of an ATP-Dependent Protease from Rabbit Reticulocyte Lysates. Journal of Biological Chemistry *261*, 2400-2408.

Hoyt, M.A., and Coffino, P. (2004). Ubiquitin-proteasome system - Ubiquitin-free routes into the proteasome. Cellular and Molecular Life Sciences *61*, 1596-1600.

Hoyt, M.A., Zhang, M., and Coffino, P. (2003). Ubiquitin-independent mechanisms of mouse ornithine decarboxylase degradation are conserved between mammalian and fungal cells. The Journal of biological chemistry *278*, 12135-12143.

Igarashi, K., and Kashiwagi, K. (2010). Modulation of cellular function by polyamines. The international journal of biochemistry & cell biology *42*, 39-51.

Inobe, T., and Matouschek, A. (2014). Paradigms of protein degradation by the proteasome. Current opinion in structural biology *24*, 156-164.

Isono, E., Nishihara, K., Saeki, Y., Yashiroda, H., Kamata, N., Ge, L., Ueda, T., Kikuchi, Y., Tanaka, K., Nakano, A.*, et al.* (2007). The assembly pathway of the 19S regulatory particle of the yeast 26S proteasome. Molecular biology of the cell *18*, 569-580.

Jariel-Encontre, I., Bossis, G., and Piechaczyk, M. (2008). Ubiquitin-independent degradation of proteins by the proteasome. Biochimica et biophysica acta *1786*, 153-177.

Ju, D., and Xie, Y. (2004). Proteasomal degradation of RPN4 via two distinct mechanisms, ubiquitin-dependent and -independent. The Journal of biological chemistry *279*, 23851-23854.

Kahana, C. (2009). Regulation of cellular polyamine levels and cellular proliferation by antizyme and antizyme inhibitor. Essays in biochemistry *46*, 47-61.

Kandasamy, G. (2014). Role of molecular chaperones in ubiquitin-dependent protein degradation. In Mathematics and Natural Sciences (Cologne, Germany: University of Cologne).

Kock, M., Nunes, M.M., Hemann, M., Kube, S., Dohmen, R.J., Herzog, F., Ramos, P.C., and Wendler, P. (2015). Proteasome assembly from 15S precursors involves major conformational changes and recycling of the Pba1-Pba2 chaperone. Nature communications *6*.

Komander, D., Clague, M.J., and Urbe, S. (2009). Breaking the chains: structure and function of the deubiquitinases. Nat Rev Mol Cell Bio *10*, 550-563.

Kurian, L., Palanimurugan, R., Godderz, D., and Dohmen, R.J. (2011). Polyamine sensing by nascent ornithine decarboxylase antizyme stimulates decoding of its mRNA. Nature *477*, 490-494.

Laemmli, U.K. (1970). Cleavage of Structural Proteins during Assembly of Head of Bacteriophage-T4. Nature *227*, 680.

Lander, G.C., Estrin, E., Matyskiela, M.E., Bashore, C., Nogales, E., and Martin, A. (2012). Complete subunit architecture of the proteasome regulatory particle. Nature *482*, 186-191.

Lander, G.C., Martin, A., and Nogales, E. (2013). The proteasome under the microscope: the regulatory particle in focus. Current opinion in structural biology *23*, 243-251.

Lee, W.C., Lee, M., Jung, J.W., Kim, K.P., and Kim, D. (2008). SCUD: Saccharomyces cerevisiae ubiquitination database. BMC genomics *9*, 440.

Li, X., and Coffino, P. (1993). Degradation of ornithine decarboxylase: exposure of the C-terminal target by a polyamine-inducible inhibitory protein. Molecular and cellular biology *13*, 2377-2383.

Li, X.Q., and Coffino, P. (1994). Distinct Domains of Antizyme Required for Binding and Proteolysis of Ornithine Decarboxylase. Molecular and cellular biology *14*, 87-92.

Li, X.Q., Stebbins, B., Hoffman, L., Pratt, G., Rechsteiner, M., and Coffino, P. (1996). The N terminus of antizyme promotes degradation of heterologous proteins. Journal of Biological Chemistry *271*, 4441-4446.

Lilienbaum, A. (2013). Relationship between the proteasomal system and autophagy. Int J Biochem Mol Biol.

Liu, B., Sutton, A., and Sternglanz, R. (2005). A yeast polyamine acetyltransferase. The Journal of biological chemistry *280*, 16659-16664.

Matsufuji, S., Matsufuji, T., Miyazaki, Y., Murakami, Y., Atkins, J.F., Gesteland, R.F., and Hayashi, S. (1995). Autoregulatory frameshifting in decoding mammalian ornithine decarboxylase antizyme. Cell *80*, 51-60.

Matyskiela, M.E., Lander, G.C., and Martin, A. (2013). Conformational switching of the 26S proteasome enables substrate degradation. Nature structural & molecular biology *20*, 781-788

McGrath, J.P., Jentsch, S., and Varshavsky, A. (1991). UBA 1: an essential yeast gene encoding ubiquitin-activating enzyme. Embo J *10*, 227-236.

Melvin, A.T., Woss, G.S., Park, J.H., Waters, M.L., and Allbritton, N.L. (2013). Measuring Activity in the Ubiquitin-Proteasome System: From Large Scale Discoveries to Single Cells Analysis. Cell biochemistry and biophysics. *67*, 75-86

Meng, L., Mohan, R., Kwok, B.H., Elofsson, M., Sin, N., and Crews, C.M. (1999). Epoxomicin, a potent and selective proteasome inhibitor, exhibits *in vivo* antiinflammatory activity. Proceedings of the National Academy of Sciences of the United States of America *96*, 10403-10408.

Meyskens, F.L., Jr., Simoneau, A.R., and Gerner, E.W. (2014). Chemoprevention of prostate cancer with the polyamine synthesis inhibitor difluoromethylornithine. Recent results in cancer research *202*, 115-120.

Michael H. Glickman, D.M.R., Hongyong Fu, Christopher N. Larsen,Olivier Coux, Inge Wefes, Günter Pfeifer, Zdenka Cjeka, Richard Vierstra,Wolfgang Baumeister, Victor Fried and Daniel Finley (1999). Functional analysis of the proteasome regulatory particle. Molecular Biology Reports *26*, 21-28.

Nickell, S., Beck, F., Scheres, S.H.W., Korinek, A., Forster, F., Lasker, K., Mihalache, O., Sun, N., Nagya, I., Sali, A.*, et al.* (2009). Insights into the molecular architecture of the 26S proteasome. Proceedings of the National Academy of Sciences of the United States of America *106*, 11943-11947.

Nillegoda, N.B., Theodoraki, M.A., Mandal, A.K., Mayo, K.J., Ren, H.Y., Sultana, R., Wu, K., Johnson, J., Cyr, D.M., and Caplan, A.J. (2010). Ubr1 and Ubr2 function in a quality control pathway for degradation of unfolded cytosolic proteins. Molecular biology of the cell *21*, 2102-2116.

Nowotarski, S.L., Woster, P.M., and Casero, R.A. (2013). Polyamines and cancer: implications for chemotherapy and chemoprevention. Expert reviews in molecular medicine *15*.

Olsen, R.R., and Zetter, B.R. (2011). Evidence of a Role for Antizyme and Antizyme Inhibitor as Regulators of Human Cancer. Molecular Cancer Research *9*, 1285-1293.

Palanimurugan, R., and Dohmen, R.J. (2012). Ultrafiltration-based in vitro assay for determining polyamine binding to proteins. Protocol Exchange *doi:10.1038/protex.2012.005*.

Palanimurugan, R., Kurian, L., Hegde, V., Hofmann, K., and Dohmen, R.J. (2014). Co-translational Polyamine Sensing Co-translational polyamine sensing by Nascent ODC Antizyme ODC antizyme. In Regulatory Nascent Polypeptides, K. Ito, ed. (Springer Japan), 203-222.

Palanimurugan, R., Scheel, H., Hofmann, K., and Dohmen, R.J. (2004). Polyamines regulate their synthesis by inducing expression and blocking degradation of ODC antizyme. Embo J *23*, 4857-4867.

Pandey, U.B., Nie, Z.P., Batlevi, Y., McCray, B.A., Ritson, G.P., Nedelsky, N.B., Schwartz, S.L., DiProspero, N.A., Knight, M.A., Schuldiner, O.*, et al.* (2007). HDAC6 rescues neurodegeneration and provides an essential link between autophagy and the UPS. Nature *447*, 859-863.

Pegg, A.E. (2006). Regulation of ornithine decarboxylase. Journal of Biological Chemistry *281*, 14529-14532.

Pegg, A.E. (2008). Spermidine/spermine-N-1-acetyltransferase: a key metabolic regulator. Am J Physiol-Endoc M *294*, E995-E1010.

Pena, M.M., Melo, S.P., Xing, Y.Y., White, K., Barbour, K.W., and Berger, F.G. (2009). The intrinsically disordered N-terminal domain of thymidylate synthase targets the enzyme to the ubiquitin-independent proteasomal degradation pathway. The Journal of biological chemistry *284*, 31597-31607.

Perez-Leal, O., and Merali, S. (2012). Regulation of polyamine metabolism by translational control. Amino acids *42*, 611-617.

Persson, L. (2009). Polyamine homoeostasis. Essays in biochemistry *46*, 11-24.

Porat, Z., Landau, G., Bercovich, Z., Krutauz, D., Glickman, M., and Kahana, C. (2008). Yeast antizyme mediates degradation of yeast ornithine decarboxylase by yeast but not by mammalian proteasome: new insights on yeast antizyme. The Journal of biological chemistry *283*, 4528-4534.

Porter, C.W., and Bergeron, R.J. (1988). Regulation of polyamine biosynthetic activity by spermidine and spermine analogs--a novel antiproliferative strategy. Advances in experimental medicine and biology *250*, 677-690.

Prakash, S., Tian, L., Ratliff, K.S., Lehotzky, R.E., and Matouschek, A. (2004). An unstructured initiation site is required for efficient proteasome-mediated degradation. Nature structural & molecular biology *11*, 830-837.

Ramos, P.C., Höckendorff, J., Johnson, E.S., Varshavsky, A., and Dohmen, R.J. (1998). Ump1p Is Required for Proper Maturation of the 20S Proteasome and Becomes Its Substrate upon Completion of the Assembly. Cell *92*, 489-499.

Rangasamy, P.M. (2005). Regulation of polyamine biosynthesis in Saccharomyces cerevisiae. In Mathematics and Natural Sciences. (Cologne, Germany: University of Cologne).

Rato, C., Amirova, S.R., Bates, D.G., Stansfield, I., and Wallace, H.M. (2011). Translational recoding as a feedback controller: systems approaches reveal polyamine-specific effects on the antizyme ribosomal frameshift. Nucleic acids research *39*, 4587-4597.

Richard W. Kriwacki , J.W., Linda Tennant , Peter E. Wright , Gary Siuzdak (1997). Probing protein structure using biochemical and biophysical methods Proteolysis, matrix-assisted laser desorption / ionization mass spectrometry, high-performance liquid chromatography and size- Waf1 /Cip1 / Sdi1 exclusion chromatography of p21. Journal of Chromatography A *777*, 23-30

Rosenberghasson, Y., Bercovich, Z., Ciechanover, A., and Kahana, C. (1989). Degradation of Ornithine Decarboxylase in Mammalian-Cells Is Atp Dependent but Ubiquitin Independent. European Journal of Biochemistry *185*, 469-474.

Sheaff, R.J., Singer, J.D., Swanger, J., Smitherman, M., Roberts, J.M., and Clurman, B.E. (2000). Proteasomal turnover of p21Cip1 does not require p21Cip1 ubiquitination. Molecular cell *5*, 403-410.

Sherr, C.J., and Roberts, J.M. (1999). CDK inhibitors: positive and negative regulators of G1-phase progression. Genes & development *13*, 1501-1512.

Stadelmayer, F. (2014). Degradation of Ornithine Decarboxylase in Yeast. Laboratory Module, University of Cologne.

Starostina, N.G., and Kipreos, E.T. (2012). Multiple degradation pathways regulate versatile CIP/KIP CDK inhibitors. Trends in cell biology *22*, 33-41.

Tomko, R.J., Jr., and Hochstrasser, M. (2013). Molecular architecture and assembly of the eukaryotic proteasome. Annual review of biochemistry *82*, 415-445.

Varshavsky, A. (1996). The N-end rule: functions, mysteries, uses. Proceedings of the National Academy of Sciences of the United States of America *93*, 12142-12149.

Wallace, H.M. (2009). The polyamines: past, present and future. Essays in biochemistry *46*, 1-9.

Walz, J., Erdmann, A., Kania, M., Typke, D., Koster, A.J., and Baumeister, W. (1998). 26S proteasome structure revealed by three-dimensional electron microscopy. Journal of structural biology *121*, 19-29.

Wang, X.J., Yu, J., Wong, S.H., Cheng, A.S.L., Chan, F.K.L., Ng, S.S.M., Cho, C.H., Sung, J.J.Y., and Wu, W.K.K. (2013). A novel crosstalk between two major protein degradation systems Regulation of proteasomal activity by autophagy. Autophagy *9*, 1500-1508.

Zhang, F., Hu, M., Tian, G., Zhang, P., Finley, D., Jeffrey, P.D., and Shi, Y.G. (2009). Structural Insights into the Regulatory Particle of the Proteasome from Methanocaldococcus jannaschii. Molecular cell *34*, 473-484.

Zhang, M., Pickart, C.M., and Coffino, P. (2003). Determinants of proteasome recognition of ornithine decarboxylase, a ubiquitin-independent substrate. Embo J *22*, 1488-1496.

List of Abbreviations

AAA	:	ATPases associated with diverse cellular activities
APS	:	Ammonium persulfate
AMP	:	Adenosine monophosphate
ATP	:	Adenosine triphosphate
BSA	:	Bovine serum albumin
CP	:	Core particle
CryoEM	:	Cryo electron microscopy
DFMO	:	α-Difluoromethylornithine
DNA	:	Deoxyribonucleic acid
dNTP	:	Nucleotide triphosphates
DTT	:	Dithiothreitol
EDTA	:	Ethylenediaminetetraacetic acid
g	:	Gravitation
GST	:	Glutathione S-transferase
HEPES	:	4-(2-hydroxyethyl)-1-piperazineethanesulfonic acid
h	:	Hours
kDa	:	Kilodalton
µL	:	Microliter
µM	:	Micromolar
mg	:	Miligram
ml	:	Mililiter
min	:	Minute
mRNA	:	Messenger RNA
OD600	:	Optical density at a wavelength of 600 nanometer
ODS	:	ODC degradation signal
PAGE	:	Polyacrylamide gel electrophoresis
PCR	:	Polymerase chain reaction
PEG	:	Polyethylene glycol
PVDF	:	Polyvinylidene fluoride
RP	:	Regulatory particle
rpm	:	Revolutions per minute
RT	:	Room temperature
sec	:	seconds
SD	:	Synthetic dextrose
SDS	:	Sodium dodecyl sulfate

Spd	:	Spermidine
Spm	:	Spermidine
TEMED	:	Tetramethylethylenediamine
Ub	:	Ubiquitin
WT	:	Wild-type
YP	:	Yeast extract-peptone
YPD	:	Yeast extract-peptone with glucose

Acknowledgement

I wish to place on record my deepest gratitude to my mentor Prof. Dr. Jürgen Dohmen for his patient guidance and support, in particular for giving me the space to experiment my own ideas. I have learned a great deal from him and feel very lucky and proud to have him as my mentor.

My sincere thanks to my thesis committee members, Prof. Dr. Kay Hofmann and Prof. Dr. Ute Höcker, for their valuable time.

I acknowledge gratefully our collaborator Prof. Dr. Philip Coffino of UCSF, USA for useful discussion and for providing us with some of the yeast strains that I used in this thesis.

I remember with gratitude my teachers, in particular my mentors, Prof. Dr. Hussain Munavar of Madurai Kamaraj University and Dr. Beulah Vijayakumar, former Head of Botany at Stella Maris College for their undying support and guidance.

I thank the International Graduate School for Development Health and Disease for funding. Dr. Isabell Witt has been a great support throughout my PhD studies and I thank her for all the effort she has put in organising the soft skill courses. I also thank Kathy and others from the graduate school for making my stay in Germany comfortable.

I have received complete support from my lab members. I sincerely acknowledge with gratitude Dr. R. Palanimurugan, for being there every step of the way during my earlier years as a PhD student. I thank him for all those hours of discussion and for spending his valuable time in teaching me the basics of yeast genetics. I thank Dr. Paula Ramos for her encouragement and for sharing with me her expertise on biochemical techniques. I thank all current and previous members of the Dohmen lab for helping me out on various occasions. My lab mates Maria, Vishal and Steffi deserves special mention for all the fun times and for making my life so wonderful with their presence.

I thank all my friends for their love and support. Michelle, Arun, Ruchika, Prachi, Vipin, Vale, Aathmaja and others have made my stay in Cologne an enjoyable one. I thank my friend Sutharsan for encouraging me to apply to the IGSDHD graduate program and Sabari for giving me the right advice at the right time.

My husband has been a pillar of support in all my endeavours and continues to be so. I thank him for his love and encouragement. I have no words to thank my parents. I thank them for being exceptionally supportive and teaching me to think and live freely. I thank my

sister for her undying support. I also thank my grandfather, my in-laws and other well-wishers for their constant encouragement.

Roshini

Eidesstattliche Erklärung

Ich versichere, dass ich die von mir vorgelegte Dissertation selbständig angefertigt, die benutzten Quellen und Hilfsmittel vollständig angegeben und die Stellen der Arbeit - einschließlich Tabellen, Karten und Abbildungen -, die anderen Werken im Wortlaut oder dem Sinn nach entnommen sind, in jedem Einzelfall als Entlehnung kenntlich gemacht habe; dass diese Dissertation noch keiner anderen Fakultät oder Universität zur Prüfung vorgelegen hat; dass noch nicht veröffentlicht worden ist sowie, dass ich eine solche Veröffentlichung vor Abschluss des Promotionsverfahrens nicht vornehmen werde. Die Bestimmungen der Promotionsordnung sind mir bekannt. Die von mir vorgelegte Dissertation ist von Herrn Prof. Dr. R. Jürgen Dohmen betreut worden.

Köln, im Mai 2015 Roshini Beenukumar Renukadevi

Teilpublikationen im Rahmen dieser Arbeit

R. Roshini Beenukumar, Daniela Gödderz, R. Palanimurugan, R. Jürgen Dohmen (2015) Polyamines directly promote antizyme-mediated degradation of ornithine decarboxylase by the proteasome. **Microbial cell**: *in press.*

Lebenslauf

Vor- und Zuname	: Roshini Beenukumar Renukadevi
Geburtstag	: 20.11.1987
Geburtsort	: Trivandrum, Indien
Familienstand	: Verheiratet
Staatsangehörigkeit	: Indien
Anschrift	: Caumannsstr. 10, 51065, Köln
Telefon	: 0049-176-70330043
Email	: roshini.br@gmail.com

Schulausbildung

2002-2003	Gymnasium Bharatiya Vidya Bhavan School, Calicut, Kerala, Indien Abschluss: All India Secondary School Certificate Examination
2003-2005	Gymnasium Kendriya Vidyalaya School Pattom, Trivandrum, Kerala, Indien Abschluss: All India Senior School Certificate Examination (Abitur)

Hochschulausbildung

2005-2008	Studium der Biologie (Plant Biology and Plant Biotechnology) University of Madras, Chennai, Indien Abschluss: Bachelor of Science
2008-2010	Studium der Biologie (Genomics) Madurai Kamaraj University, Madurai, Indien Abschluss: Master of Science
seit 10/2010	International Graduate School for Development Health and Disease, Universität zu Köln
seit 04/2011	Doktorarbeit am Institut für Genetik der Universität zu Köln in der Arbeitsgruppe von Prof. Dr. Jürgen Dohmen. Dissertation zum Thema “Ubiquitin-Independent Proteolytic Targeting of Ornithine Decarboxylase”.